

**Probing gluon saturation with forward di-hadron correlations in
proton-proton and proton-nucleus collisions**

Wenbin Zhao

Central China Normal University

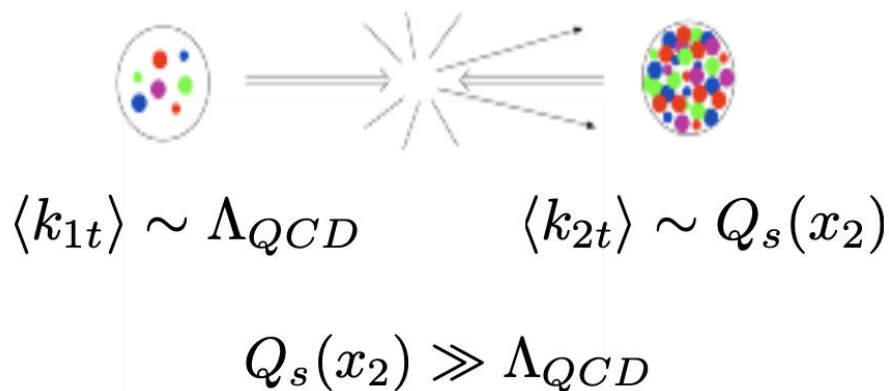
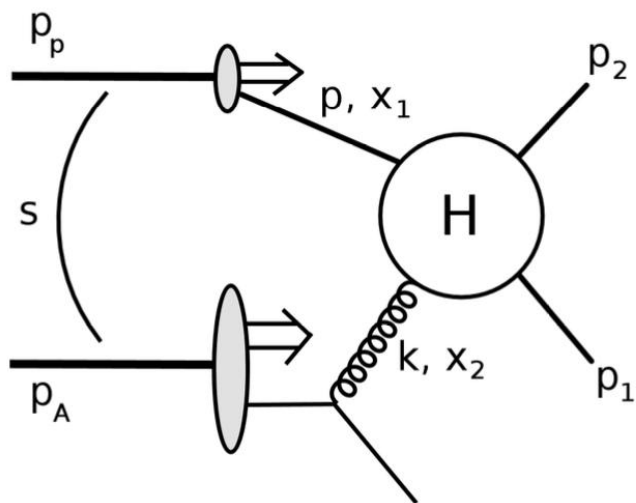


The 1st Annual Conference on Electron-Ion Collider Physics in China

2026.04.21 Shandong

Forward di-hadrons productions (dilute-dense)

- large-x projectile (proton) on small-x target (proton or nucleus)



so-called “dilute-dense” kinematics

Incoming partons' energy fractions:

$$x_1 = \frac{1}{\sqrt{s}} (|p_{1t}|e^{y_1} + |p_{2t}|e^{y_2}) \quad \xrightarrow{y_1, y_2 \gg 0} \quad x_1 \sim 1$$

$$x_2 = \frac{1}{\sqrt{s}} (|p_{1t}|e^{-y_1} + |p_{2t}|e^{-y_2}) \quad \xrightarrow{y_1, y_2 \gg 0} \quad x_2 \ll 1$$

CM (2007)

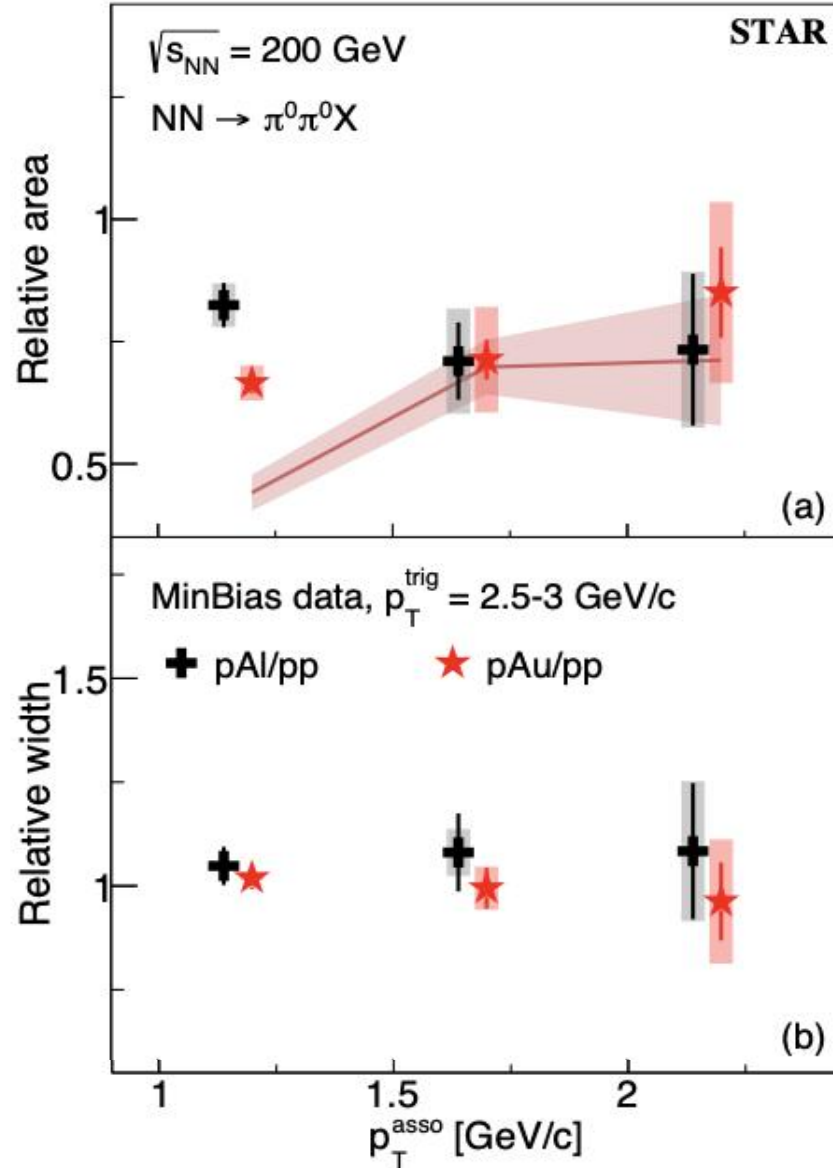
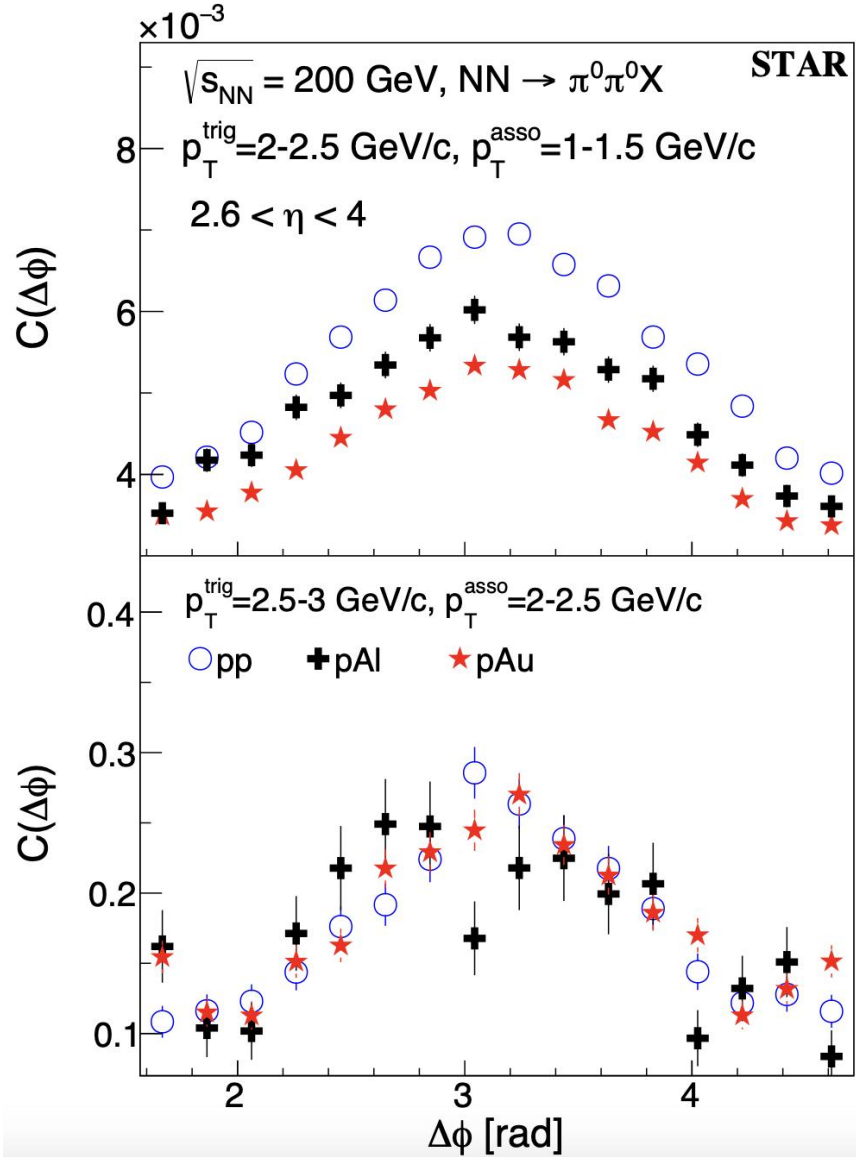
Gluon's transverse momentum (p_{1t} , p_{2t} imbalance):

$$|k_t|^2 = |p_{1t} + p_{2t}|^2 = |p_{1t}|^2 + |p_{2t}|^2 + 2|p_{1t}||p_{2t}|\cos\Delta\phi$$

prediction: modification of the k_t distribution in p+Pb vs p+p collisions

Borrow from Cyrille Marquet's slide (2020).

STAR measurements



STAR data: PhysRevLett.129.092501.

CGC model: J. L. Albacete, G. Giacalone, C. Marquet and M. Matas, PhysRevD.99.014002

Color Glass Condensate Calculations

- We use the improved TMD factorization (iTMD), which resums the $\left(\frac{Q_s}{k_T}\right)^n$ and $\left(\frac{k_T}{P_T}\right)^n$.

$$\frac{d\sigma^{pA \rightarrow \text{dijets}+X}}{dy_1 dy_2 d^2p_{1t} d^2p_{2t}} = \frac{\alpha_s^2}{(x_1 x_2 s)^2} \sum_{a,c,d} x_1 f_{a/p}(x_1, \mu^2) \sum_i H_{ag \rightarrow cd}^{(i)} \mathcal{F}_{ag}^{(i)}(x_2, k_t) \frac{1}{1 + \delta_{cd}},$$

$f_{a/p}$: Collinear pdf for the large-x projectile (dilute part)

$F_{ag}^i(x, k_t)$: Several gluon TMDs for small-x target (dense part)

$H_{ag \rightarrow cd}^i$: The associated hard matrix elements.

$$\frac{d\sigma^{qA \rightarrow qgX}}{dP.S.} = \mathcal{F}_{qg}^{(1)}(x_A, \mathbf{k}) \mathcal{H}_{qg \rightarrow qg}^{(1)} + \mathcal{F}_{qg}^{(2)}(x_A, \mathbf{k}) \mathcal{H}_{qg \rightarrow qg}^{(2)} \quad (2)$$

$$\frac{d\sigma^{gA \rightarrow q\bar{q}X}}{dP.S.} = \mathcal{F}_{gq}^{(1)}(x_A, \mathbf{k}) \mathcal{H}_{gq \rightarrow q\bar{q}}^{(1)} + \mathcal{F}_{gq}^{(2)}(x_A, \mathbf{k}) \mathcal{H}_{gq \rightarrow q\bar{q}}^{(2)} \quad (3)$$

$$\begin{aligned} \frac{d\sigma^{gA \rightarrow ggX}}{dP.S.} &= (\mathcal{F}_{gg}^{(1)}(x_A, \mathbf{k}) + \mathcal{F}_{gg}^{(3)}(x_A, \mathbf{k})) \mathcal{H}_{gg \rightarrow gg}^{(1)} \\ &+ (\mathcal{F}_{gg}^{(2)}(x_A, \mathbf{k}) + \mathcal{F}_{gg}^{(3)}(x_A, \mathbf{k})) \mathcal{H}_{gg \rightarrow gg}^{(2)} \end{aligned} \quad (4)$$

Soft gluon resummation

A. H. Mueller, B. W. Xiao and F. Yuan, PhysRevLett.110.082301.
 P. Sun, C. P. Yuan, and F. Yuan, Phys. Rev. Lett. 113 23, (2014)
 S. y. Wei, Phys. Lett. B 817, 136356 (2021)

$$\frac{d\sigma}{d^2p_{T1}d^2p_{T2}} \propto \int \frac{d^2b_{\perp}}{(2\pi)^2} e^{-i\vec{q}_T \cdot \vec{b}_{\perp}} f(x_1) \otimes F(x_2, b_{\perp}) \otimes H \otimes e^{-S_{\text{Sudakov}}}$$

- Sudakov factors : $S_{\text{Sud}}^{a+b \rightarrow c+d}(b_{\perp}) = \sum_{i=a,b,c,d} S_p^i(b_{\perp}) + \mathbf{C}_{np} \times \sum_{i=a,c,d} S_{np}^i(b_{\perp})$,

$$S_p^{q+g \rightarrow q+g}(Q, b_{\perp}) = \int_{\mu_b^2}^{Q^2} \frac{d\mu^2}{\mu^2} \left[2(C_F + C_A) \frac{\alpha_s}{2\pi} \ln \left(\frac{Q^2}{\mu^2} \right) - \left(\frac{3}{2}C_F + C_A\beta_0 \right) \frac{\alpha_s}{\pi} \right],$$

$$S_p^{g+g \rightarrow g+g}(Q, b_{\perp}) = \int_{\mu_b^2}^{Q^2} \frac{d\mu^2}{\mu^2} \left[4C_A \frac{\alpha_s}{2\pi} \ln \left(\frac{Q^2}{\mu^2} \right) - 3C_A\beta_0 \frac{\alpha_s}{\pi} \right].$$

$$S_{np}^{q+g \rightarrow q+g}(Q, b_{\perp}) = \left(2 + \frac{C_A}{C_F} \right) \frac{g_1}{2} b_{\perp}^2 + \left(2 + \frac{C_A}{C_F} \right) \frac{g_2}{2} \ln \frac{Q}{Q_0} \ln \frac{b_{\perp}}{b_*},$$

$$S_{np}^{g+g \rightarrow g+g}(Q, b_{\perp}) = \frac{3C_A}{C_F} \frac{g_1}{2} b_{\perp}^2 + \frac{3C_A}{C_F} \frac{g_2}{2} \ln \frac{Q}{Q_0} \ln \frac{b_{\perp}}{b_*}.$$

Using the b^* -prescription: $\beta_0 = (11 - 2n_f/3)/12$, $\mu_b = 2e^{-\gamma_E}/b_*$, and $b_* = b_{\perp}/\sqrt{1 + b_{\perp}^2/b_{\text{max}}^2}$.

\mathbf{C}_{np} as the tuneable parameter in our model calculations.

Initial conditions for rcBK

- The dipole-nucleus amplitude is obtained by solving the rcBK evolution equation.
- The initial conditions at $x_0 = 0.01$ is model by parametrization, based on McLerran-Venugopalan model

$$\mathcal{N}(\mathbf{r}_T) = 1 - \exp \left[-\frac{(\mathbf{r}_T^2 Q_{s0}^2)^\gamma}{4} \ln \left(\frac{1}{|\mathbf{r}_T| \Lambda_{\text{QCD}}} + e_c \cdot e \right) \right]$$

- The BK equation with strong coupling constant α_s as a function of the transverse separation $r = |\mathbf{r}_T|$

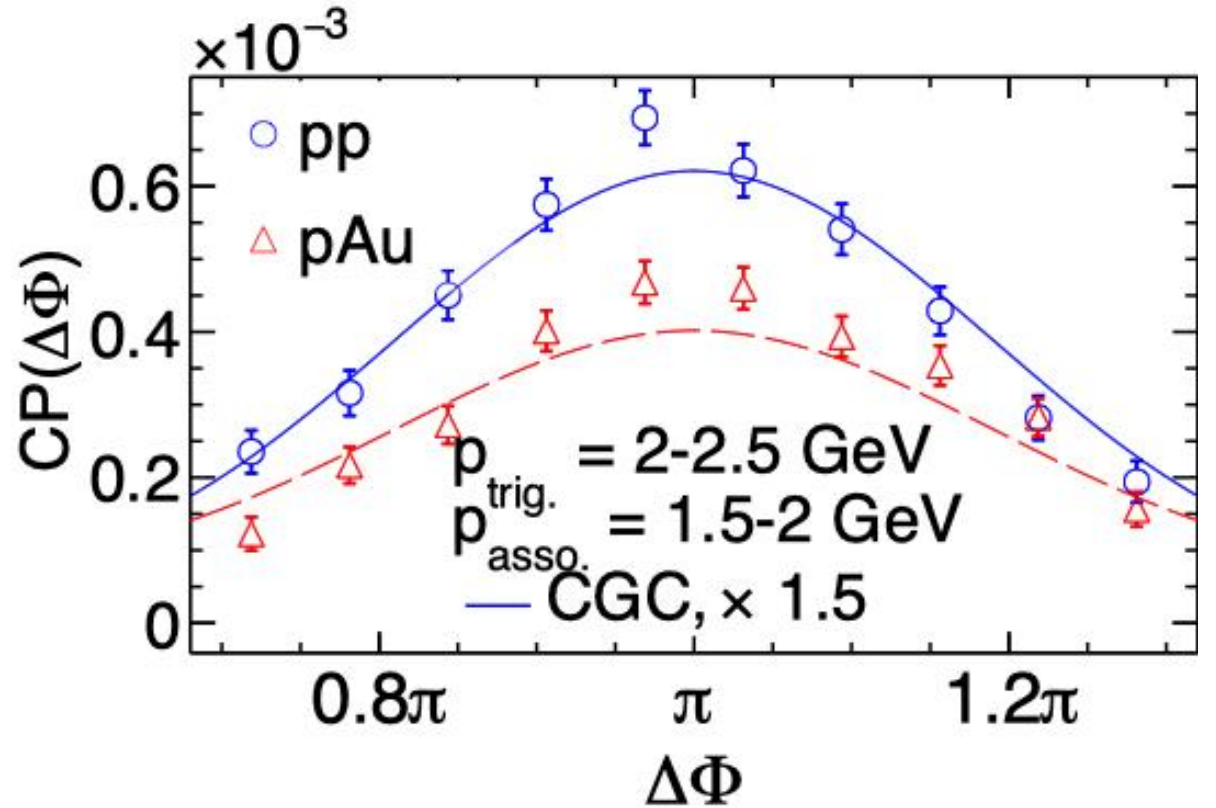
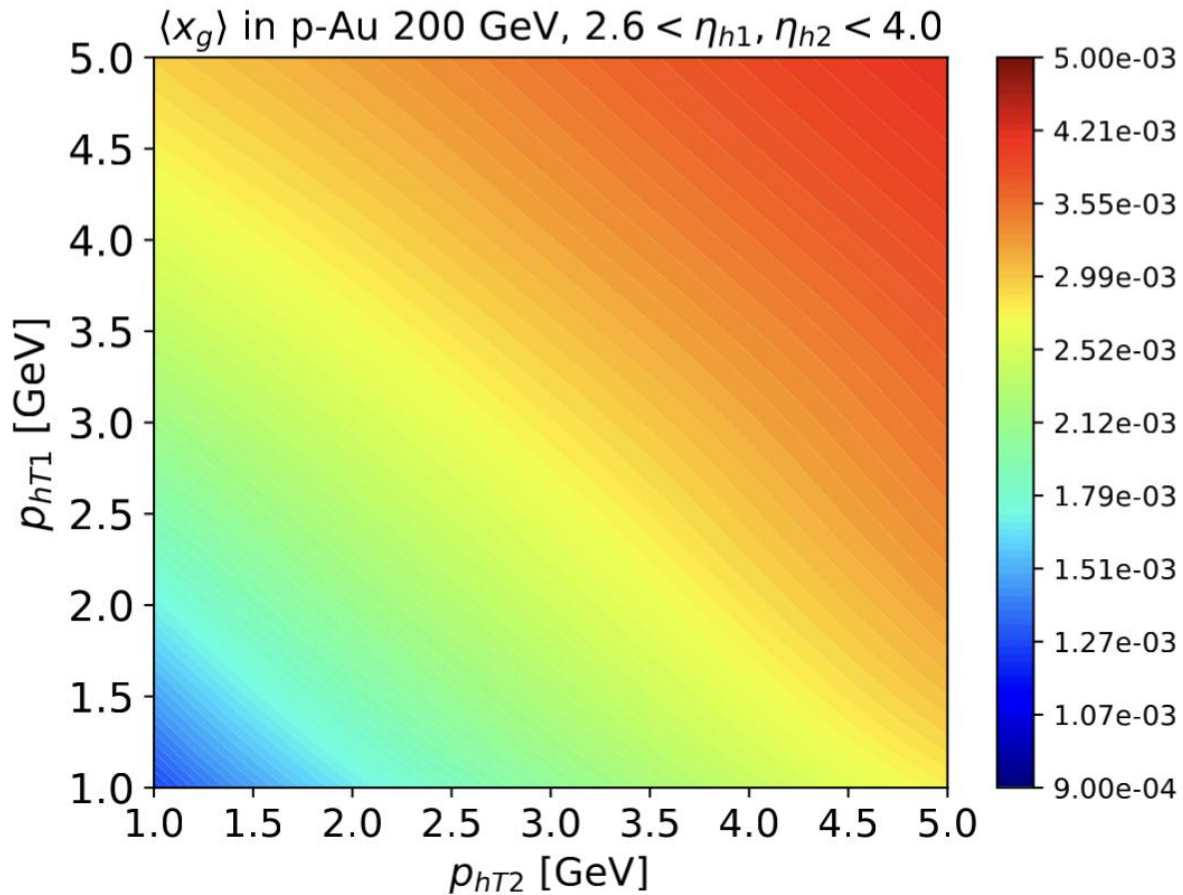
$$\alpha_s(r) = \frac{12\pi}{(33 - 2N_f) \log \left(\frac{4C^2}{r^2 \Lambda_{\text{QCD}}^2} \right)},$$

- We use $Q_{p,s0}^2 = 0.168 \text{ GeV}^2$, $\gamma = 1.119$, $C = 1.1715$, $\Lambda_{\text{QCD}} = 0.24 \text{ GeV}$, $e_c = 1$.
- For nucleus, we set $Q_{Al,s0}^2 = 1.2 Q_{p,s0}^2$; $Q_{Au,s0}^2 = 2.75 Q_{p,s0}^2$; $Q_{Pb,s0}^2 = 2.84 Q_{p,s0}^2$

J. L. Albacete, N. Armesto, J. G. Milhano, P. Quiroga-Arias and C. A. Salgado, Eur. Phys. J. C71 (2011) 1705. (AAMQS collaboration)

F. Deganutti, C. Royon and S. Schlichting, JHEP 01(2024)159.

Dihadron Correlations in Forward pp and pA collisions

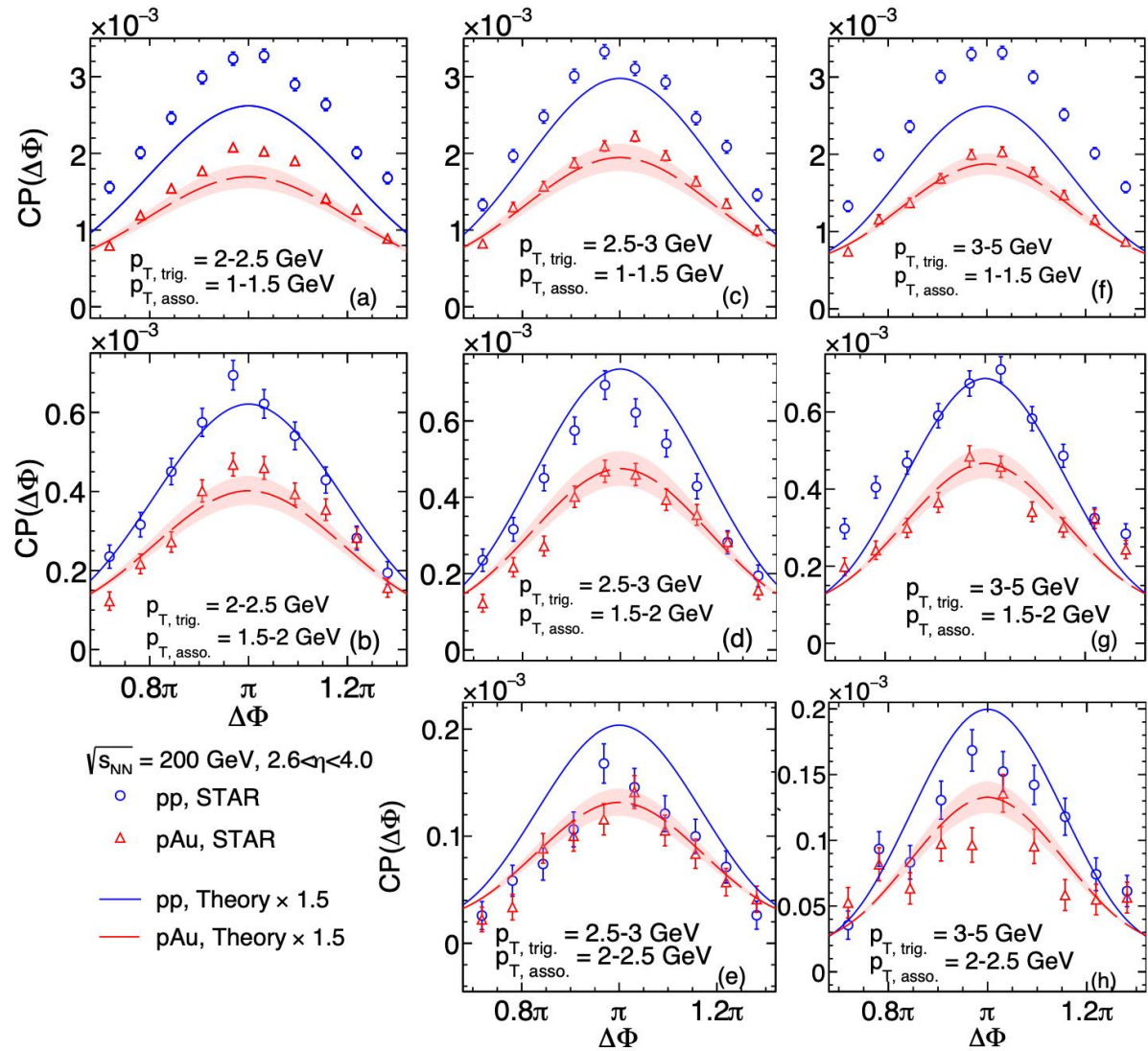


STAR data: PhysRevLett.129.092501

P. Caucal, Z. B.Kang, P. Korcyl, F. Salazar, B. Schenke, T.Stebel, R.Venugopalan and W.Zhao, [arXiv:2512.21466].

- $\langle x_g \rangle$ probed by di-hadron at STAR is small.
- CGC model reasonably describe the STAR data; Suppression: **pp > pAu.**

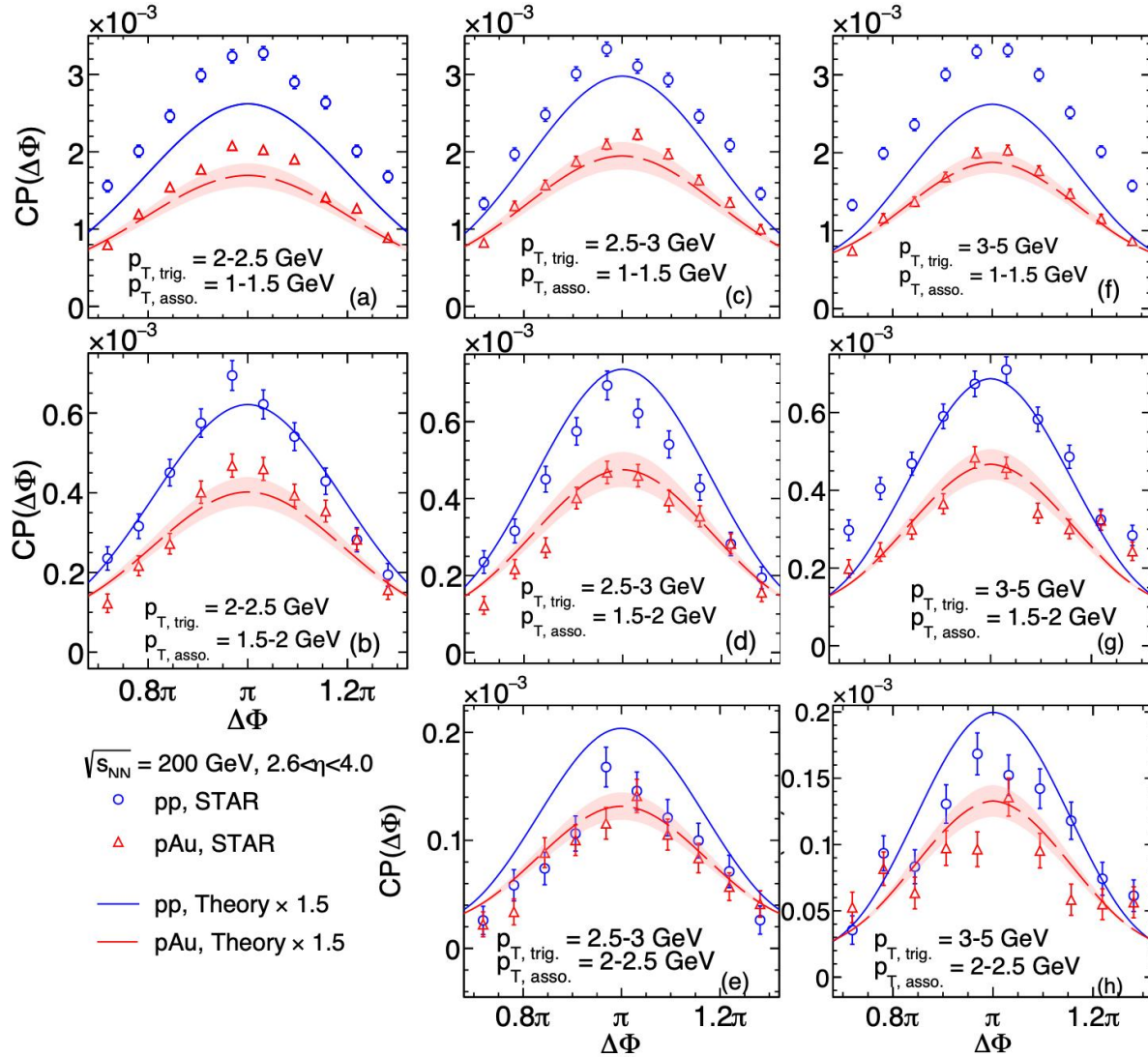
Dihadron Correlations in Forward collisions



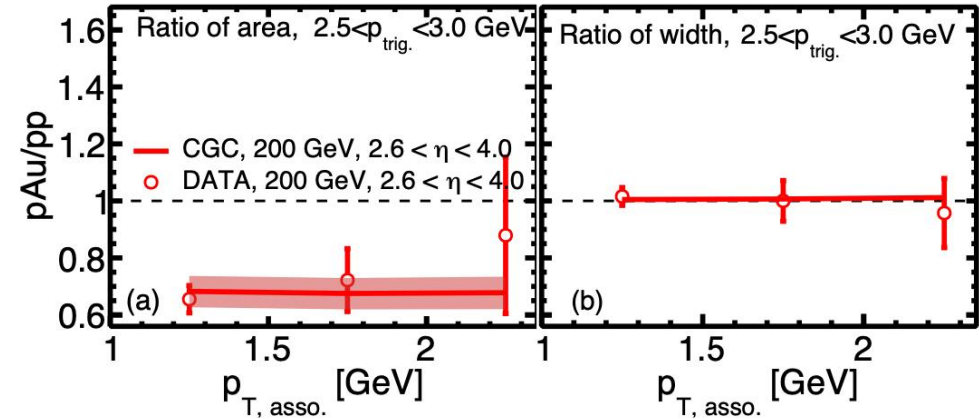
- Overall, it's good;
- Need an **additional normalization factor**. (There are uncertainties from FF).
- The first line is not well described.

P. Caucal, Z. B.Kang, P. Korcyl, F. Salazar, B. Schenke, T.Stebel, R.Venugopalan and W.Zhao, [arXiv:2512.21466].
 STAR data: PhysRevLett.129.092501

Dihadron Correlations in Forward collisions



- Overall, it's good;
- Need an **additional normalization factor**. (There are uncertainties from FF).
- The first line is not well described.



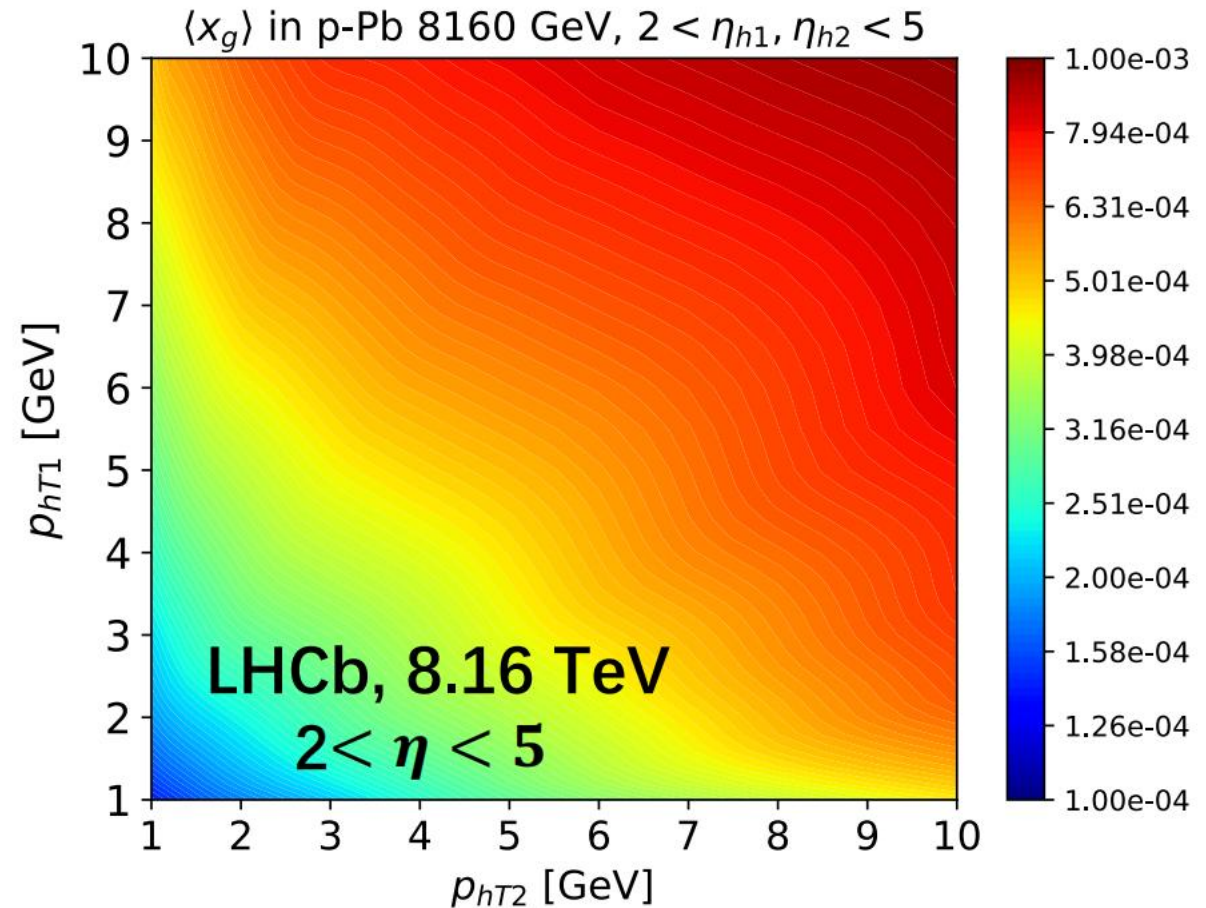
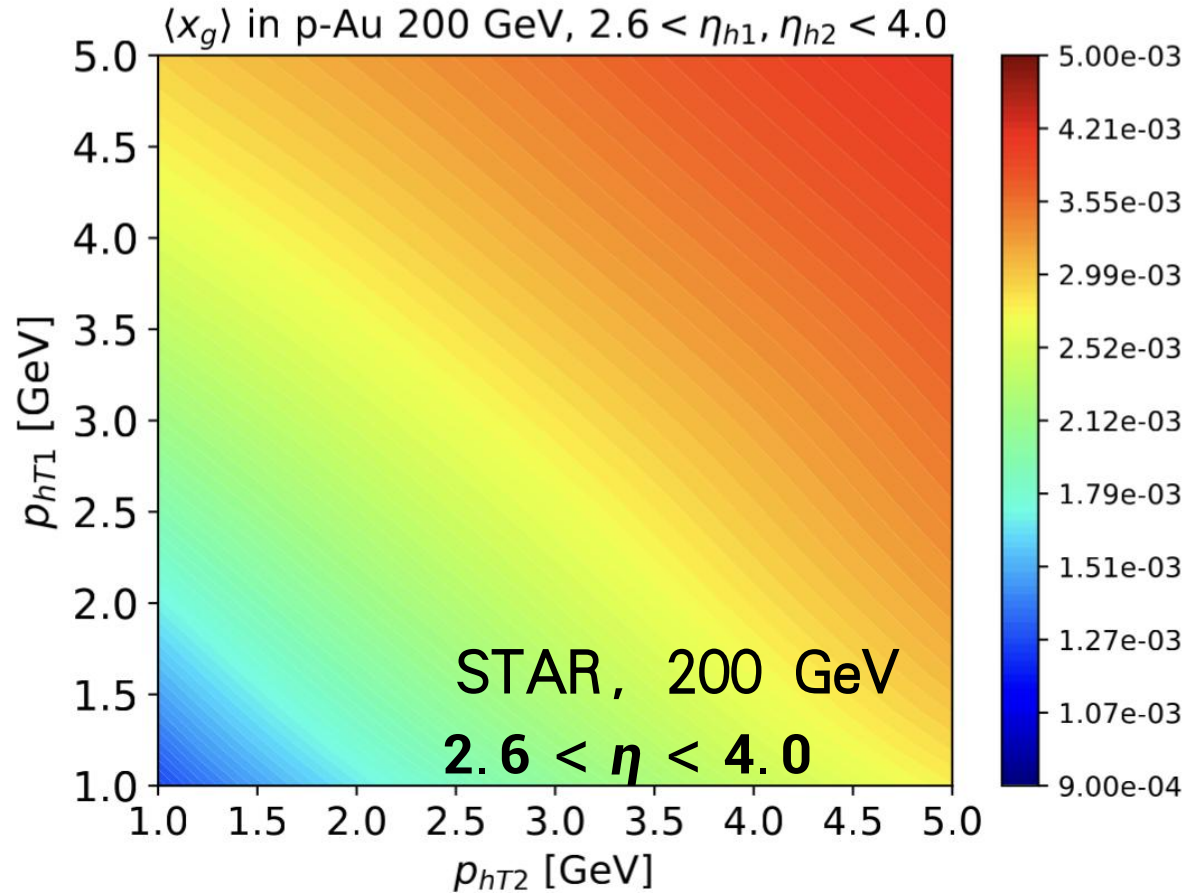
- CGC predicts very **weak p_T dependence**.
- The width ratio is very **close to 1, width is dominated by the Sudakov factor**.

P. Caucal, Z. B.Kang, P. Korcyl, F. Salazar, B. Schenke, T.Stebel, R.Venugopalan and W.Zhao, [arXiv:2512.21466].
 STAR data: PhysRevLett.129.092501

Predictions for LHCb at the LHC

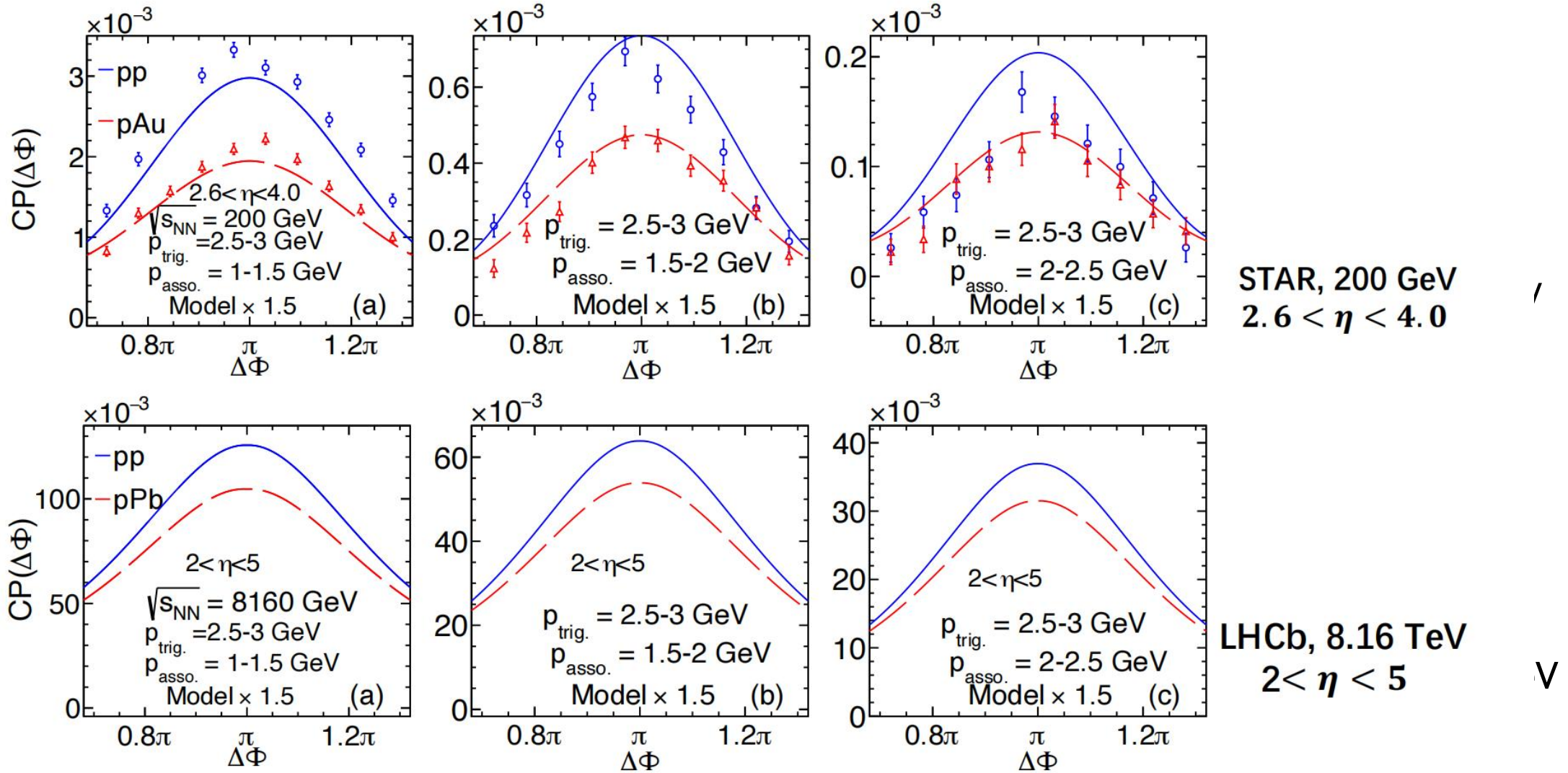
p-p and p-Pb at $\sqrt{s_{nn}} = 8.16 \text{ TeV}$, $2 < \eta < 5$

$\langle x_g \rangle$ probed by STAR and LHCb



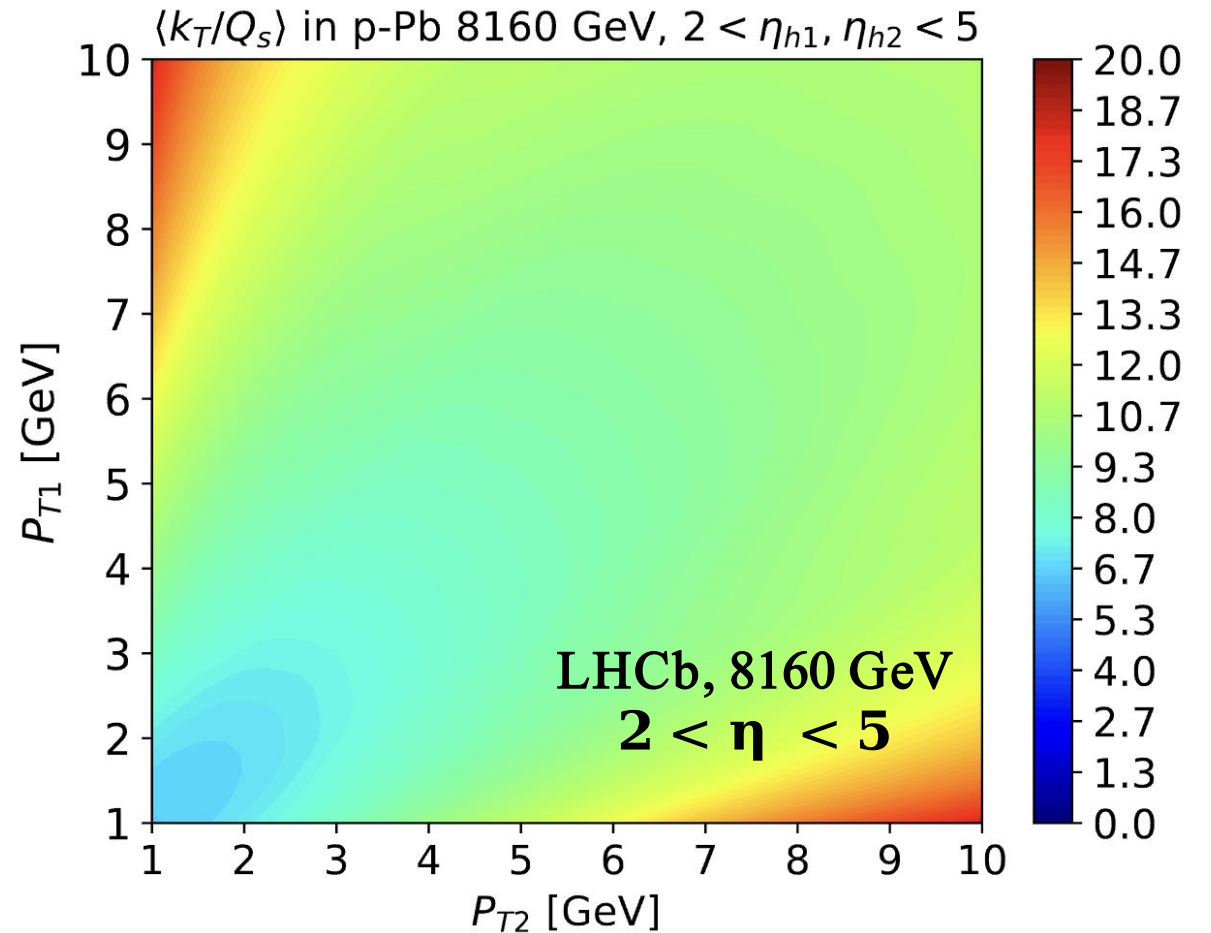
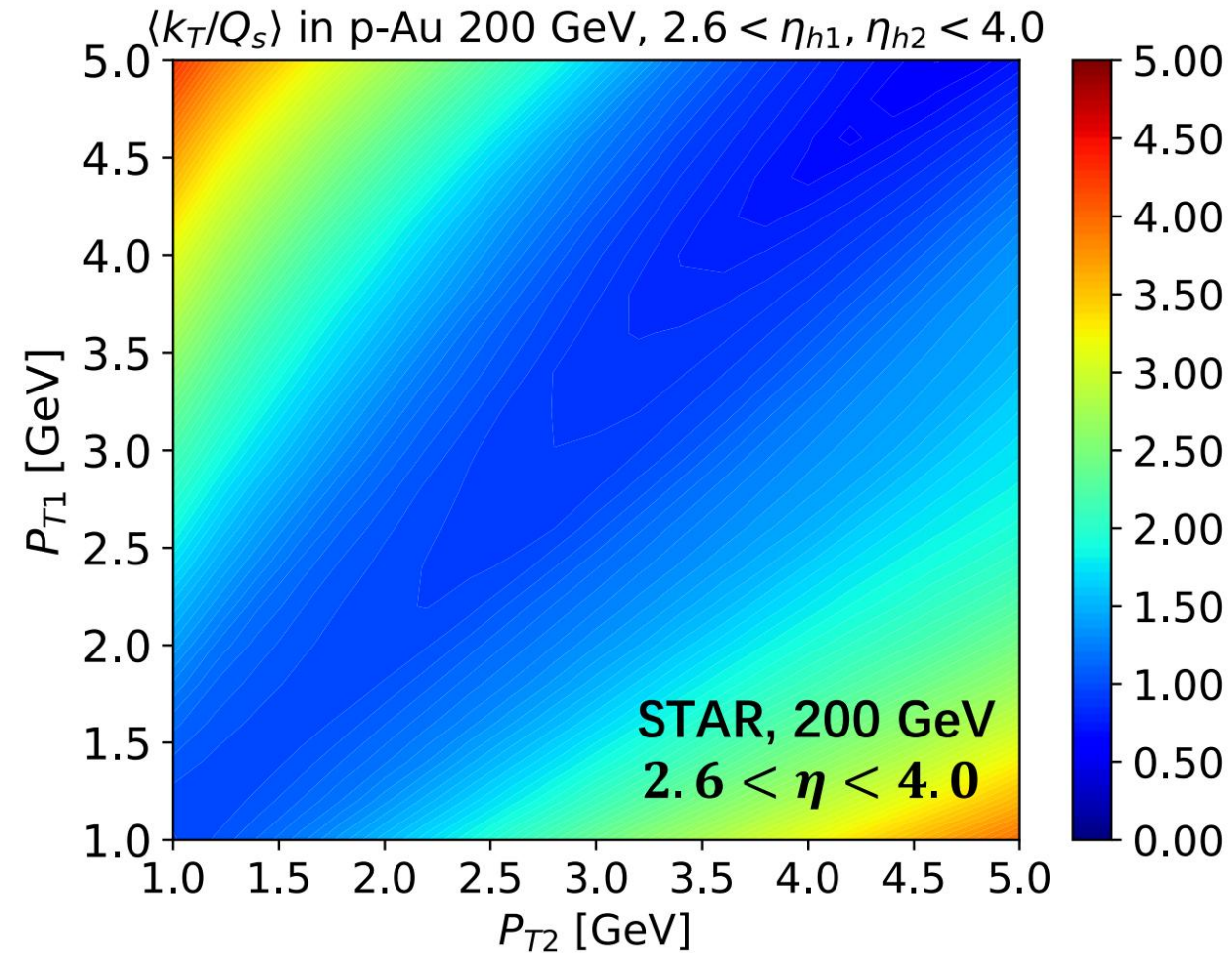
- $\langle x_g \rangle$ probed by di-hadron at LHCb is **much smaller** than that at STAR.

Dihadron Correlations in LHCb



- Surprisingly, LHCb has the **smaller suppression** than STAR, even LHCb has smaller x_g .

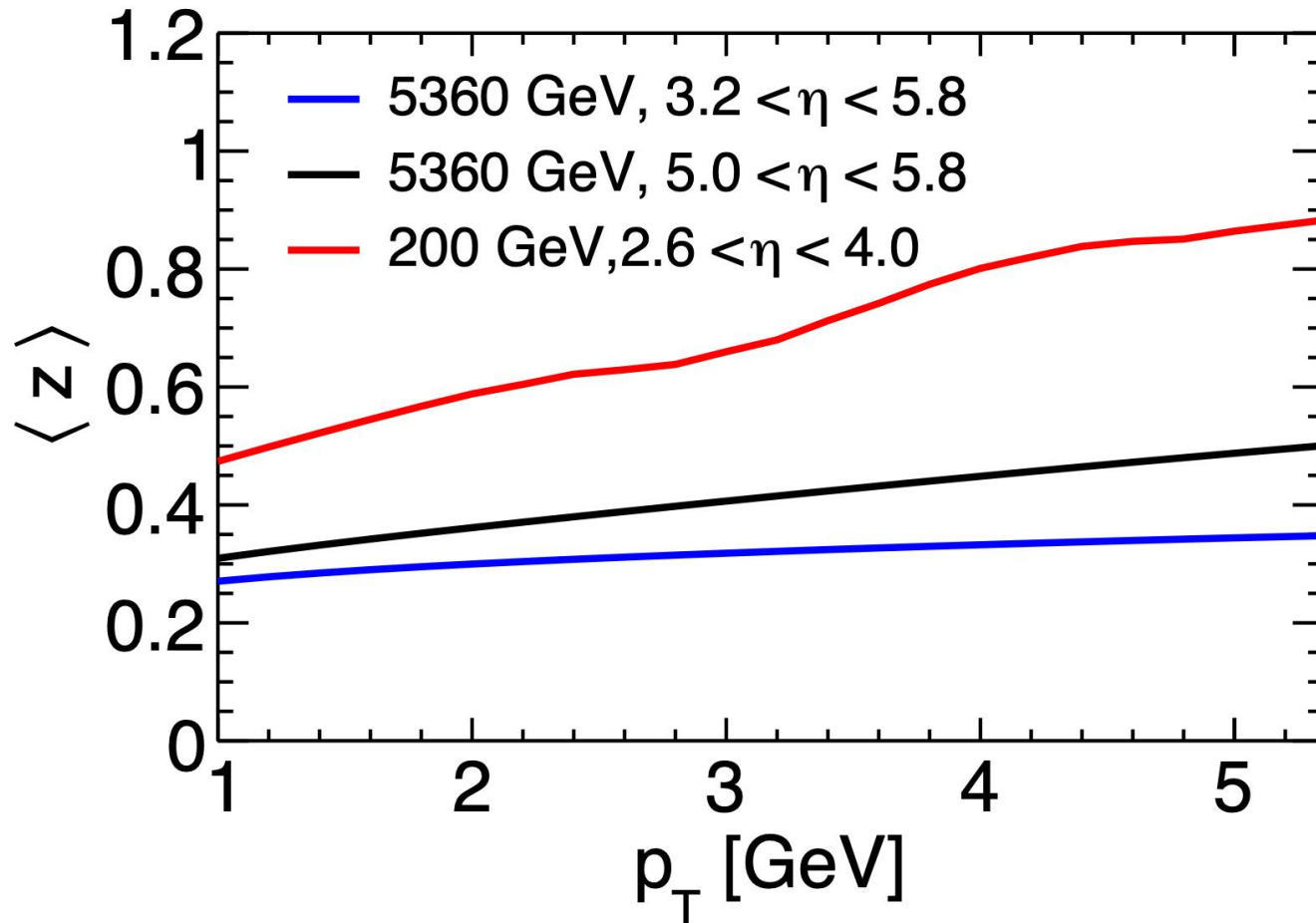
$\langle k_T/Q_s \rangle$ probed by STAR and LHCb



- $\langle k_T/Q_s \rangle$ probed by di-hadron at **LHCb is much larger than that at STAR**, which partially explains the less saturation effects in LHCb than STAR.

P. Caucal, Z. B.Kang, P. Korcyl, F. Salazar, B. Schenke, T.Stebel, R.Venugopalan and W.Zhao, [arXiv:2512.21466].

Fragmentation fraction probed by STAR and LHCb



- STAR has much **larger** $\langle z \rangle$, than that at LHCb.

Heavy Flavour

Color Glass Condensate for Heavy Flavour

$$\frac{d\sigma^{pA \rightarrow Q\bar{Q}X}}{d^2\mathbf{k}_{1\perp}d^2\mathbf{k}_{2\perp}dy_1dy_2} = x_p g(x_p, \mu^2) \int \frac{d^2\mathbf{x}_\perp d^2\mathbf{x}'_\perp d^2\mathbf{y}_\perp d^2\mathbf{y}'_\perp}{(2\pi)^6} e^{-i\mathbf{k}_{1\perp} \cdot (\mathbf{x}_\perp - \mathbf{x}'_\perp)} e^{-i\mathbf{k}_{2\perp} \cdot (\mathbf{y}_\perp - \mathbf{y}'_\perp)}$$

$$\times \psi^{g \rightarrow Q\bar{Q}}(\mathbf{x}_\perp - \mathbf{y}_\perp) \psi^{g \rightarrow Q\bar{Q}, \dagger}(\mathbf{x}'_\perp - \mathbf{y}'_\perp) \left[S_{q\bar{q}q\bar{q}}^{(4)}(\mathbf{x}_\perp, \mathbf{y}_\perp, \mathbf{x}'_\perp, \mathbf{y}'_\perp; x_A) + S_{gg}^{(2)}(z\mathbf{x}_\perp + (1-z)\mathbf{y}_\perp, z\mathbf{x}'_\perp + (1-z)\mathbf{y}'_\perp; x_A) \right.$$

$$\left. - S^{(3)}(\mathbf{x}_\perp, z\mathbf{x}'_\perp + (1-z)\mathbf{y}'_\perp, \mathbf{y}_\perp; x_A) - S^{(3)}(\mathbf{y}'_\perp, z\mathbf{x}_\perp + (1-z)\mathbf{y}_\perp, \mathbf{x}'_\perp; x_A) \right]$$

- In the large N_c limite, we can have

$$S_{q\bar{q}q\bar{q}}^{(4)}(\mathbf{x}_\perp, \mathbf{y}_\perp, \mathbf{x}'_\perp, \mathbf{y}'_\perp; x_A) = S_{q\bar{q}}^{(2)}(\mathbf{x}_\perp, \mathbf{x}'_\perp; x_A) S_{q\bar{q}}^{(2)}(\mathbf{y}'_\perp, \mathbf{y}_\perp; x_A)$$

$$S_{gg}^{(2)}(\mathbf{v}_\perp, \mathbf{v}'_\perp; x_A) = S_{q\bar{q}}^{(2)}(\mathbf{v}_\perp, \mathbf{v}'_\perp; x_A) S_{q\bar{q}}^{(2)}(\mathbf{v}'_\perp, \mathbf{v}_\perp; x_A)$$

$$S^{(3)}(\mathbf{x}_\perp, \mathbf{v}'_\perp, \mathbf{y}_\perp; x_A) = S_{q\bar{q}}^{(2)}(\mathbf{x}_\perp, \mathbf{v}'_\perp; x_A) S_{q\bar{q}}^{(2)}(\mathbf{v}'_\perp, \mathbf{y}_\perp; x_A)$$

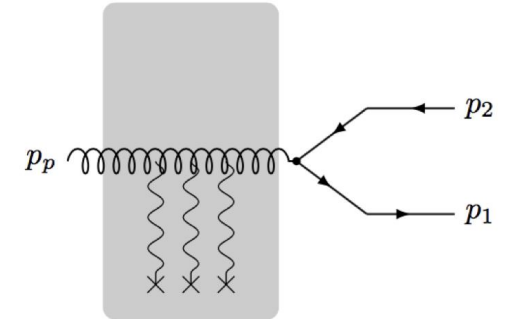
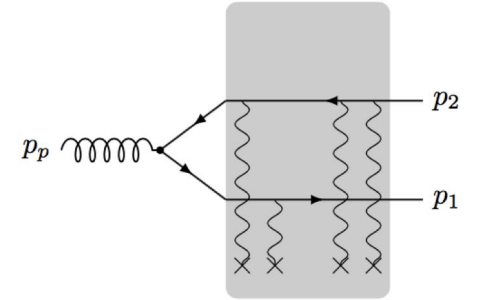
$$S^{(3)}(\mathbf{y}'_\perp, \mathbf{v}_\perp, \mathbf{x}'_\perp; x_A) = S_{q\bar{q}}^{(2)}(\mathbf{y}'_\perp, \mathbf{v}_\perp; x_A) S_{q\bar{q}}^{(2)}(\mathbf{v}_\perp, \mathbf{x}'_\perp; x_A)$$

Thus

$$\frac{d\sigma^{pA \rightarrow Q\bar{Q}X}}{d^2\mathbf{k}_{1\perp}d^2\mathbf{k}_{2\perp}dy_1dy_2} = S_\perp x_p g(x_p, \mu^2) \int \frac{d^2\mathbf{l}_\perp}{(2\pi)^2} F(\mathbf{l}_\perp; x_A) F(\mathbf{K}_\perp - \mathbf{l}_\perp; x_A)$$

$$\int \frac{d^2\mathbf{u}_\perp d^2\mathbf{u}'_\perp}{(2\pi)^2} \psi^{g \rightarrow Q\bar{Q}}(\mathbf{u}_\perp) \psi^{g \rightarrow Q\bar{Q}, \dagger}(\mathbf{u}'_\perp) \left[e^{-i\mathbf{P}_\perp \cdot \mathbf{u}_\perp} - e^{-i(z\mathbf{K}_\perp + \mathbf{P}_\perp - \mathbf{l}_\perp) \cdot \mathbf{u}_\perp} \right] \left[e^{i\mathbf{P}_\perp \cdot \mathbf{u}'_\perp} - e^{i(z\mathbf{K}_\perp + \mathbf{P}_\perp - \mathbf{l}_\perp) \cdot \mathbf{u}'_\perp} \right]$$

$$F(\mathbf{l}_\perp; x_A) = \int \frac{d^2(\mathbf{x}_\perp - \mathbf{x}'_\perp)}{(2\pi)^2} e^{-i\mathbf{l}_\perp \cdot (\mathbf{x}_\perp - \mathbf{x}'_\perp)} S_{q\bar{q}}^{(2)}(\mathbf{x}_\perp, \mathbf{x}'_\perp; x_A)$$



F. Dominguez, C. Marquet, B. W. Xiao and F. Yuan, Phys. Rev. D 83 (2011), 105005.

C. Marquet, C. Roiesnel and P. Taelis, Phys. Rev. D 97,014004 (2018).

Put Sudakov factor

$$\frac{d\sigma^{pA \rightarrow H_1 H_2 X}}{d^2\mathbf{k}_{h1\perp} d^2\mathbf{k}_{h2\perp} dy_1 dy_2} = 2S_\perp \int \frac{dz_{h1}}{z_{h1}^2} \int \frac{dz_{h2}}{z_{h2}^2} \int d^2\mathbf{l}_\perp \frac{[H(\mathbf{P}_\perp, \mathbf{P}_\perp) - 2H(\mathbf{P}_\perp + z\mathbf{K}_\perp - \mathbf{l}_\perp, \mathbf{P}_\perp) + H(\mathbf{P}_\perp + z\mathbf{K}_\perp - \mathbf{l}_\perp, \mathbf{P}_\perp + z\mathbf{K}_\perp - \mathbf{l}_\perp)]}{(z\mathbf{K}_\perp - \mathbf{l}_\perp)^2} \quad (315)$$

$$\times \int \frac{d^2\mathbf{K}'_\perp}{(2\pi)^2} W(z_{h1}, z_{h2}, x_p, \mathbf{K}'_\perp - \mathbf{K}_\perp, \mu_F) \boxed{(z\mathbf{K}'_\perp - \mathbf{l}_\perp)^2 F(\mathbf{l}_\perp; x_A) F(\mathbf{K}'_\perp - \mathbf{l}_\perp; x_A)} \quad (316)$$

Unintegrated Gluon Distributions (UGD)s

where:

$$W_{(z_{h1}, z_{h2}, x_p, \mathbf{k}'_\perp - \mathbf{k}_\perp, \mu_F)} = \int d^2\mathbf{b}_\perp e^{i(\mathbf{k}'_\perp - \mathbf{k}_\perp) \cdot \mathbf{b}_\perp} x_1 g(x_1, \mu_b^2) D_{h1/c}(z_{h1}, \mu_b^2) D_{h2/\bar{c}}(z_{h2}, \mu_b^2) e^{-S_{gg \rightarrow q\bar{q}}(\mathbf{b}_\perp, \mu_F)}$$

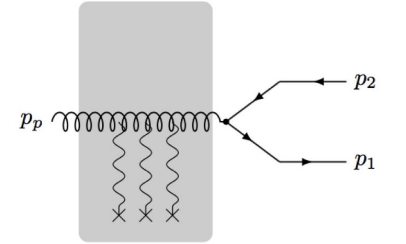
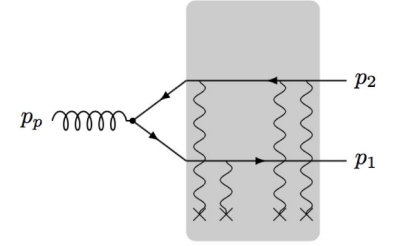
$$H(\mathbf{q}_{1\perp}, \mathbf{q}_{2\perp}) = \int \frac{d^2\mathbf{u}_\perp d^2\mathbf{u}'_\perp}{(2\pi)^2} e^{-i\mathbf{q}_{1\perp} \cdot \mathbf{u}_\perp} e^{i\mathbf{q}_{2\perp} \cdot \mathbf{u}'_\perp} \psi^{g \rightarrow Q\bar{Q}}(\mathbf{u}_\perp) \psi^{g \rightarrow Q\bar{Q}, \dagger}(\mathbf{u}'_\perp)$$

- Dead Cone effects:

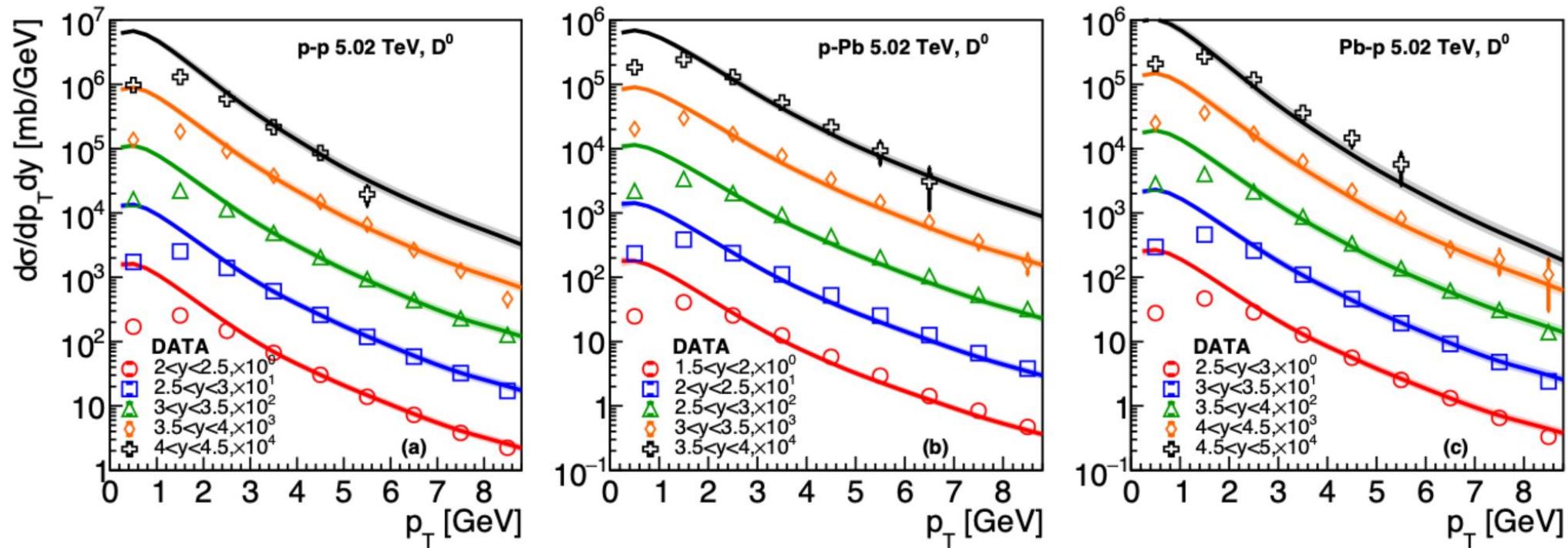
$$S_{gg \rightarrow q\bar{q}}(\mathbf{b}_\perp, \mu_F) = \int_{\mu_b^2}^{\mu_F^2} \frac{d\mu^2}{\mu^2} \frac{\alpha_s(\mu)}{2\pi} \left[2C_A \left(\ln \left(\frac{\mu_F^2}{\mu^2} \right) \right) + 2C_F \left(\ln \left(\frac{\mu_F^2}{\mu^2} \right) - \theta(M_Q^2 - \mu_b^2) \ln \left(\frac{M_Q^2}{\mu^2} \right) \right) - (3C_F + 2\beta_0) \right] \\ + \left(2 + \frac{C_A}{C_F} \right) \left[\frac{g_1}{2} \mathbf{b}_\perp^2 + \frac{1}{4} \frac{g_2}{2} \ln \left(\frac{\mu_F^2}{Q_0^2} \right) \ln \left(\frac{\mathbf{b}_\perp^2}{b_*^2} \right) \right] \quad (C16)$$

C. Marquet, Y. Shi and B. W. Xiao, [arXiv:2510.18949].

W. Zhao etc.al, in progress.

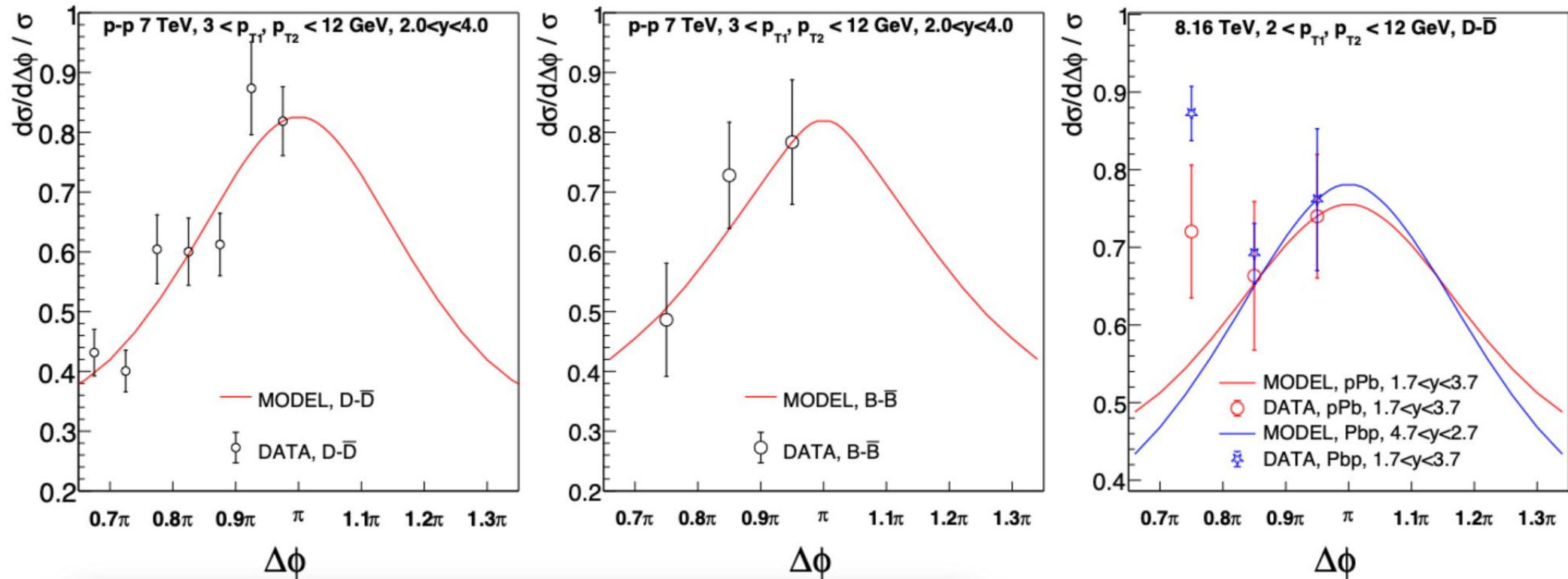


Single Inclusive Heavy Flavour



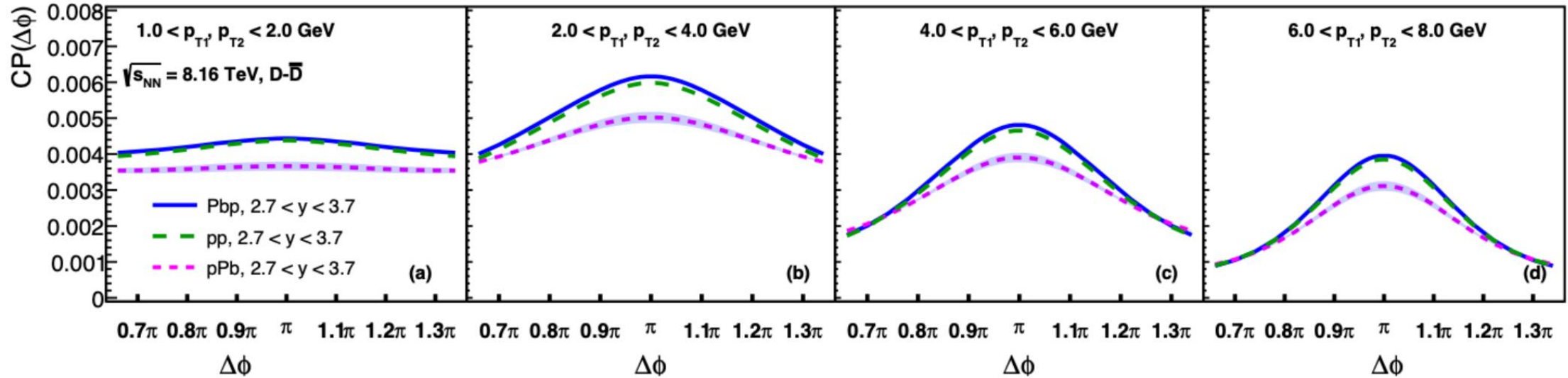
- Well describe **single inclusive** D spectra at the LHC.

Dihadron Correlations for Heavy Flavour in p-p, p-A and A-p



- Well describe the correlation in p-p, p-Pb (Pb dense) and Pb-p (p dense) with $\Delta\phi$ at **back-to-back region**.

Dihadron Correlations for Heavy Flavour in p-p, p-A and A-p



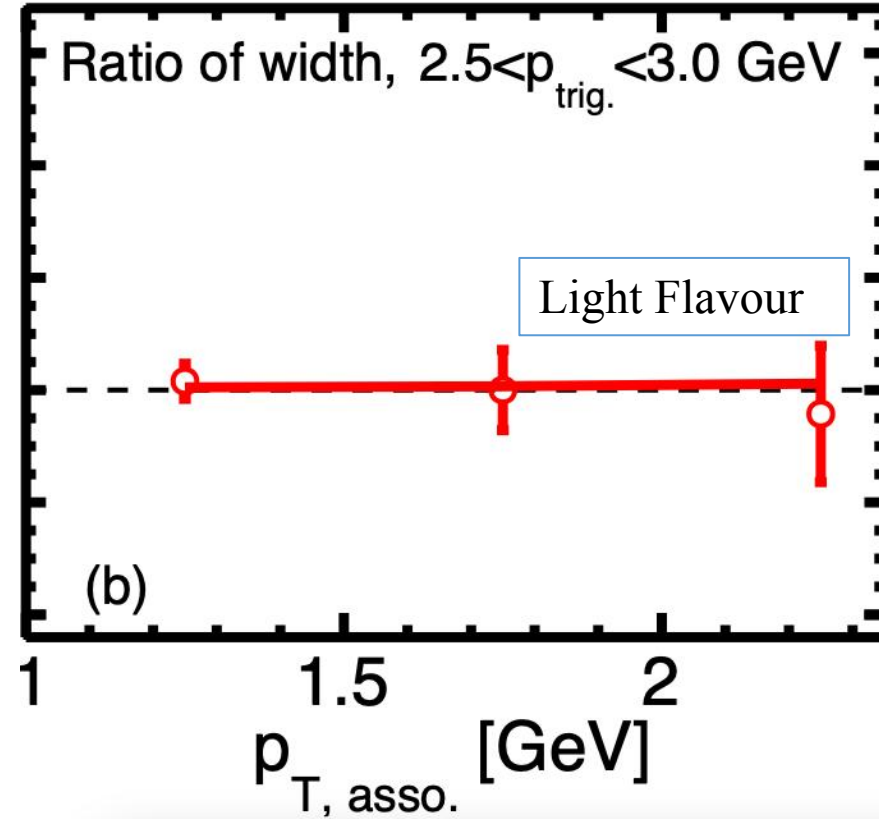
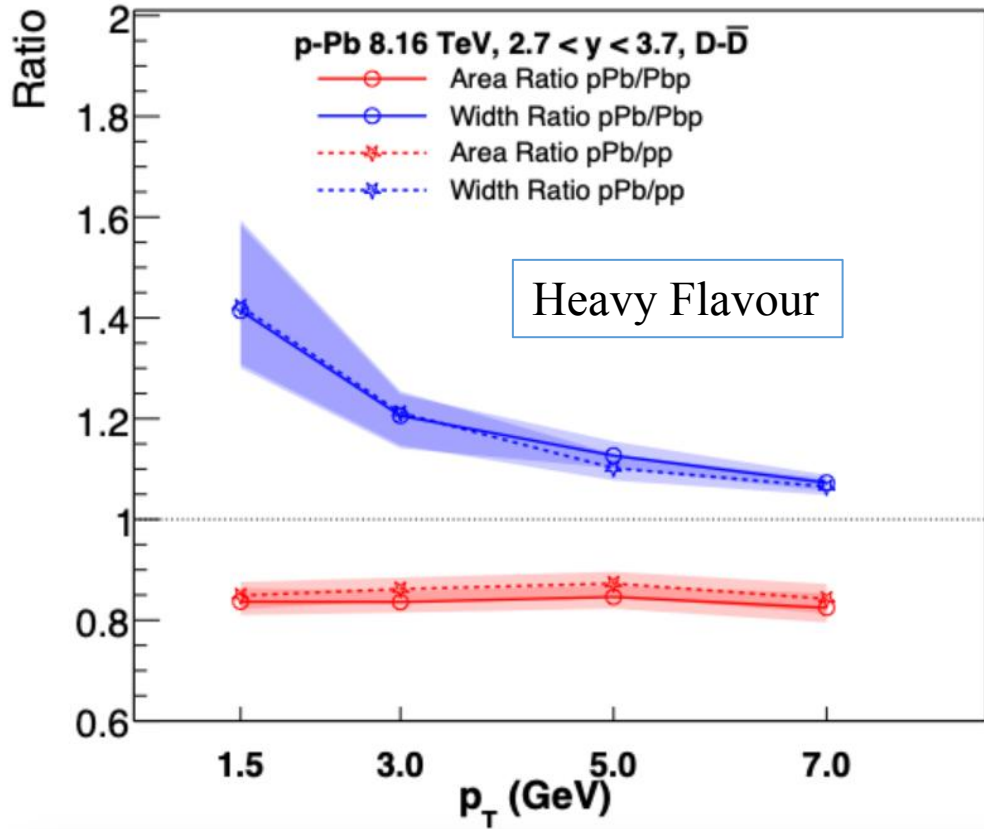
- Model predictions of di-D correlations. **Clean suppression** in p-Pb than p-p and Pb-p is observed.

$$CP(\Delta\Phi) = N_{\text{pair}}(\Delta\Phi)/N_{\text{trig}}.$$

$$N_{\text{pair}}(\Delta\Phi) = \int d\eta_{h_1} \int d\eta_{h_2} \int d\mathbf{p}_{h_1}^2 \int d\mathbf{p}_{h_2}^2 \frac{d\sigma^{pA \rightarrow h_1 h_2 X}}{d(\Delta\Phi) d\eta_{h_1} d\eta_{h_2} d\mathbf{p}_{h_1}^2 d\mathbf{p}_{h_2}^2}$$

$$N_{\text{trig}} = \int d\eta_{h_1} \int d\mathbf{p}_{h_1}^2 \frac{d\sigma^{pA \rightarrow h_1 X}}{d\eta_{h_1} d\mathbf{p}_{h_1}^2}$$

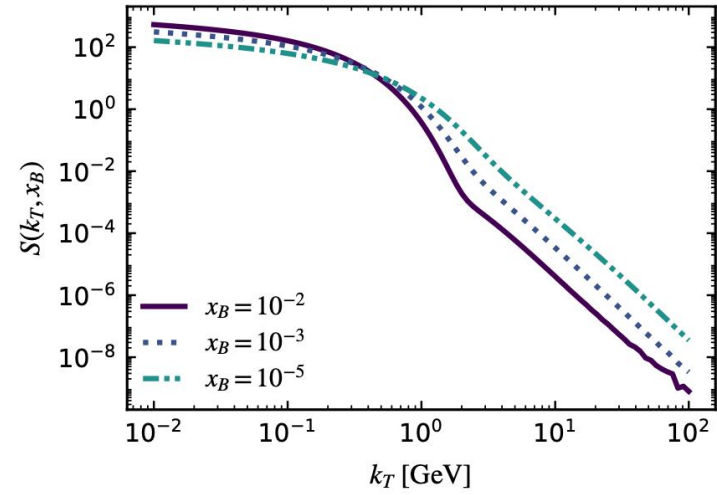
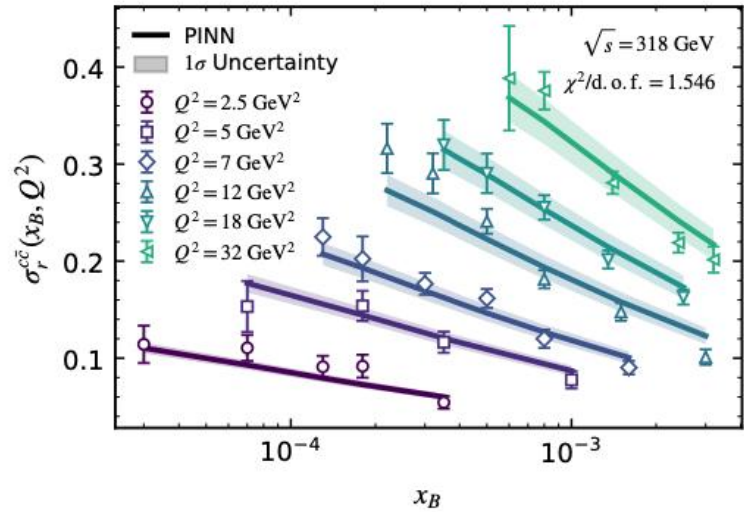
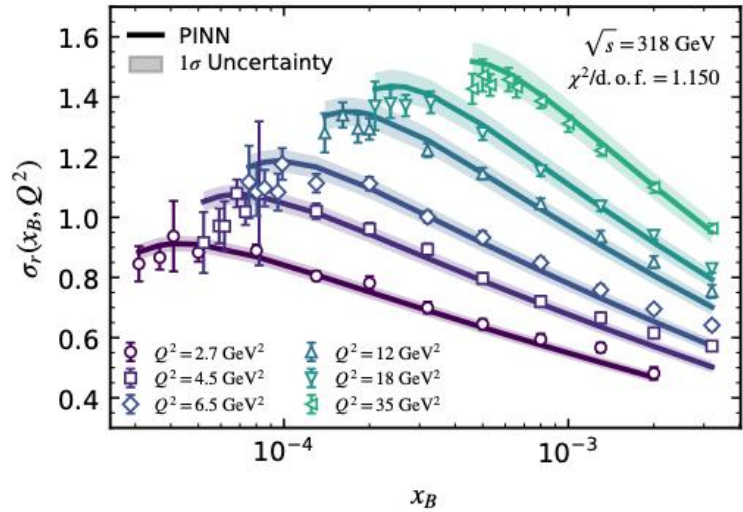
Area and Width Ratio between pPb, Pbp and p-p



- Width **ratio pPb/pp (or pPb/Pbp) > 1.4** at 1-2 GeV bin, larger than light hadron.
- Npdf doesn't affect the width, but slightly decreases the area.

Global Extraction of the Universal Dipole Amplitude

Physics-Informed Global Extraction of the Universal Dipole Amplitude



Loss function in the PINN $\mathcal{L}(\theta, \mathbf{p}) = w_1 \mathcal{L}_{\text{ciBK}} + w_2 \mathcal{L}_{\text{data}} + w_3 \mathcal{L}_{\text{phy}}$

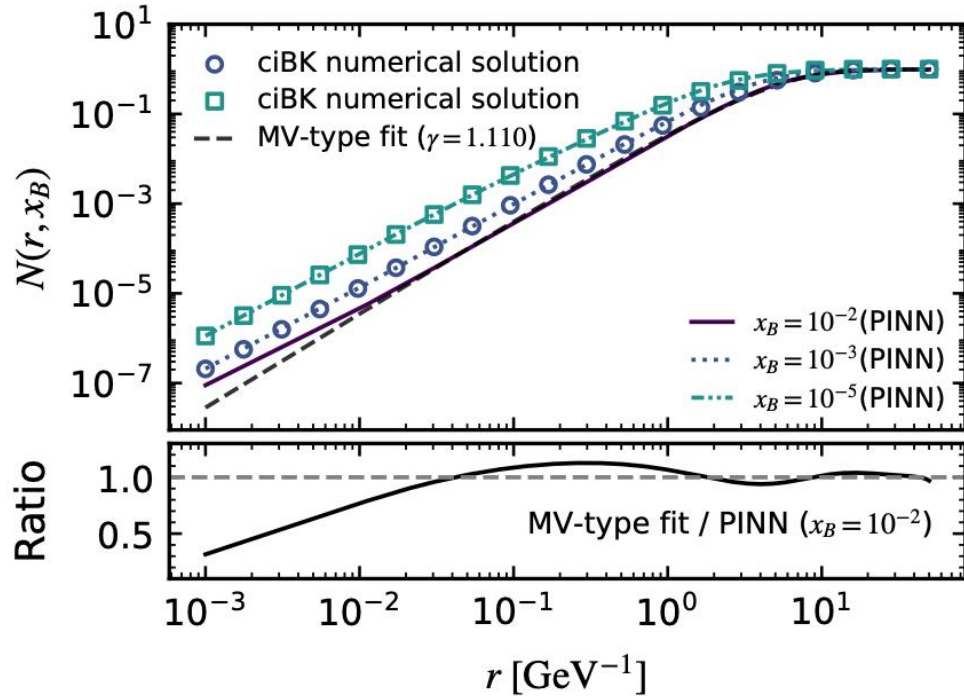
for ciBK evolution
quantifies agreement with data
additional physical constraints

- PINN extracts an **universal** dipole amplitude that constrained by the **collinearly improved Balitsky–Kovchegov**,
- and **simultaneously** constrained by the reduced **total** and **charm quark** DIS cross sections, exclusive J/ψ data, and the **positivity for the momentum-space amplitude**.

S. W. Dai, F. P. Li, L. G. Pang, G. Y. Qin, S. Y. Wei, H. Z. Zhang and W. Zhao, arXiv:2603.08008.

The dipole amplitude is available: <https://doi.org/10.5281/zenodo.18826120>

Physics-Informed Global Extraction of the Universal Dipole Amplitude

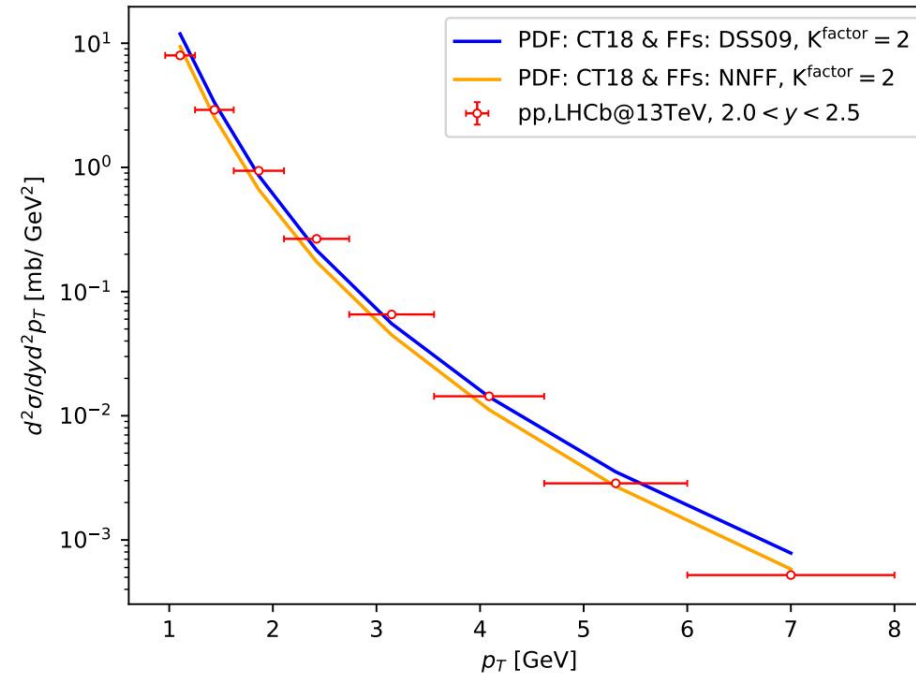
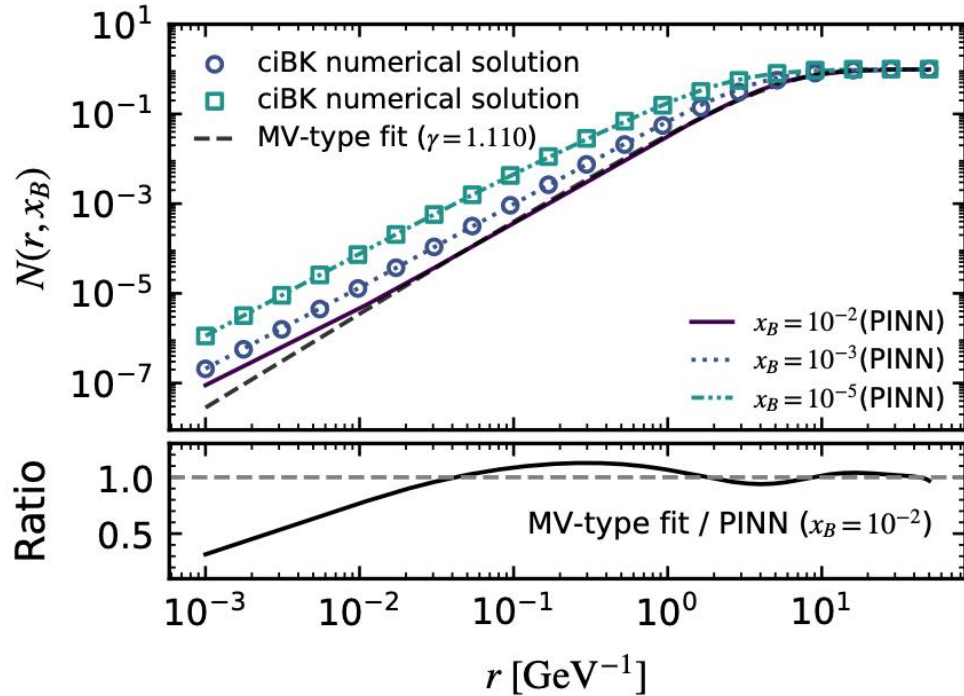


- **Without** imposing priori MV-type parametrization of initial condition.

S. W. Dai, F. P. Li, L. G. Pang, G. Y. Qin, S. Y. Wei, H. Z. Zhang and W. Zhao, arXiv:2603.08008.

The dipole amplitude is available: <https://doi.org/10.5281/zenodo.18826120>

Physics-Informed Global Extraction of the Universal Dipole Amplitude



- **Without** imposing priori MV-type parametrization of initial condition.
- PINN alleviates the tension between **total** and **charm channels**, and **positivity** for the momentum-space amplitude, and fit the **single inclusive p-p spectra**.

S. W. Dai, F. P. Li, L. G. Pang, G. Y. Qin, S. Y. Wei, H. Z. Zhang and W. Zhao, arXiv:2603.08008.

The dipole amplitude is available: <https://doi.org/10.5281/zenodo.18826120>

Summary

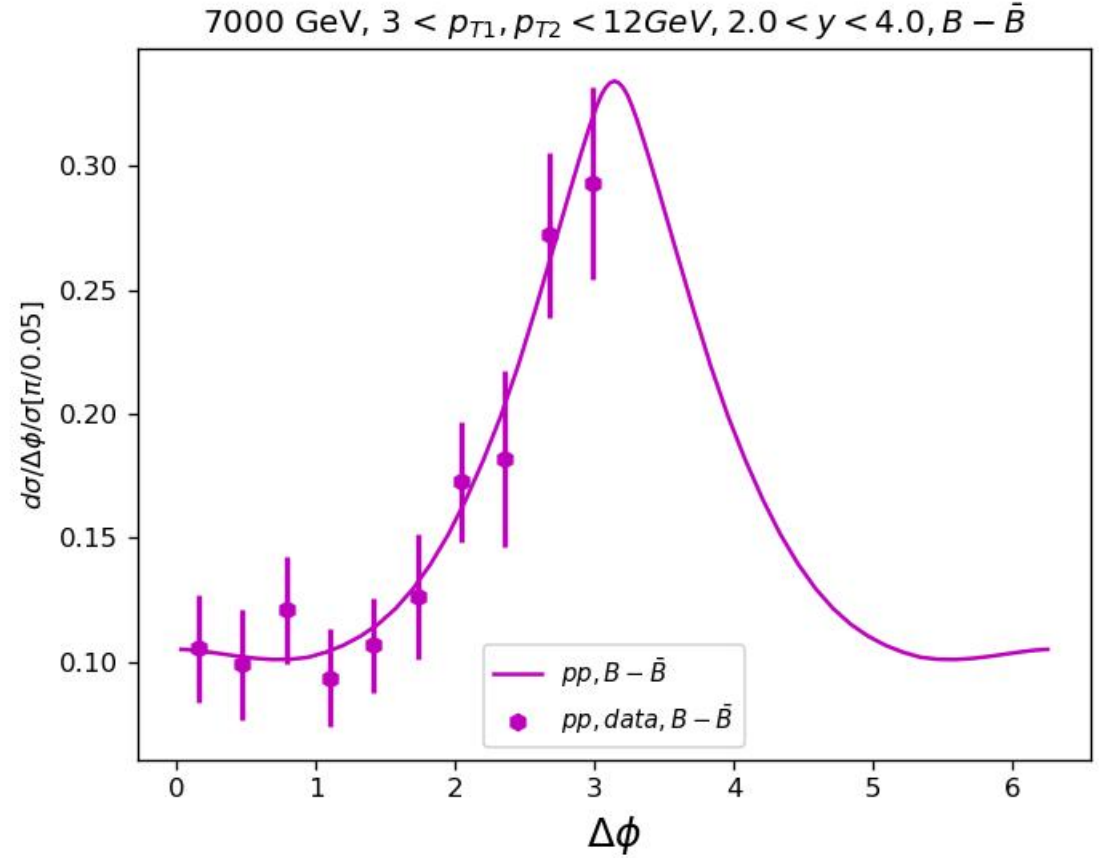
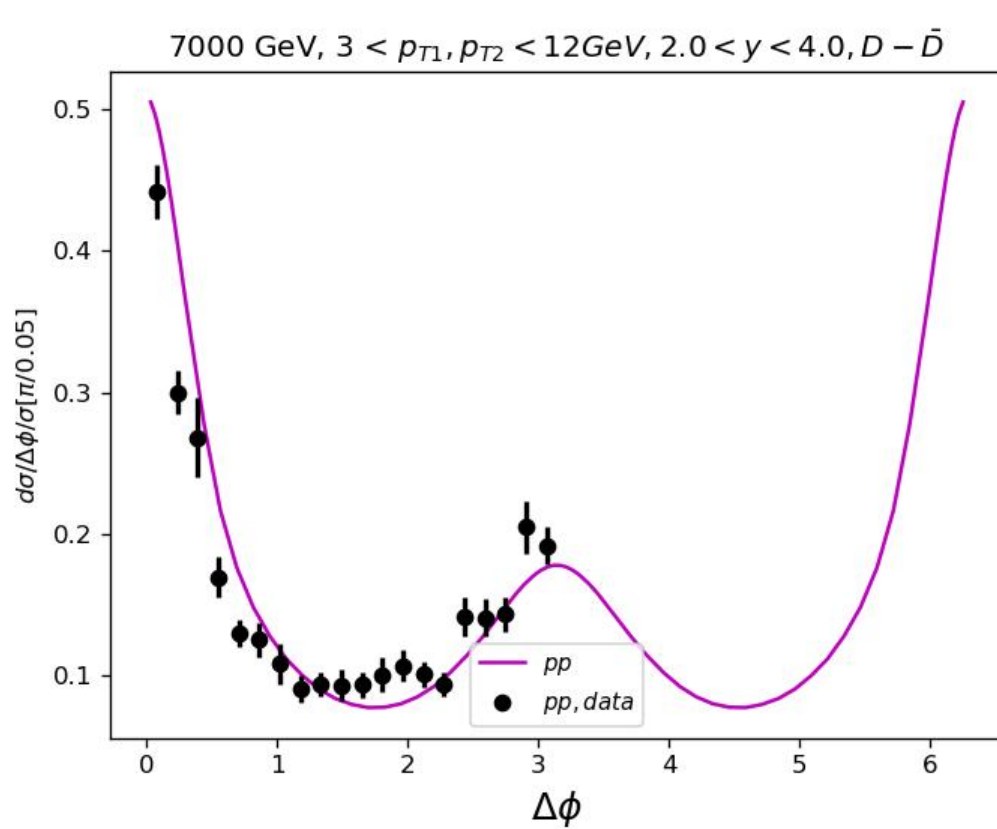
- The CGC model can reasonably reproduce the STAR data and predicts that suppression effects at the **LHC are weaker than STAR.**
- The CGC model provides a good description of both **di-heavy-flavor** and **single inclusive** production processes.
- The **neural network** method offers a novel approach to solving problems in the small-x regime.

Thanks for Your Attentions!

Back Up

Back Up

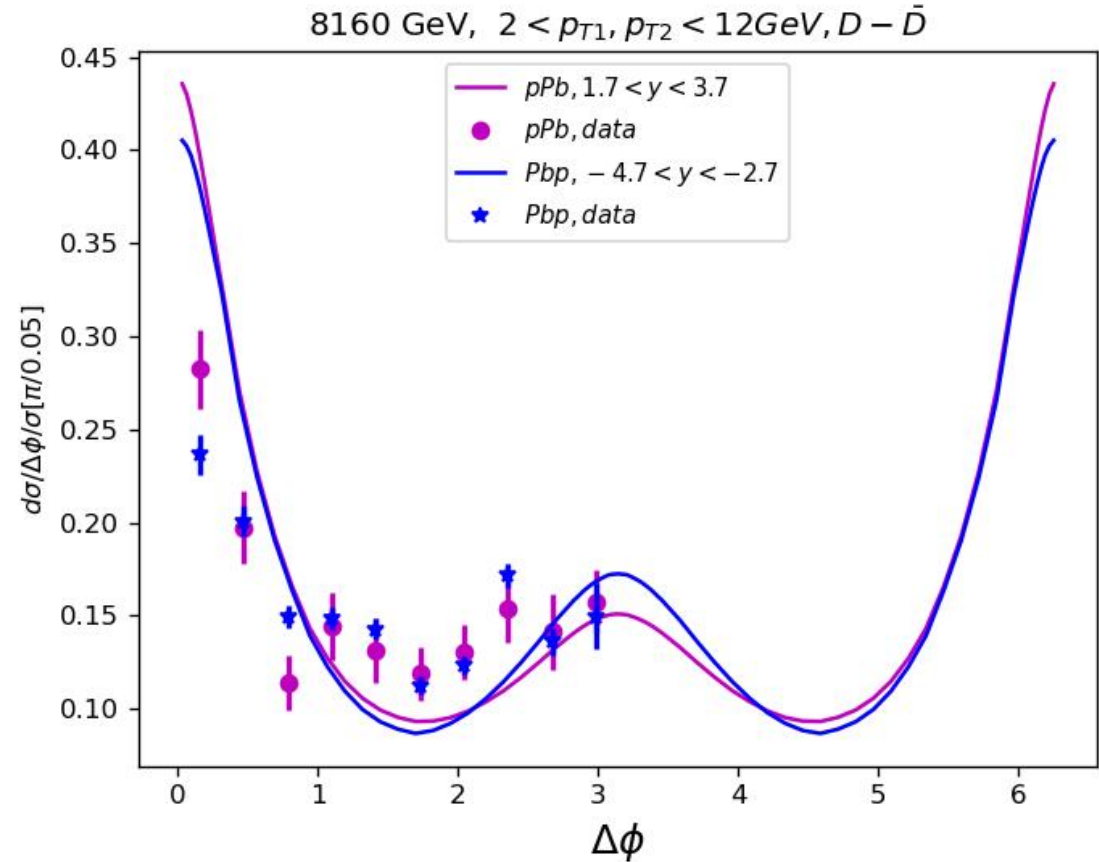
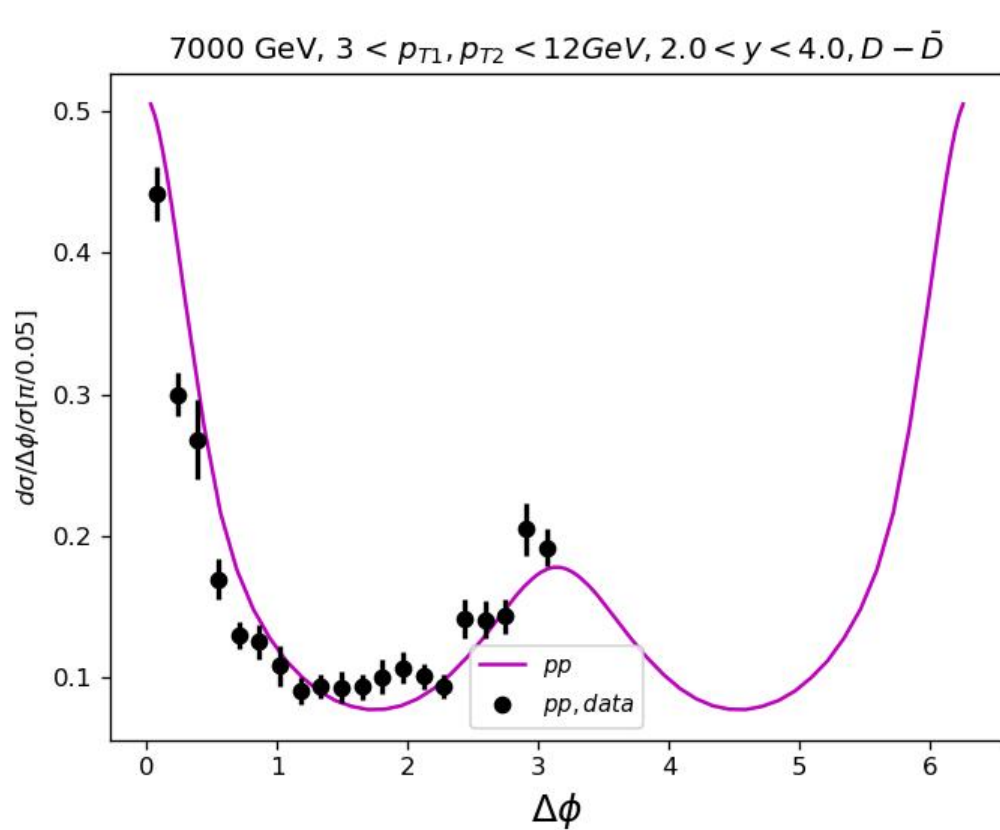
Dihadron Correlations for Heavy Flavour in p-p



- Well describe the B-B and D-D correlation in p-p with $\Delta\phi$ from 0 to 2π . **Parameter Free.**
- Clear “**Dead Cone**” effects in B-B correlations.

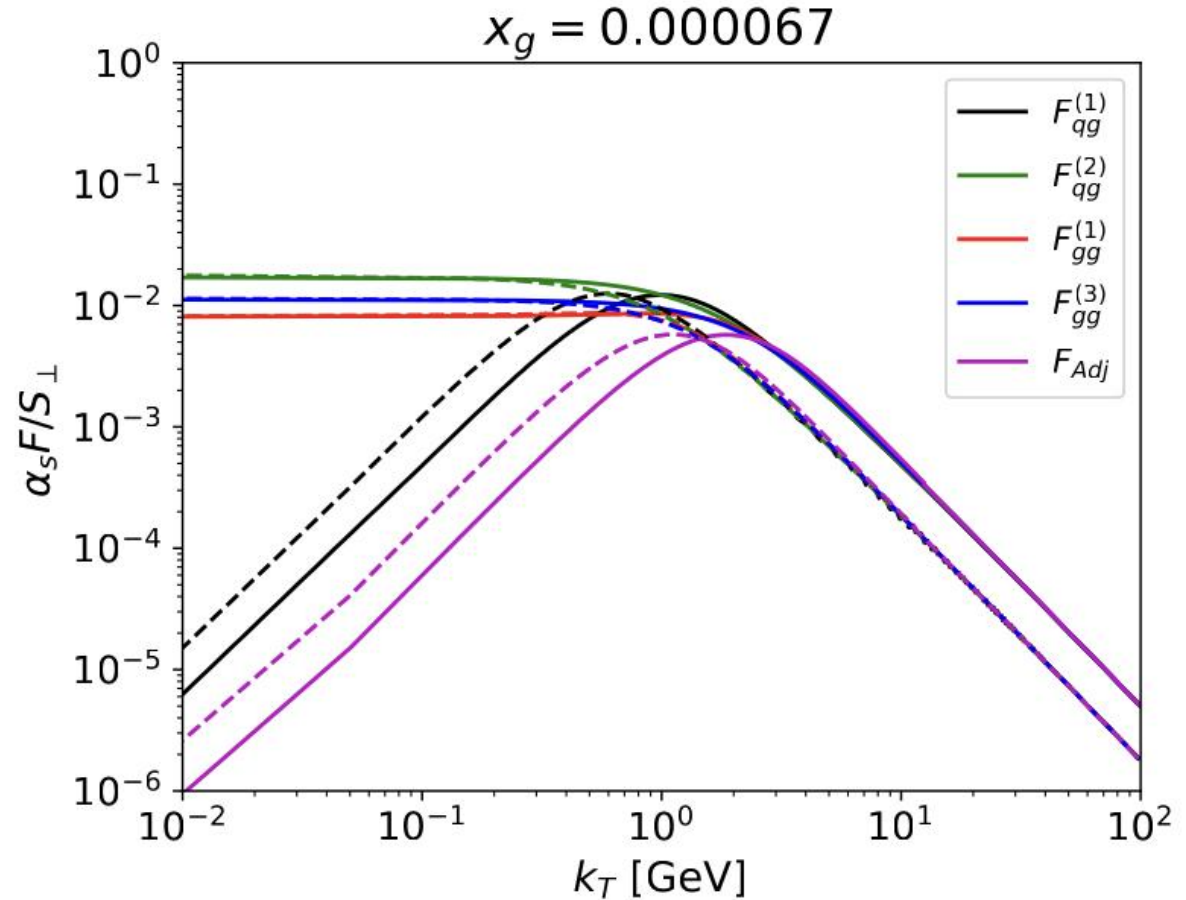
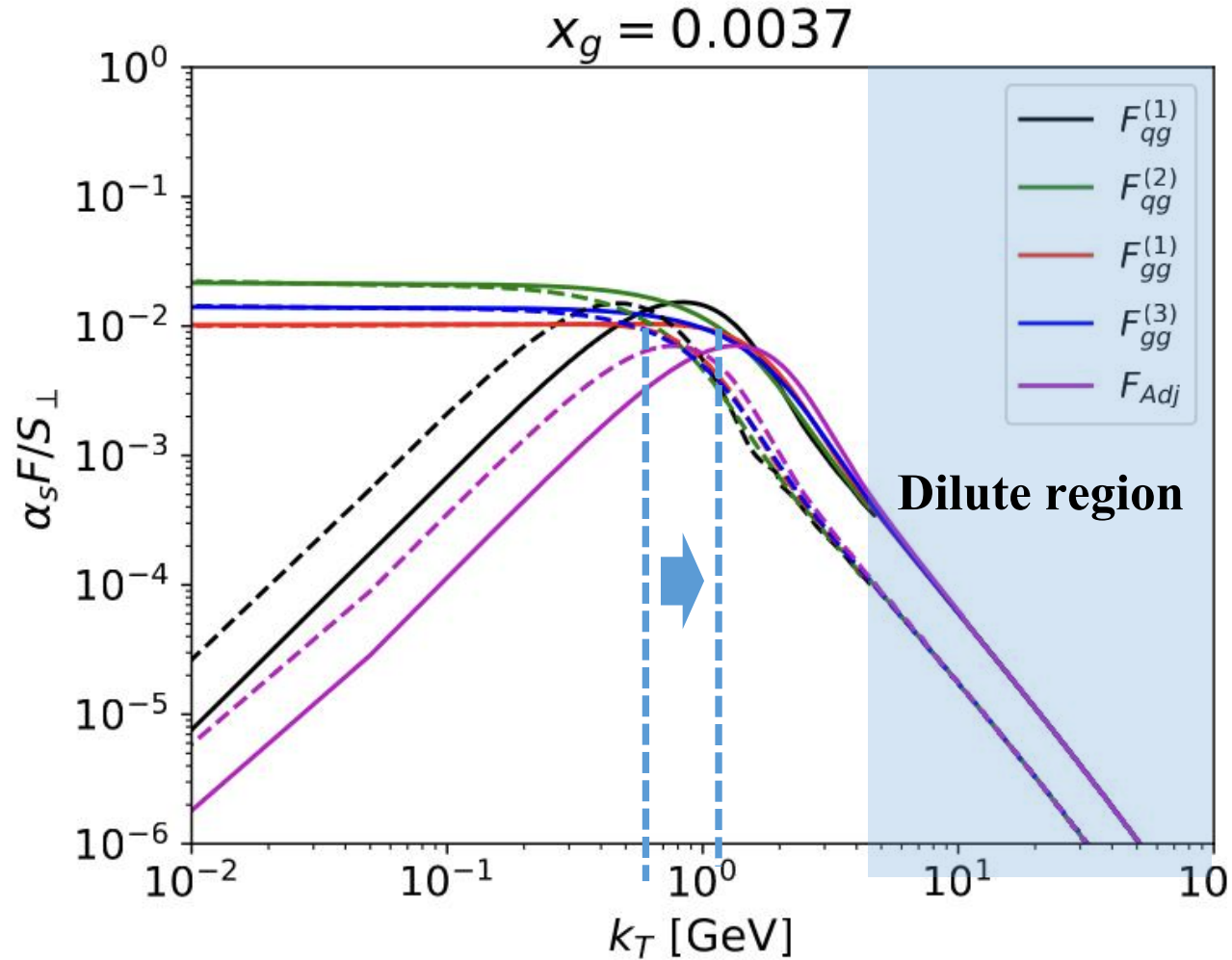
W. Zhao, etc, al. in progress.

Dihadron Correlations for Heavy Flavour in p-A and A-p



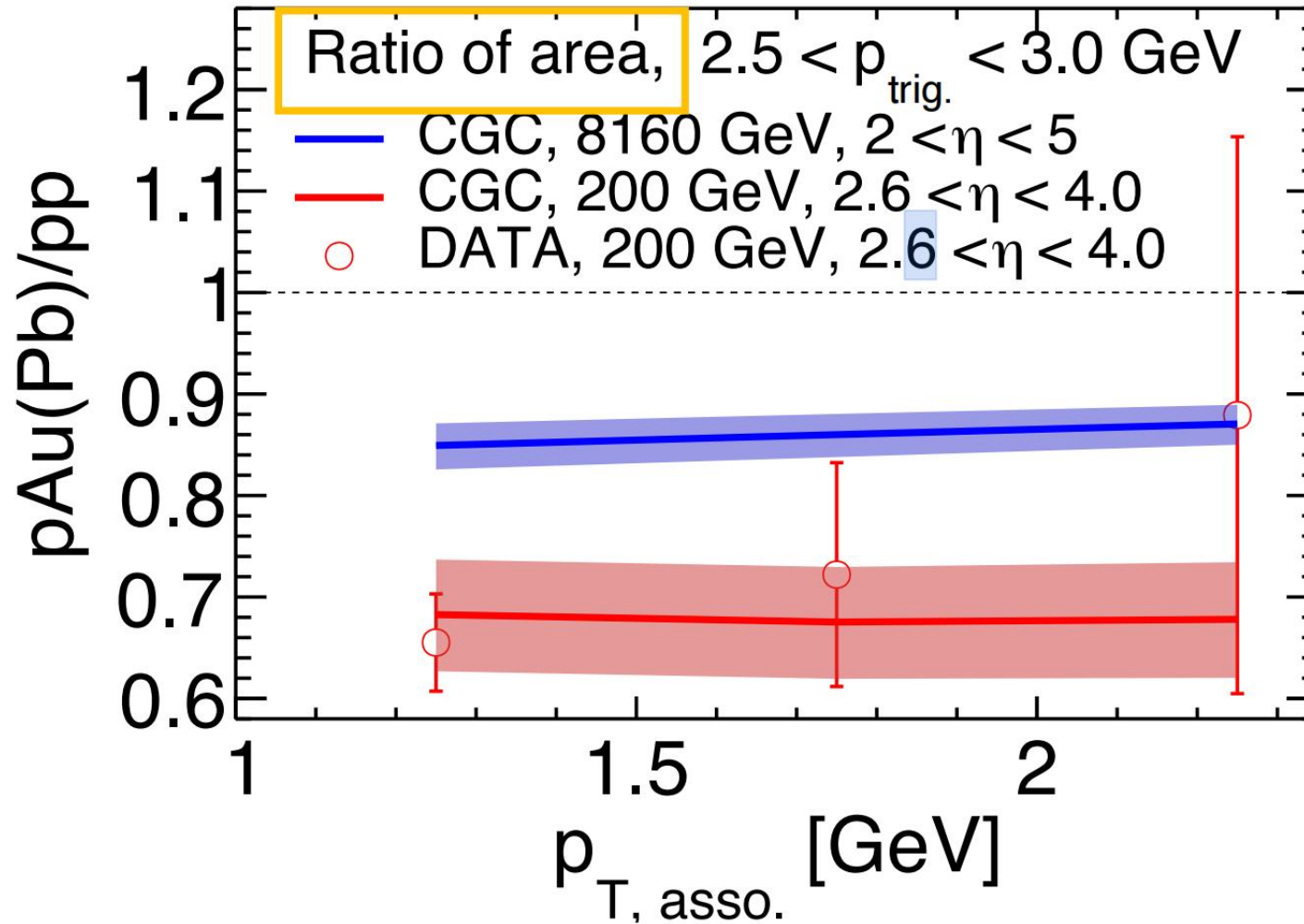
- Well describe the D-D correlation in p-Pb (Pb dense) and Pb-p (p dense) with **$\Delta\phi$ from 0 to 2π .**

TMDs



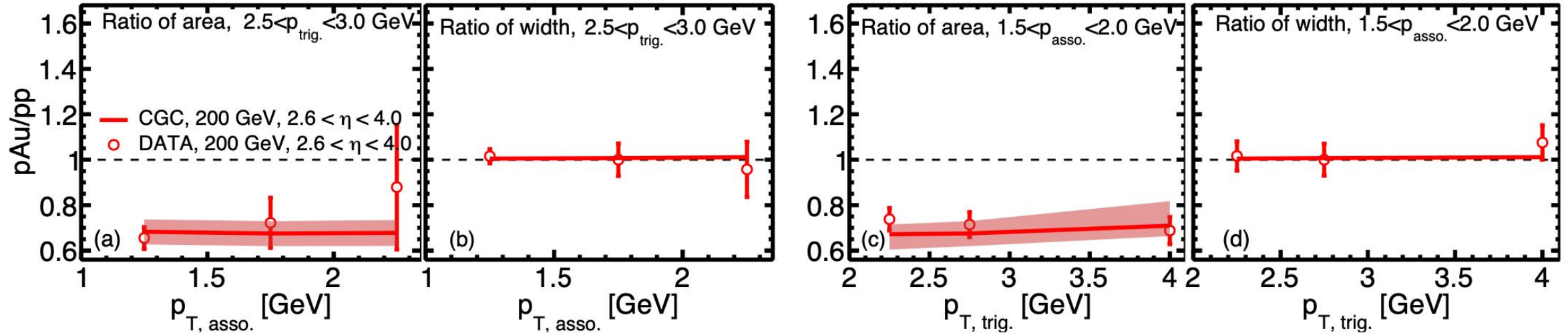
- Saturation scale moves to higher number from proton to nucleus.
- Saturation scale moves to higher number at smaller x_g .

Dihadron Correlations in LHCb



- Surprisingly, LHCb has the **smaller suppression** than STAR, even LHCb has smaller x_g .

Area ratio and width ratio between pAu and pp



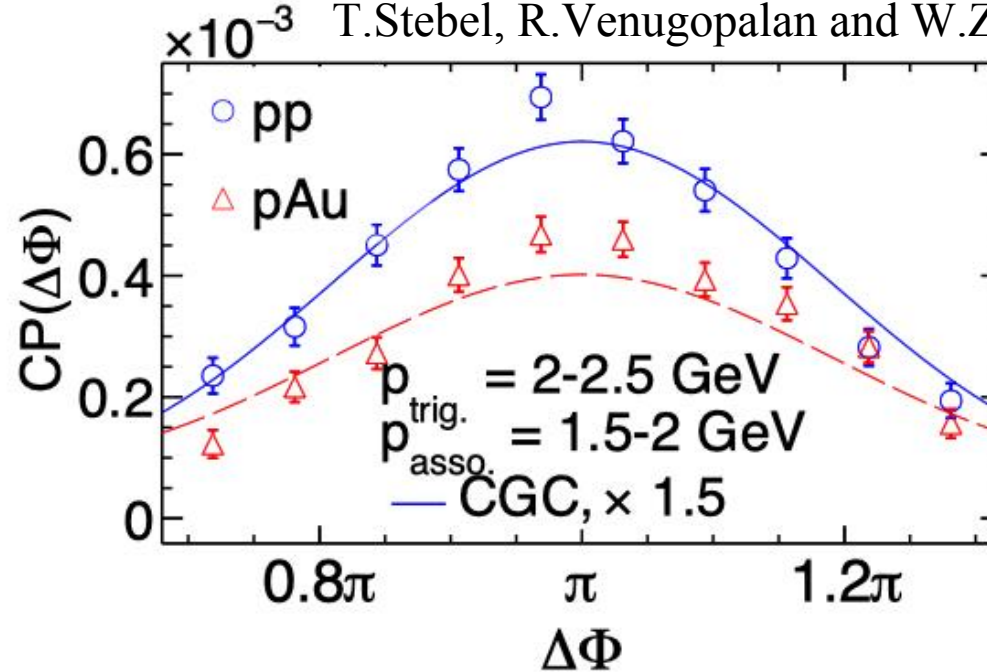
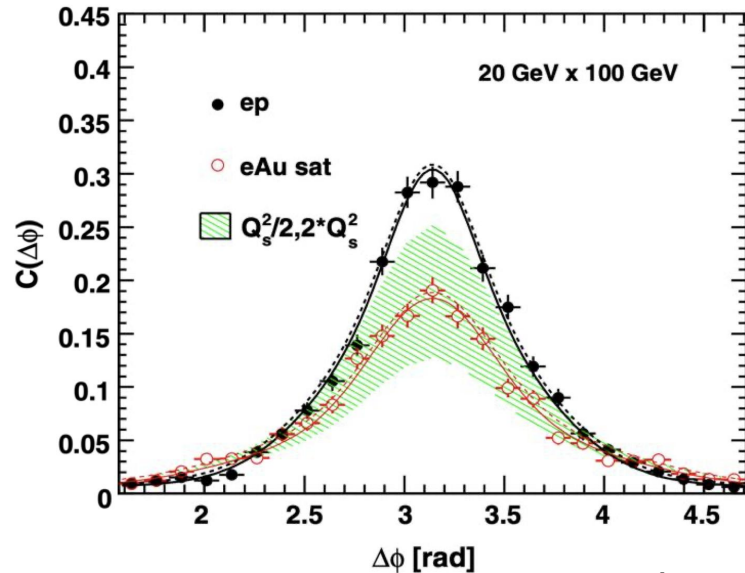
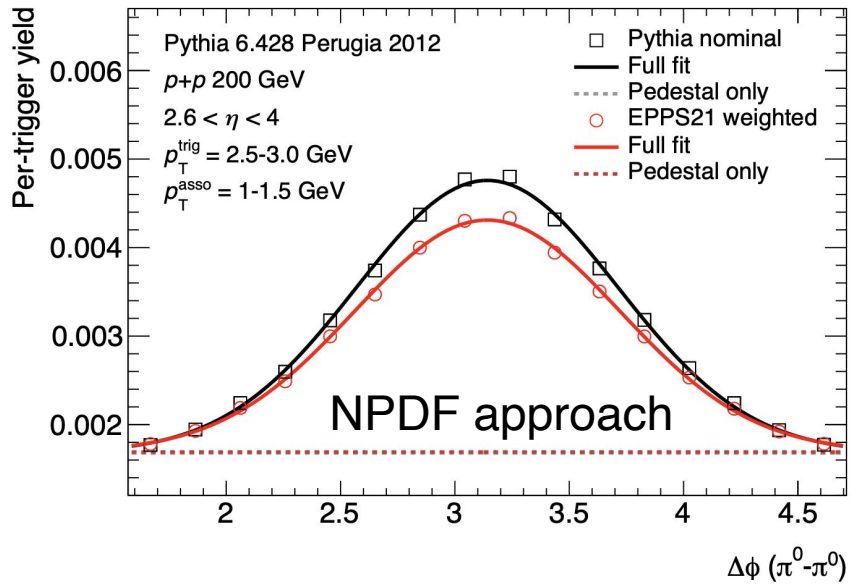
- CGC predicts very **weak p_T dependence** (as a function of associate or trigger p_T).
- The width ratio is very **close to 1, width is dominated by the Sudakov factor (or parton shower)**.

P. Caucal, Z. B.Kang, P. Korcyl, F. Salazar, B. Schenke, T.Stebel, R.Venugopalan and W.Zhao, [arXiv:2512.21466].
 STAR data: PhysRevLett.129.092501

NPDF and CGC results

P. Caucal, Z. B.Kang, P. Korcyl, F. Salazar, B. Schenke,
T.Stebel, R.Venugopalan and W.Zhao, [arXiv:2512.21466].

D. V. Perepelitsa, PRC.111.054901



- NPDF and CGC approaches have the similar results.
- EIC/UPC provide the **clean environment** for dihadron correlations

See also:

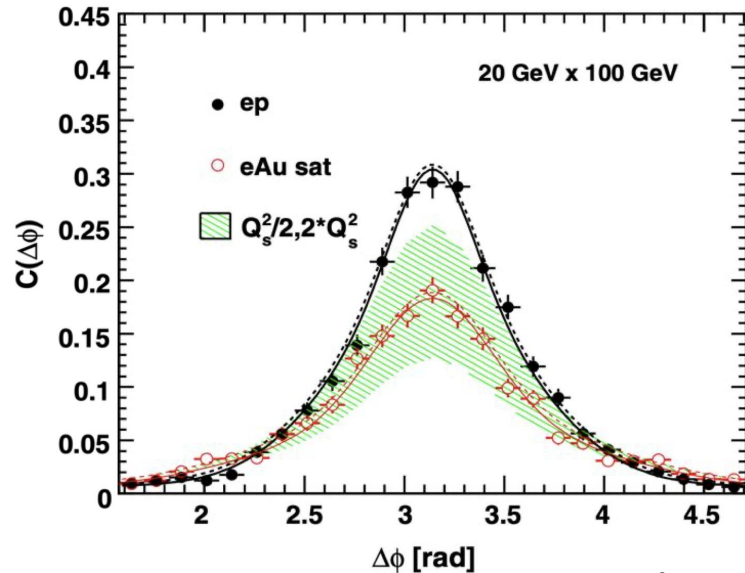
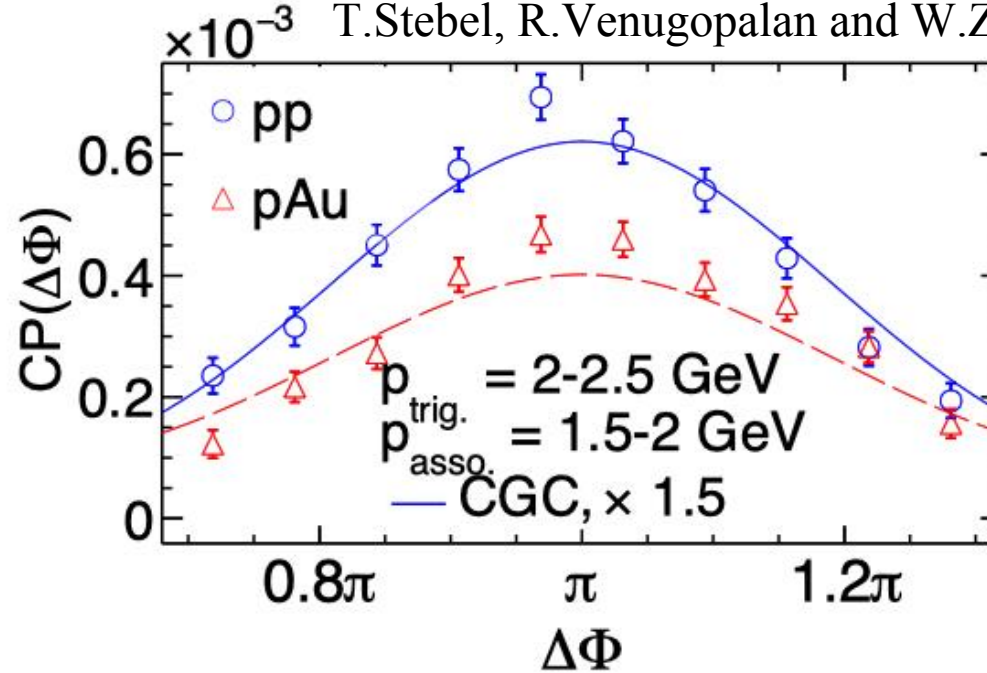
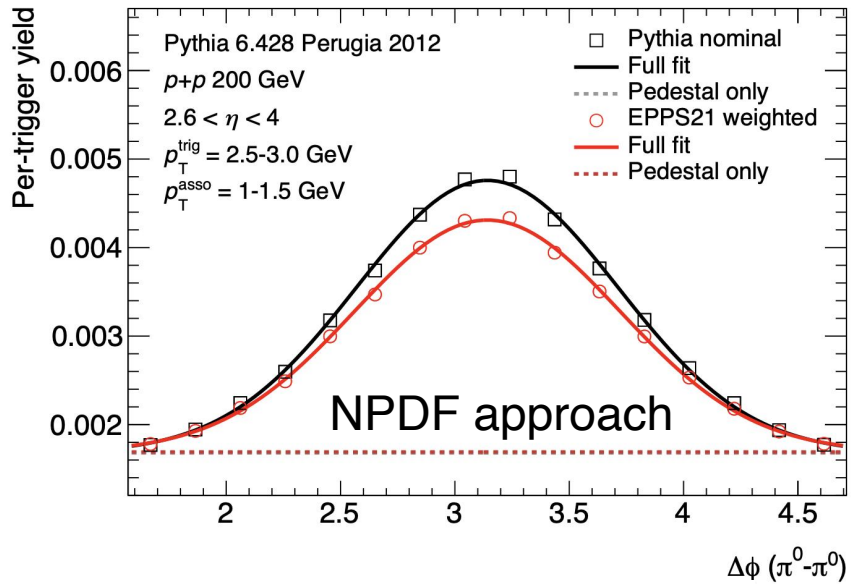
- J. L. Albacete and C. Marquet, Phys. Rev. Lett. 105, 162301 (2010)
- T. Lappi and H. Mantysaari, Nucl. Phys. 908, 51-72 (2013).
- van Hameren, etc, al. JHEP 12, 034 (2016).
- A. Stasto, etc. al, Phys. Lett. B 784, 301-306 (2018).
- J. L. Albacete, etc, al. Phys. Rev. D 99, 014002 (2019).

L. Zheng et al., PRD 89 (2014) 074037

NPDF and CGC results

P. Caucal, Z. B.Kang, P. Korcyl, F. Salazar, B. Schenke,
T.Stebel, R.Venugopalan and W.Zhao, [arXiv:2512.21466].

D. V. Perepelitsa, PRC.111.054901



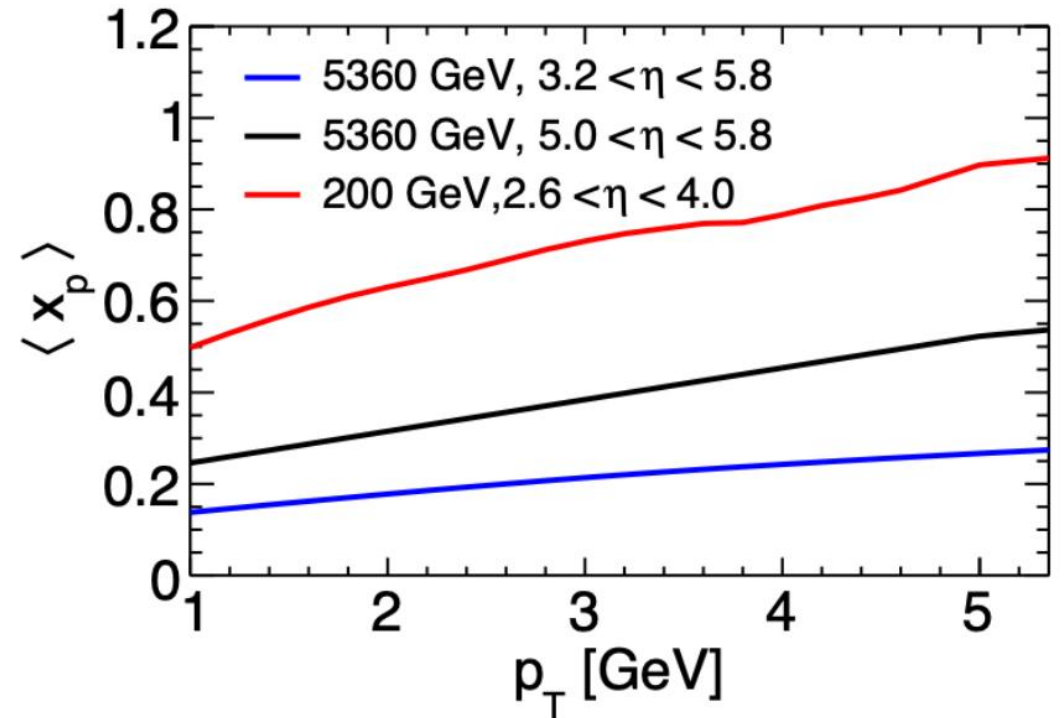
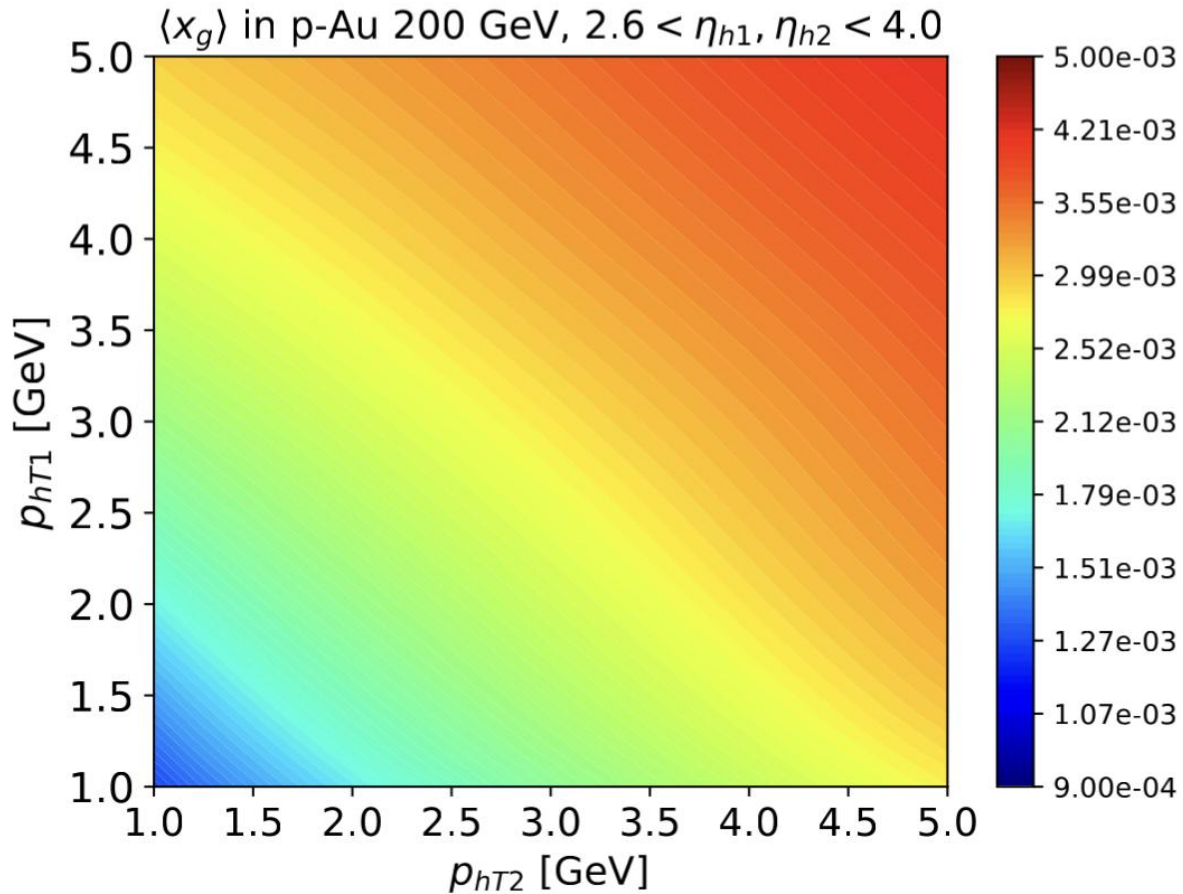
- NPDF and CGC approaches have the similar results.
- EIC/UPC provide the **clean environment** for dihadron correlations

See also:

- J. L. Albacete and C. Marquet, Phys. Rev. Lett. 105, 162301 (2010)
- T. Lappi and H. Mantysaari, Nucl. Phys. 908, 51-72 (2013).
- van Hameren, etc, al. JHEP 12, 034 (2016).
- A. Stasto, etc. al, Phys. Lett. B 784, 301-306 (2018).
- J. L. Albacete, etc, al. Phys. Rev. D 99, 014002 (2019). 34

L. Zheng et al., PRD 89 (2014) 074037

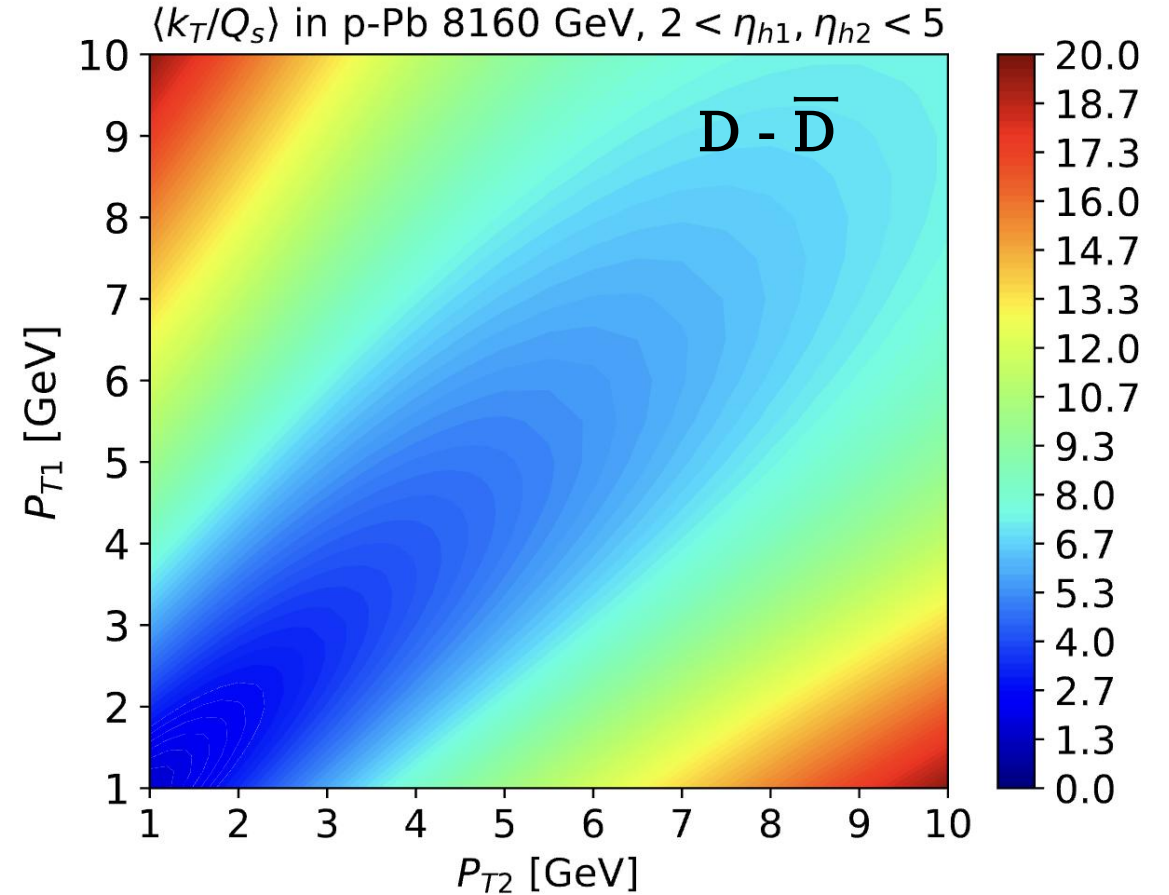
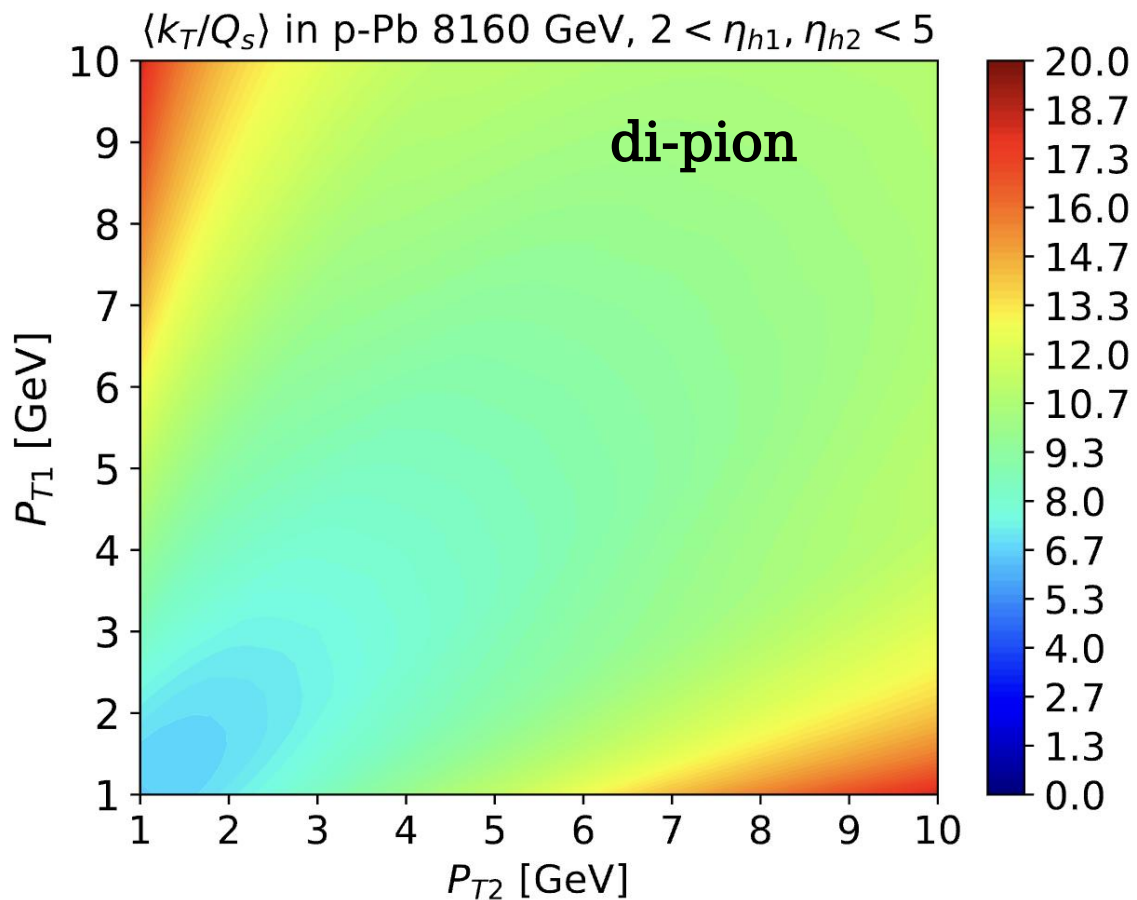
Dihadron Correlations in Forward pp and pA collisions



P. Caucal, Z. B.Kang, P. Korcyl, F. Salazar, B. Schenke, T.Stebel, R.Venugopalan and W.Zhao, [arXiv:2512.21466]

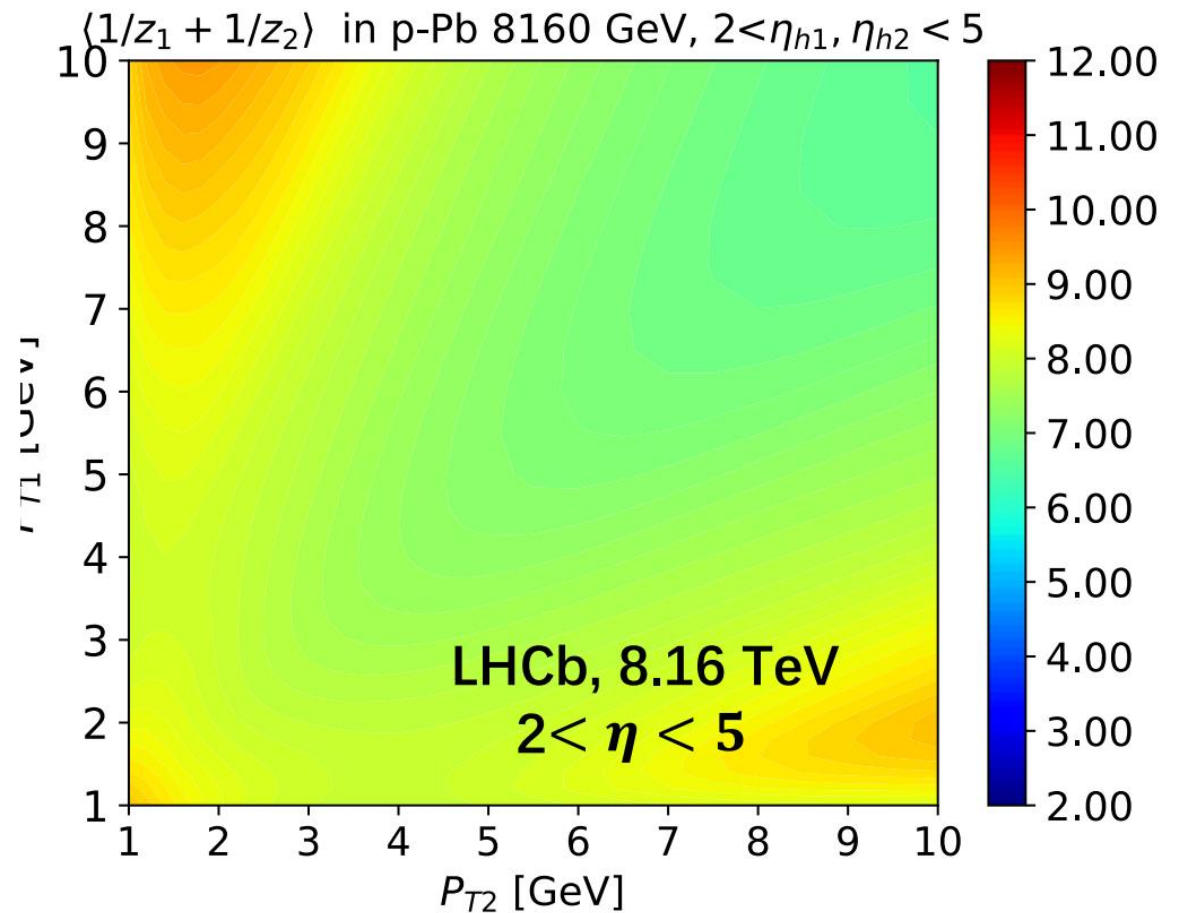
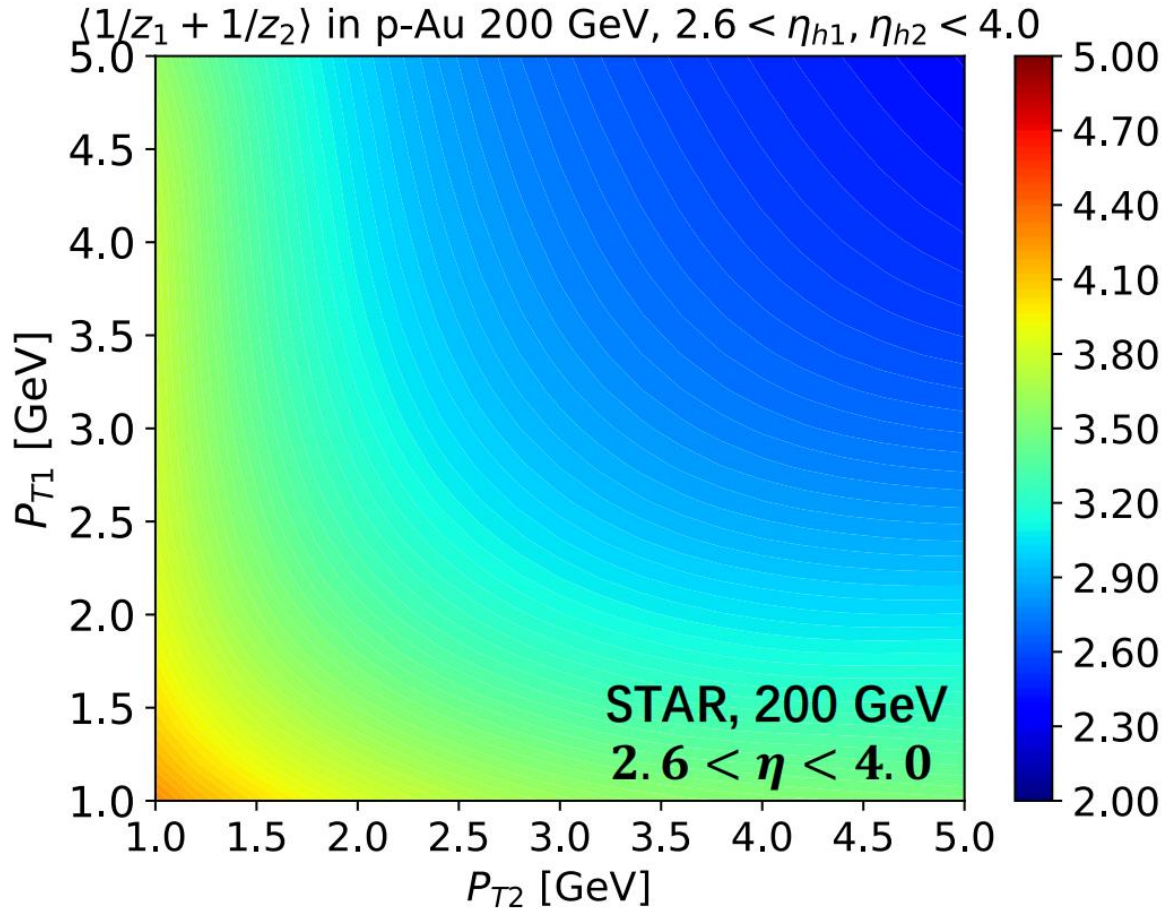
- $\langle x_g \rangle$ probed by di-hadron at STAR is small.
- $\langle x_p \rangle$ probed by di-hadron at STAR is large.

$\langle k_T/Q_s \rangle$ probed by light and heavy meson at LHCb



- $\langle k_T/Q_s \rangle$ probed by di-D meson **is much smaller than that by light hadrons.**

Fragmentation fraction probed by STAR and LHCb

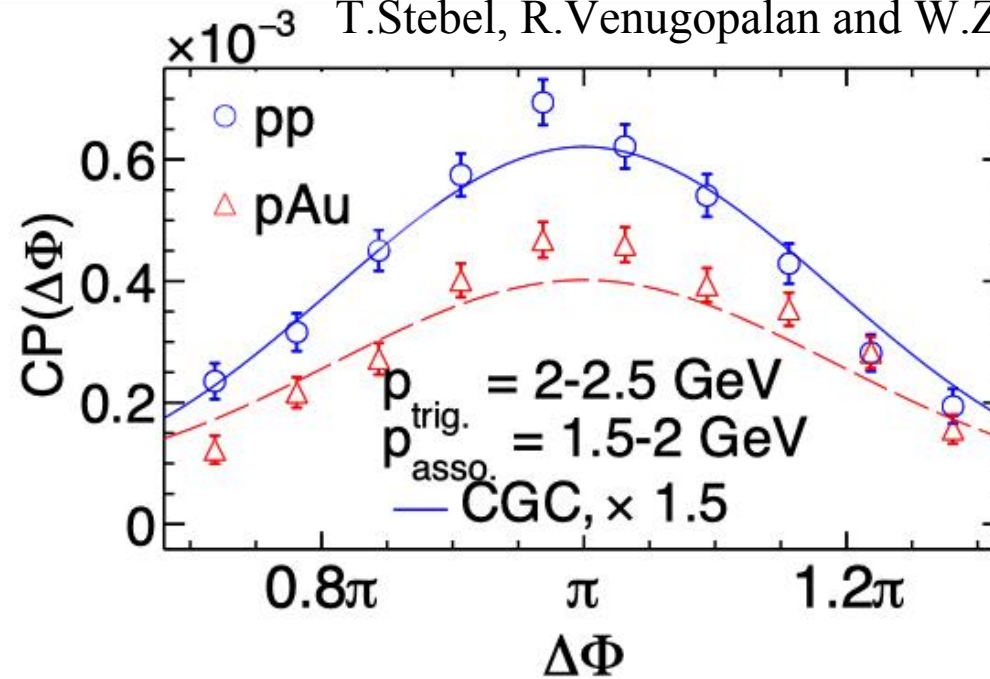
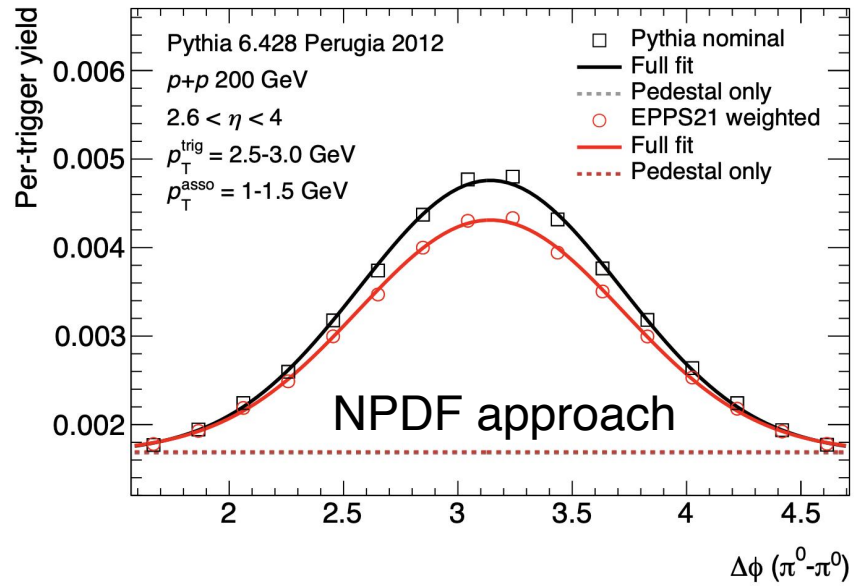


- STAR has much smaller $\langle 1/z_1 + 1/z_2 \rangle$, or **larger** $\langle z \rangle$, than that at LHCb.

NPDF and CGC results

P. Caucal, Z. B.Kang, P. Korcyl, F. Salazar, B. Schenke,
T.Stebel, R.Venugopalan and W.Zhao, [arXiv:2512.21466].

D. V. Perepelitsa, PRC.111.054901



- NPDF and CGC approaches have the similar results.

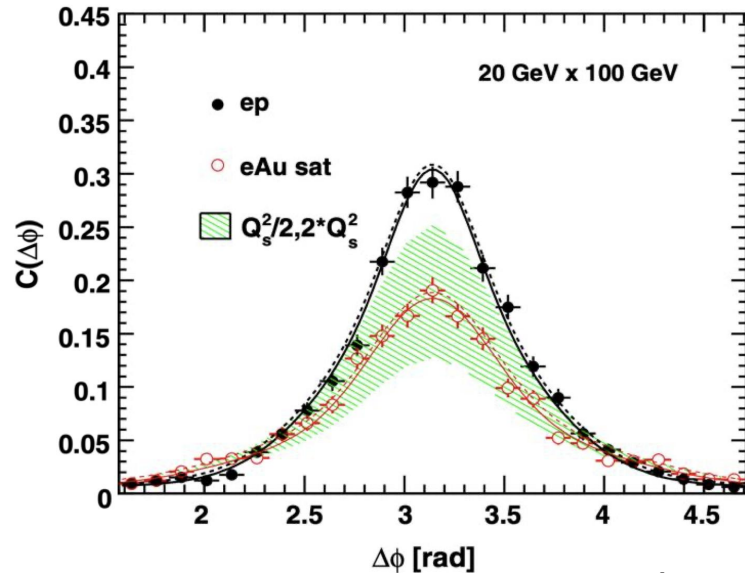
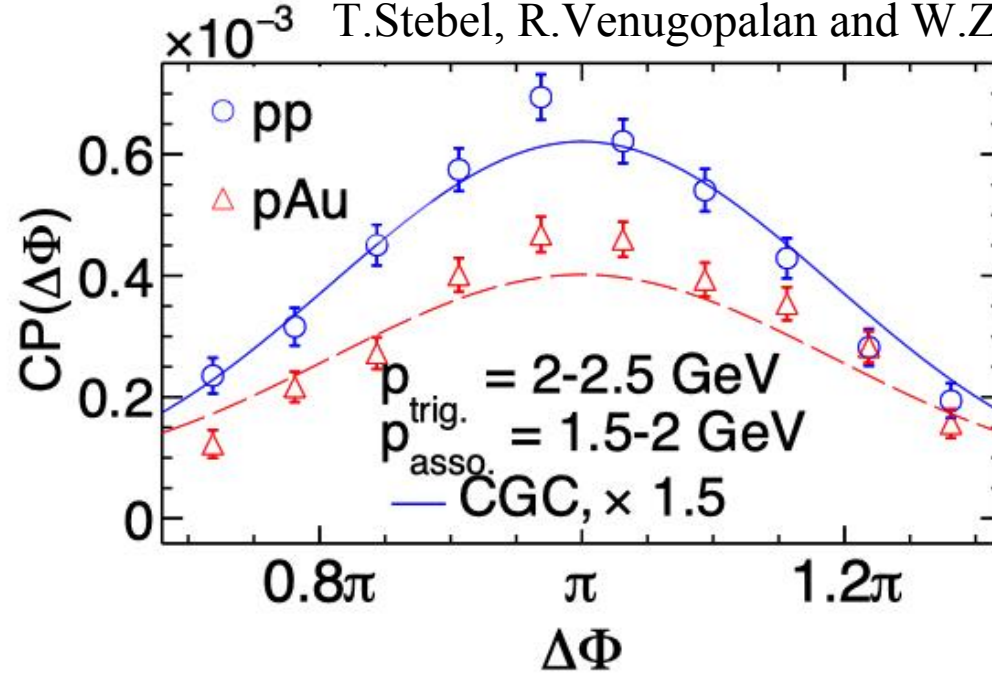
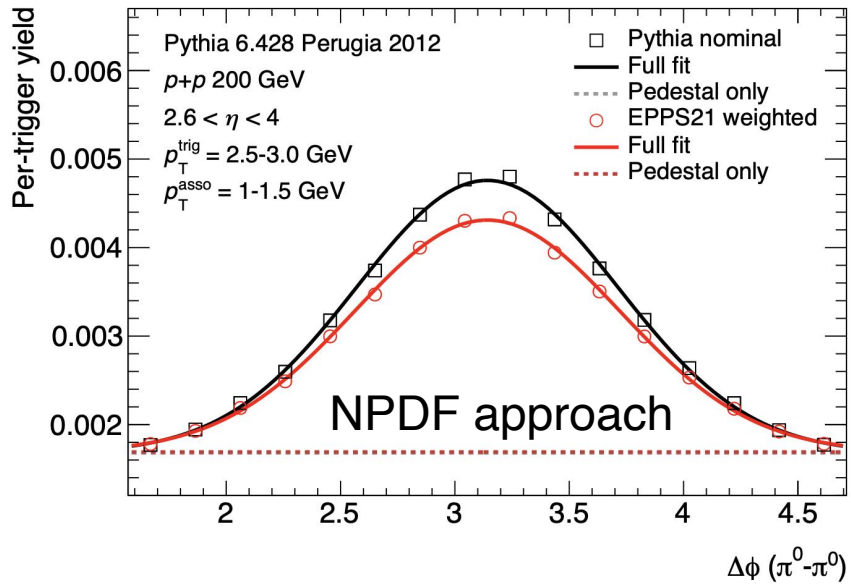
See also:

- J. L. Albacete and C. Marquet, Phys. Rev. Lett. 105, 162301 (2010)
- T. Lappi and H. Mantysaari, Nucl. Phys. 908, 51-72 (2013).
- van Hameren, etc, al. JHEP 12, 034 (2016).
- A. Stasto, etc. al, Phys. Lett. B 784, 301-306 (2018).
- J. L. Albacete, etc, al. Phys. Rev. D 99, 014002 (2019). 38

NPDF and CGC results

P. Caucal, Z. B.Kang, P. Korcyl, F. Salazar, B. Schenke,
T.Stebel, R.Venugopalan and W.Zhao, [arXiv:2512.21466].

D. V. Perepelitsa, PRC.111.054901



- NPDF and CGC approaches have the similar results.
- EIC/UPC provide the **clean environment** for dihadron correlations

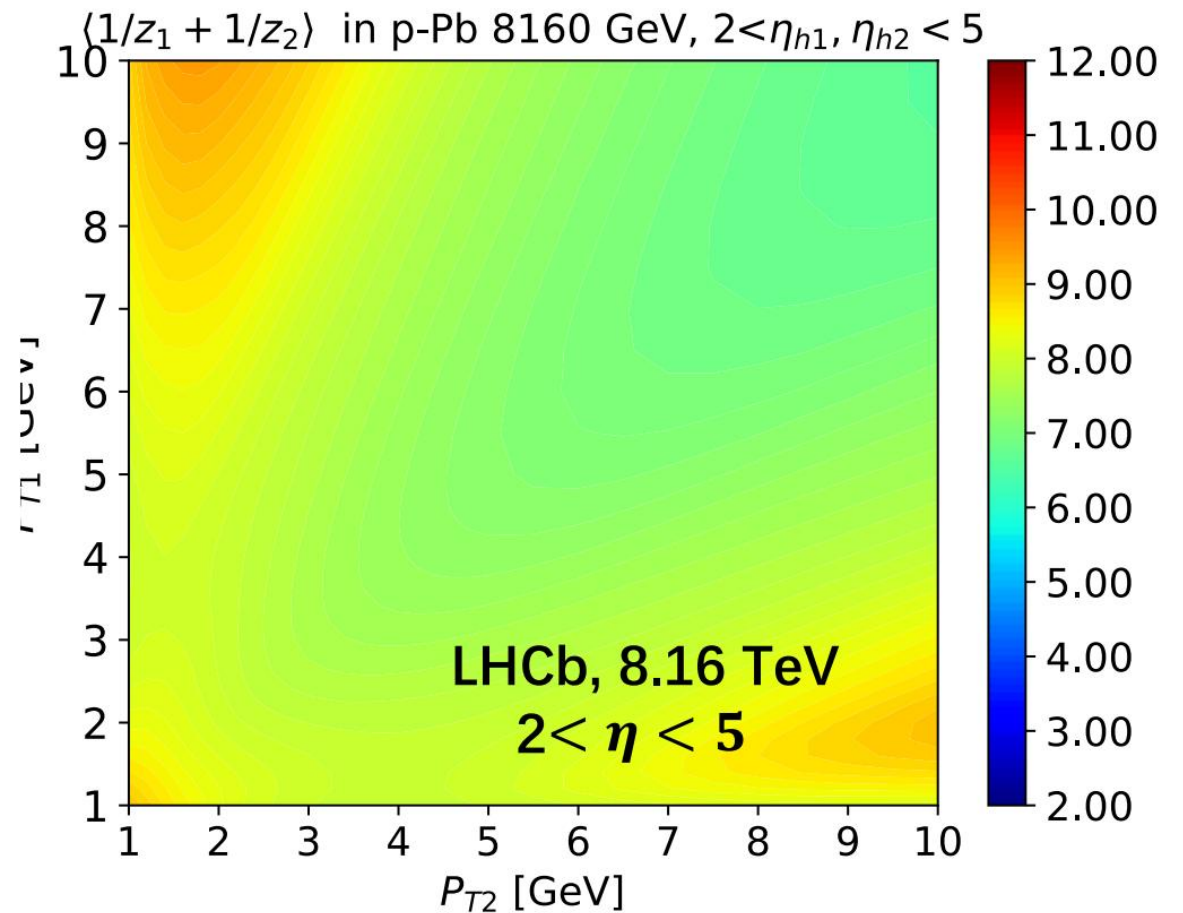
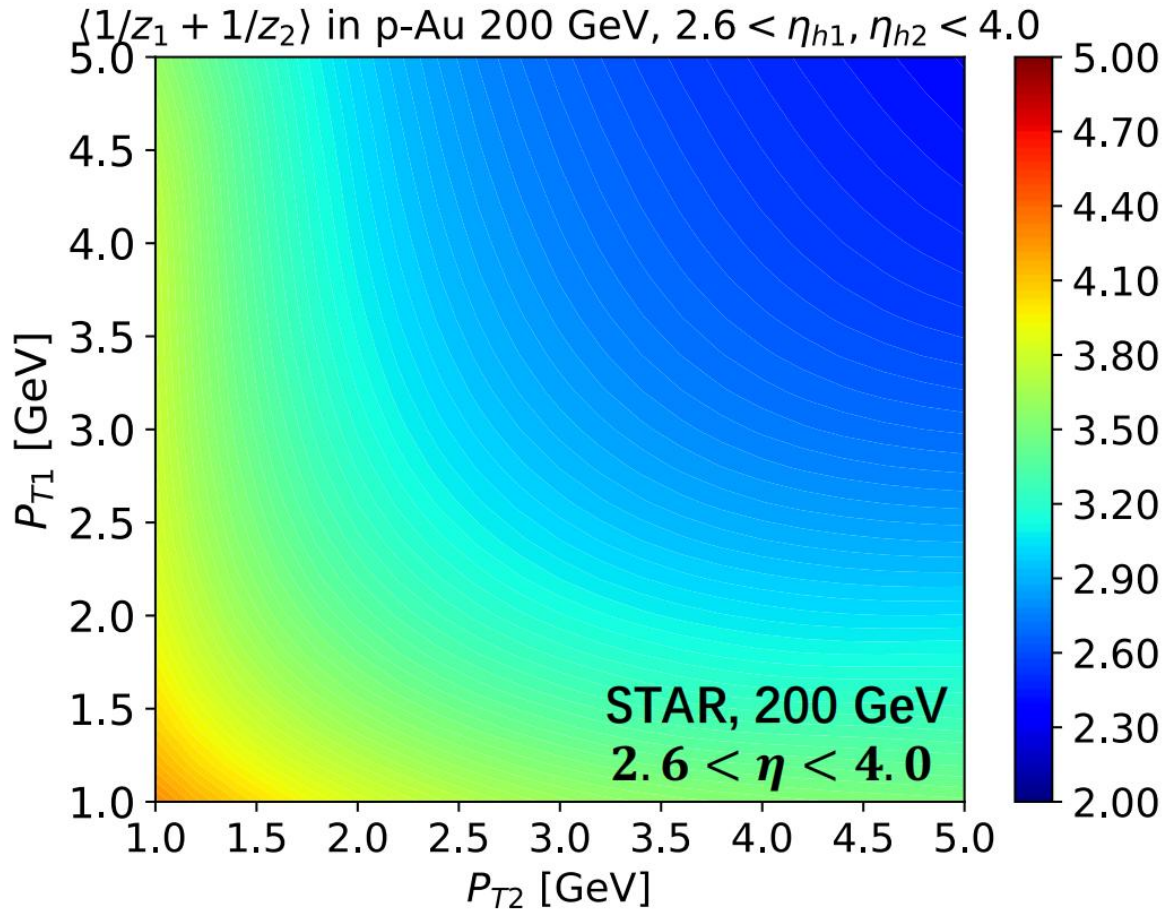
See also:

- J. L. Albacete and C. Marquet, Phys. Rev. Lett. 105, 162301 (2010)
- T. Lappi and H. Mantysaari, Nucl. Phys. 908, 51-72 (2013).
- van Hameren, etc, al. JHEP 12, 034 (2016).
- A. Stasto, etc. al, Phys. Lett. B 784, 301-306 (2018).
- J. L. Albacete, etc, al. Phys. Rev. D 99, 014002 (2019). 39

L. Zheng et al., PRD 89 (2014) 074037

CGC + Pythia8

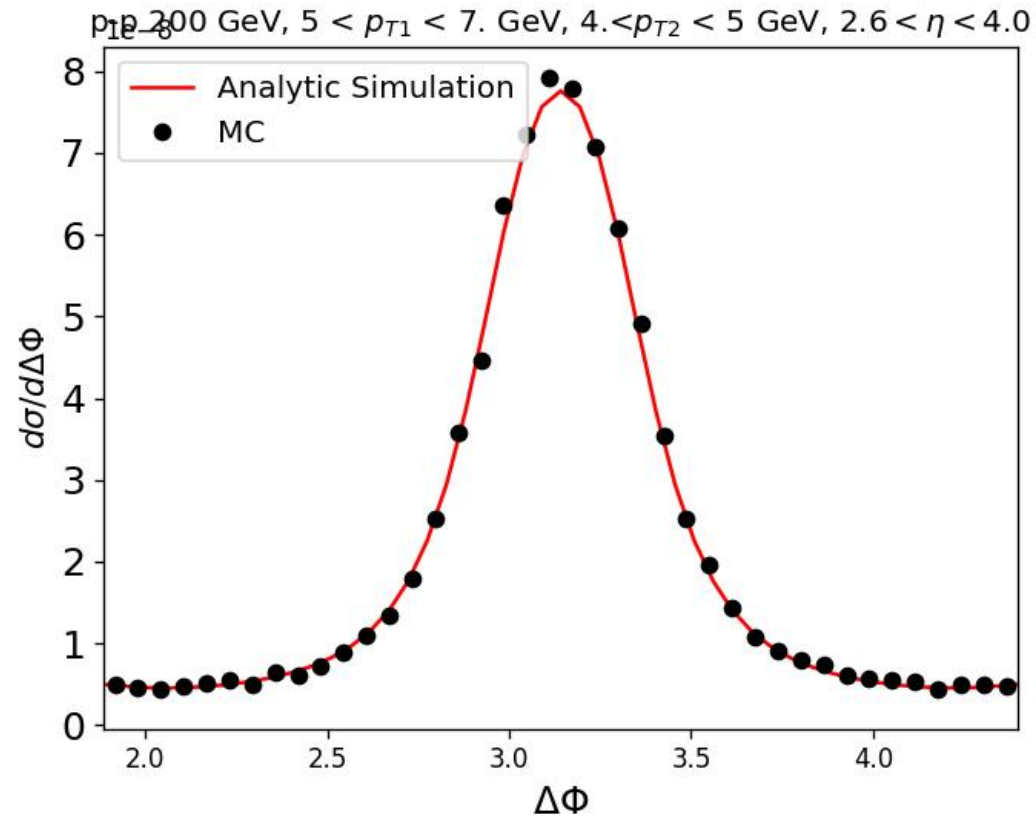
Fragmentation fraction probed by STAR and LHCb



- STAR has much smaller $\langle 1/z_1 + 1/z_2 \rangle$, or **larger** $\langle z \rangle$, than that at LHCb.

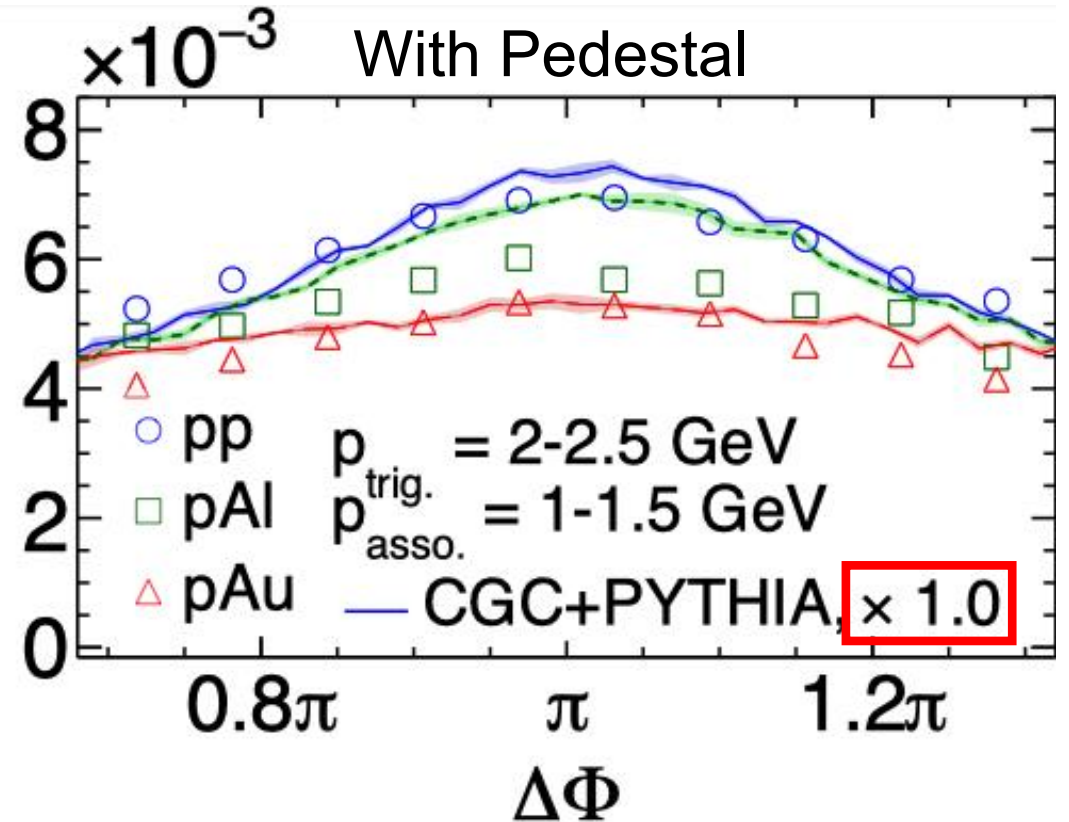
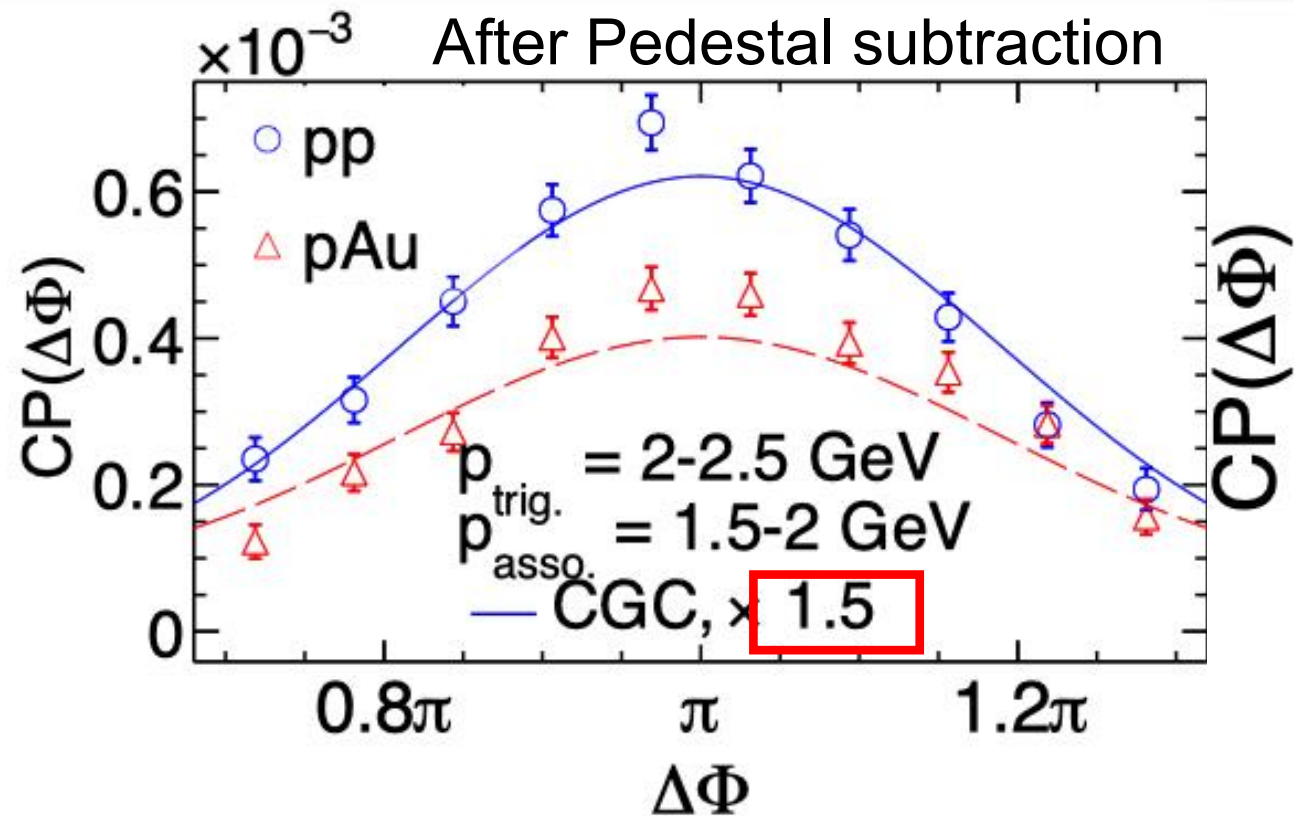
CGC + Pythia

- We sample the partons calculated by the CGC model, without FF or Sudakov factors. Then connect to PYTHIA for the parton shower and string fragmentation.



Compare between the Monte Carlo sample and semi-analytic calculations.

CGC + Pythia



- CGC+Pythia (similar to an event generator) might help to describe the data with the pedestal.
- CGC+Pythia might help to describe the data without additional factor.

TMD gluon distributions

$$\alpha_s \mathcal{F}_{qg}^{(1)}(\mathbf{k}_\perp, x) = \frac{N_c S_\perp}{2\pi^2} \int \frac{r_\perp dr_\perp}{2\pi} J_0(k_\perp r_\perp) \nabla_\perp^2 [1 - S(r_\perp, x)]$$

$$\alpha_s \mathcal{F}_{qg}^{(2)}(\mathbf{k}_\perp, x) = \frac{C_F S_\perp}{2\pi^2} \int \frac{r_\perp dr_\perp}{2\pi} J_0(k_\perp r_\perp) \mathcal{K}(r_\perp, x) \left[1 - (S(r_\perp, x))^{N_c/C_F} \right] S(r_\perp, x)$$

$$\alpha_s \mathcal{F}_{gg}^{(1)}(\mathbf{k}_\perp, x) = \frac{N_c S_\perp}{2\pi^2} \int \frac{r_\perp dr_\perp}{2\pi} J_0(k_\perp r_\perp) S(r_\perp, x) \nabla_\perp^2 [1 - S(r_\perp, x)]$$

$$\alpha_s \mathcal{F}_{gg}^{(2)}(\mathbf{k}_\perp, x) = \alpha_s \mathcal{F}_{gg}^{(1)}(\mathbf{k}_\perp, x) - \alpha_s \mathcal{F}_{adj}(\mathbf{k}_\perp, x)$$

$$\alpha_s \mathcal{F}_{gg}^{(3)}(\mathbf{k}_\perp, x) = \frac{C_F S_\perp}{2\pi^2} \int \frac{r_\perp dr_\perp}{2\pi} J_0(k_\perp r_\perp) \mathcal{K}(r_\perp, x) \left[1 - (S(r_\perp, x))^{N_c/C_F} \right] (S(r_\perp, x))^2$$

$$\alpha_s \mathcal{F}_{adj}(\mathbf{k}_\perp, x) = \frac{C_F S_\perp}{2\pi^2} \int \frac{r_\perp dr_\perp}{2\pi} J_0(k_\perp r_\perp) \nabla_\perp^2 \left[1 - (S(r_\perp, x))^{N_c/C_F} \right]$$

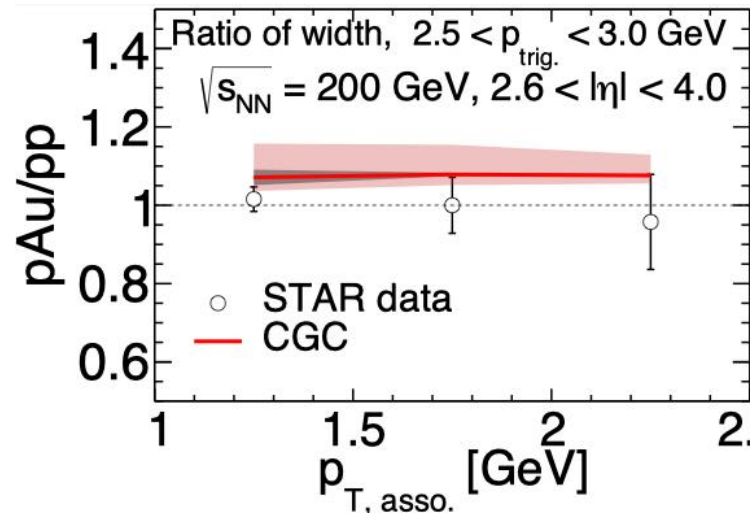
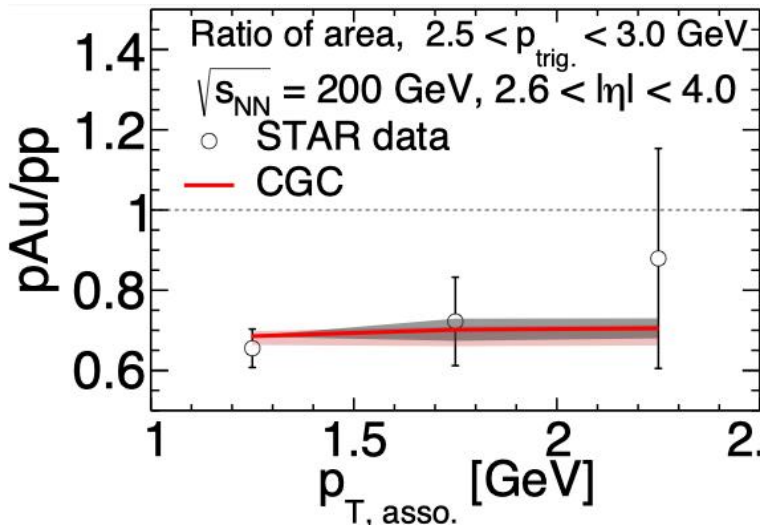
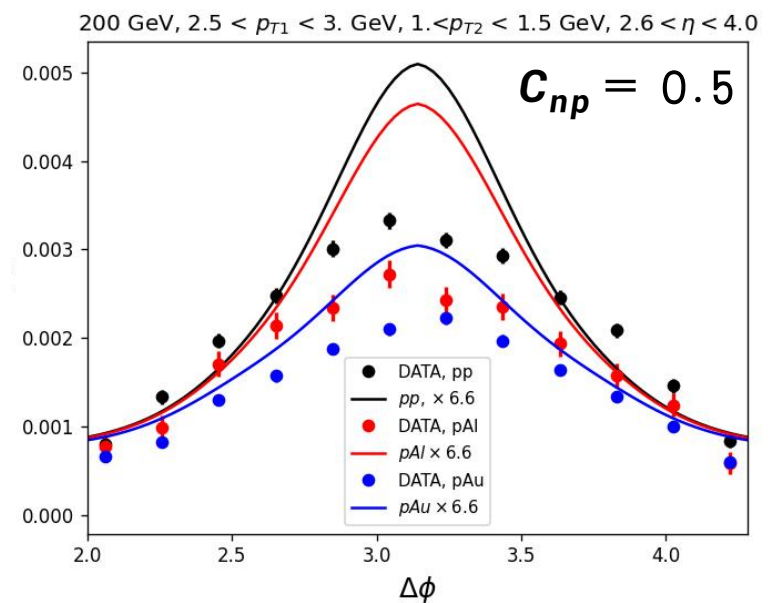
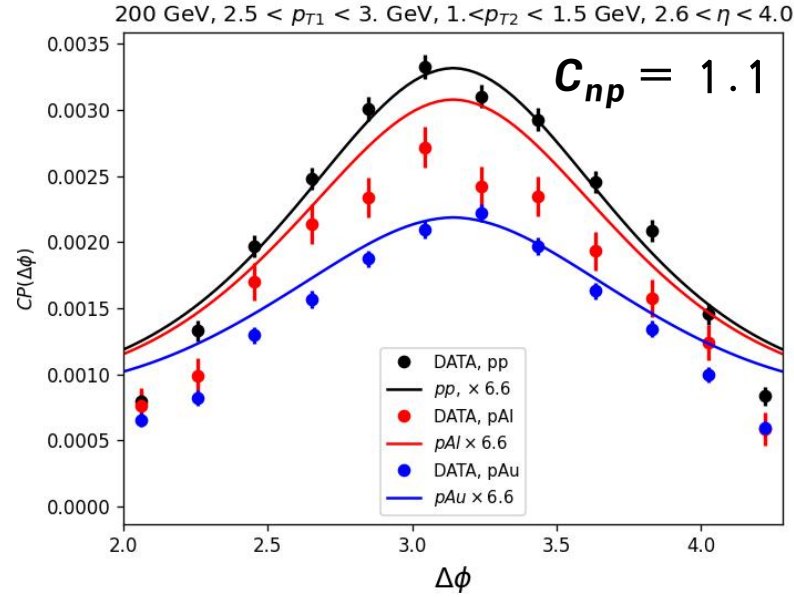
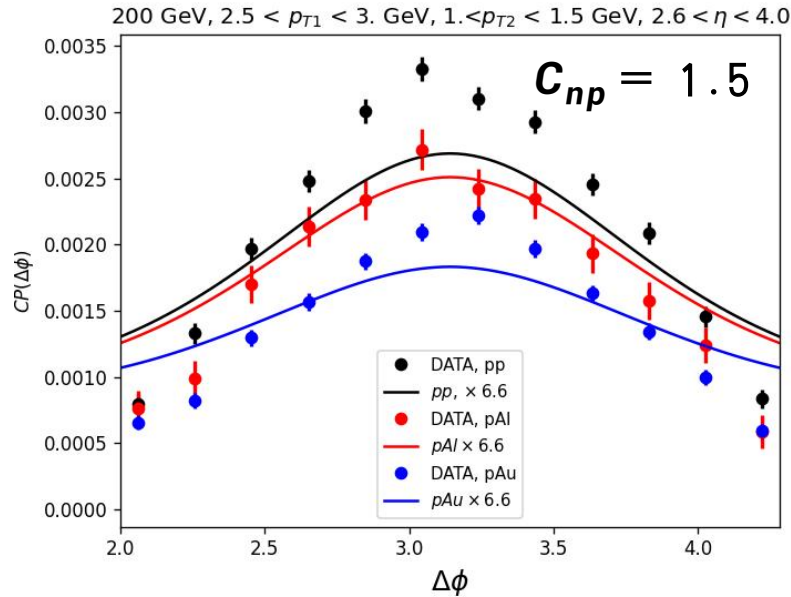
• Here we use the Gaussian approximation: $S(\mathbf{x}_\perp, \mathbf{y}_\perp, x) = \frac{1}{N_c} \langle \text{Tr} [V(\mathbf{x}_\perp) V^\dagger(\mathbf{y}_\perp)] \rangle_x$

Assume translational invariance: $S(|\mathbf{x}_\perp - \mathbf{y}_\perp|, x) = \frac{1}{N_c} \langle \text{Tr} [V(\mathbf{x}_\perp) V^\dagger(\mathbf{y}_\perp)] \rangle_x$

Mean-field approximation: $\langle \text{Tr} [\mathcal{O}_1] \text{Tr} [\mathcal{O}_2] \rangle_x = \langle \text{Tr} [\mathcal{O}_1] \rangle_x \langle \text{Tr} [\mathcal{O}_2] \rangle_x$

CP($\Delta\Phi$) for different C_{np}

$$S_{\text{Sud}}^{a+b \rightarrow c+d}(b_{\perp}) = \sum S_p^i(b_{\perp}) + C_{np} \times \sum S_{np}^i(b_{\perp}),$$



Initial conditions of rcBK for Nucleus

$$\eta = \frac{1}{\mathcal{A}_p} : \quad \mathcal{A}_p = \int_{T(\mathbf{b}) \geq T_{\text{cut}}} d^2\mathbf{b} T_p(\mathbf{b}) ,$$
$$\sigma = \frac{1}{\mathcal{T}_p} : \quad \mathcal{A}_p \mathcal{T}_p = \int_{T_p(\mathbf{b}) \geq T_{\text{cut}}} d^2\mathbf{b} T_p^2(\mathbf{b}) .$$

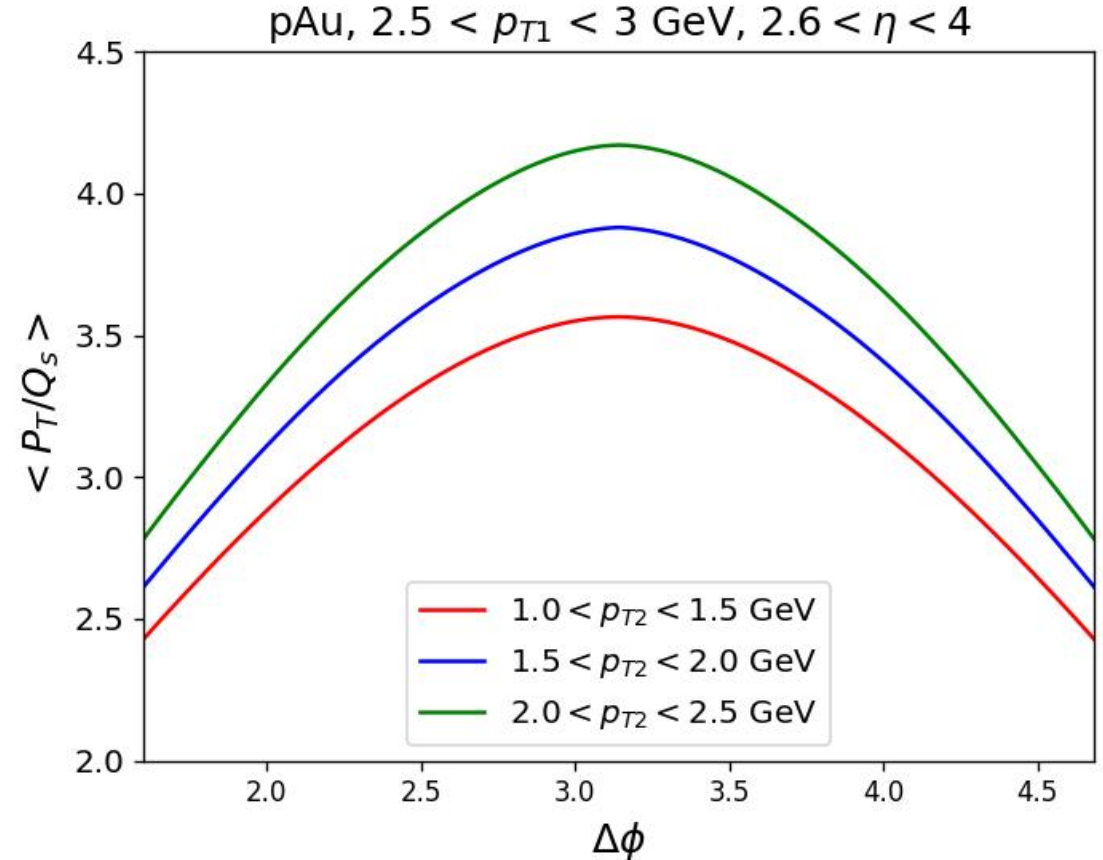
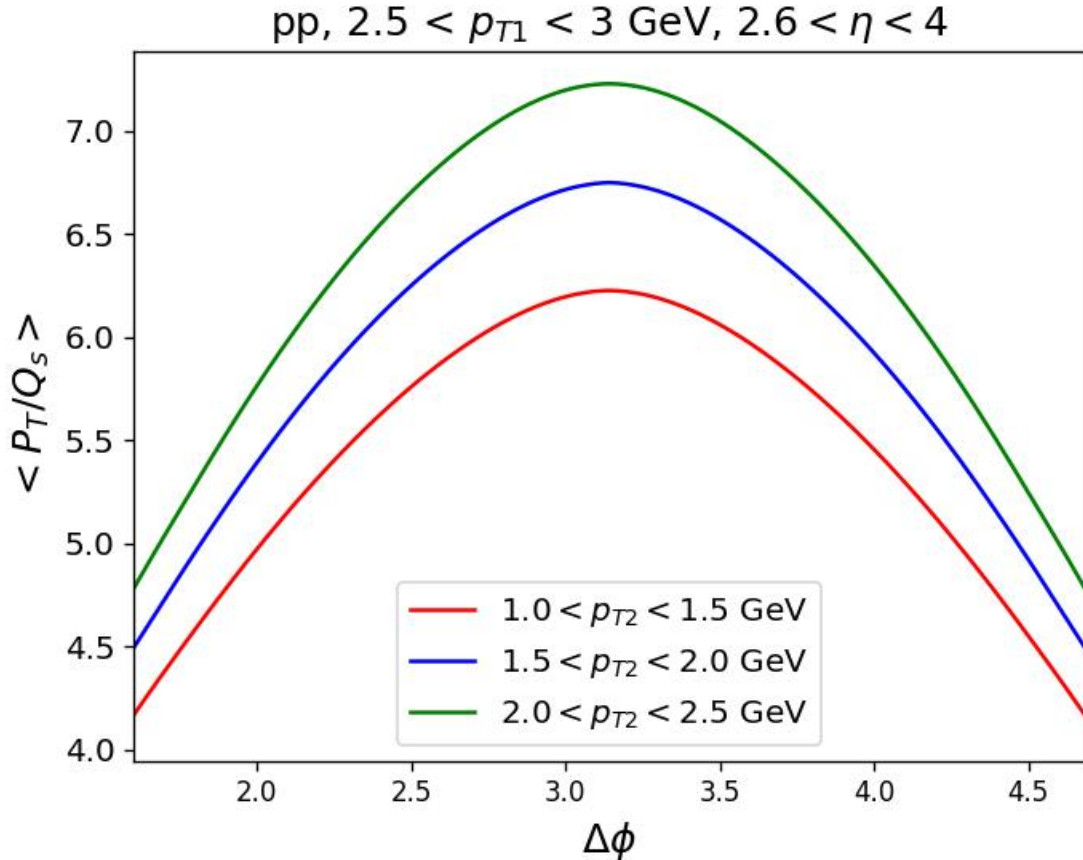
$$Q_s^A(x) \equiv Q_s(x) \sqrt{\sigma \mathcal{T}_A} ,$$

- We use $Q_{p,s0}^2 = 0.168 \text{ GeV}^2$, $\gamma = 1.119$, $C = 1.1715$, $\Lambda_{QCD} = 0.24 \text{ GeV}$, $e_c = 1$.
- For nucleus, we set $Q_{Al,s0}^2 = 1.2 Q_{p,s0}^2$; $Q_{Au,s0}^2 = 2.75 Q_{p,s0}^2$; $Q_{Pb,s0}^2 = 2.84 Q_{p,s0}^2$

J. L. Albacete, N. Armesto, J. G. Milhano, P. Quiroga-Arias and C. A. Salgado, Eur. Phys. J. C71 (2011) 1705.

F. Deganutti, C. Royon and S. Schlichting, JHEP 01(2024)159.

Why asymmetric bins not so good?



$$P_t = (1 - z)p_{1t} - zp_{2t}$$

- Partially because $\langle P_T/Q_s \rangle$ is not so large in pAu at asymmetric bins.
- How to estimate this model uncertainty when P_T/Q_s is not so large.

Initial conditions of rcBK for Nucleus

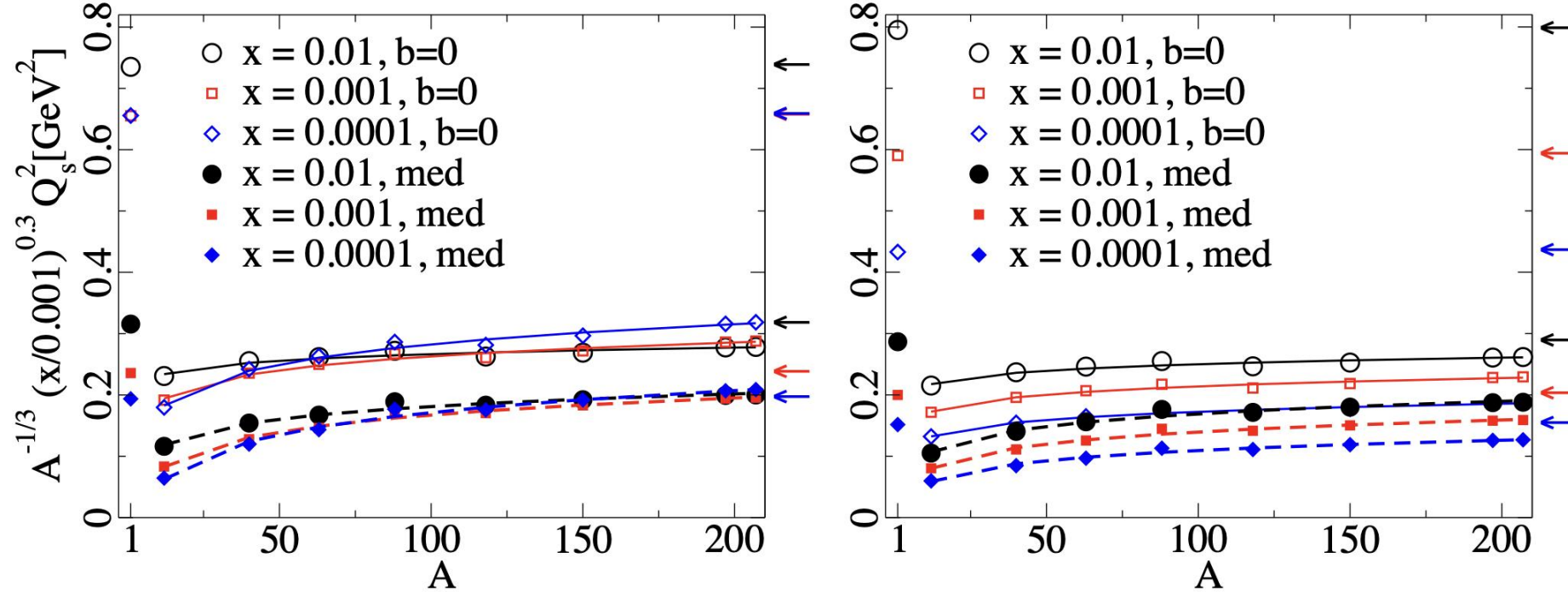
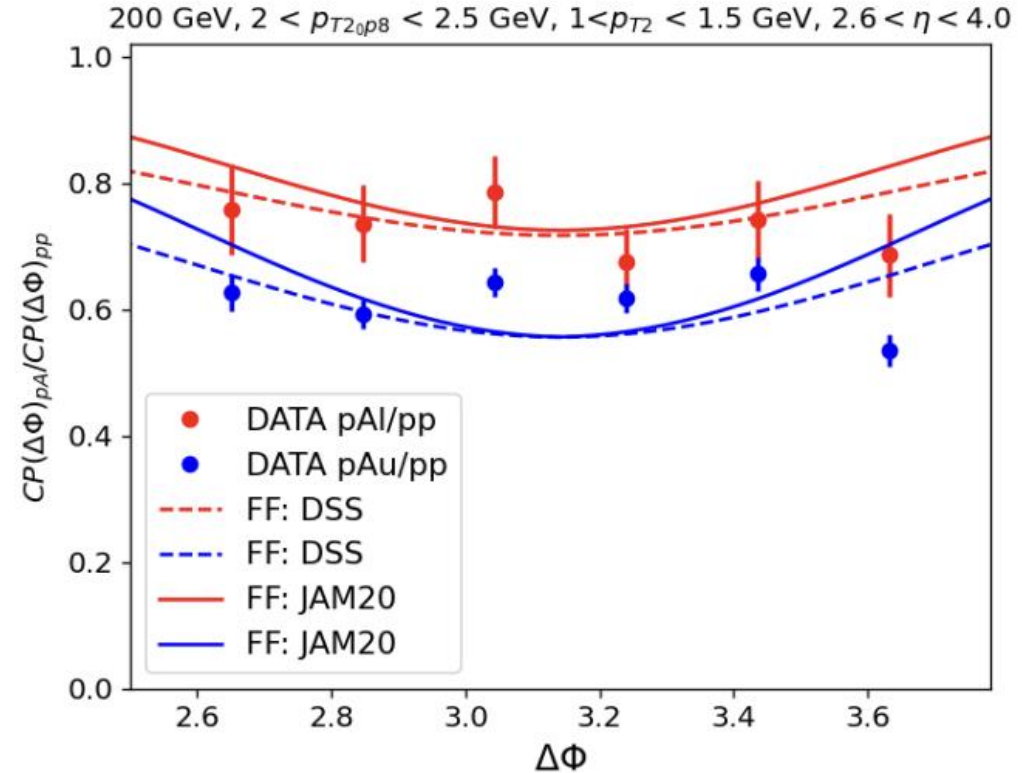
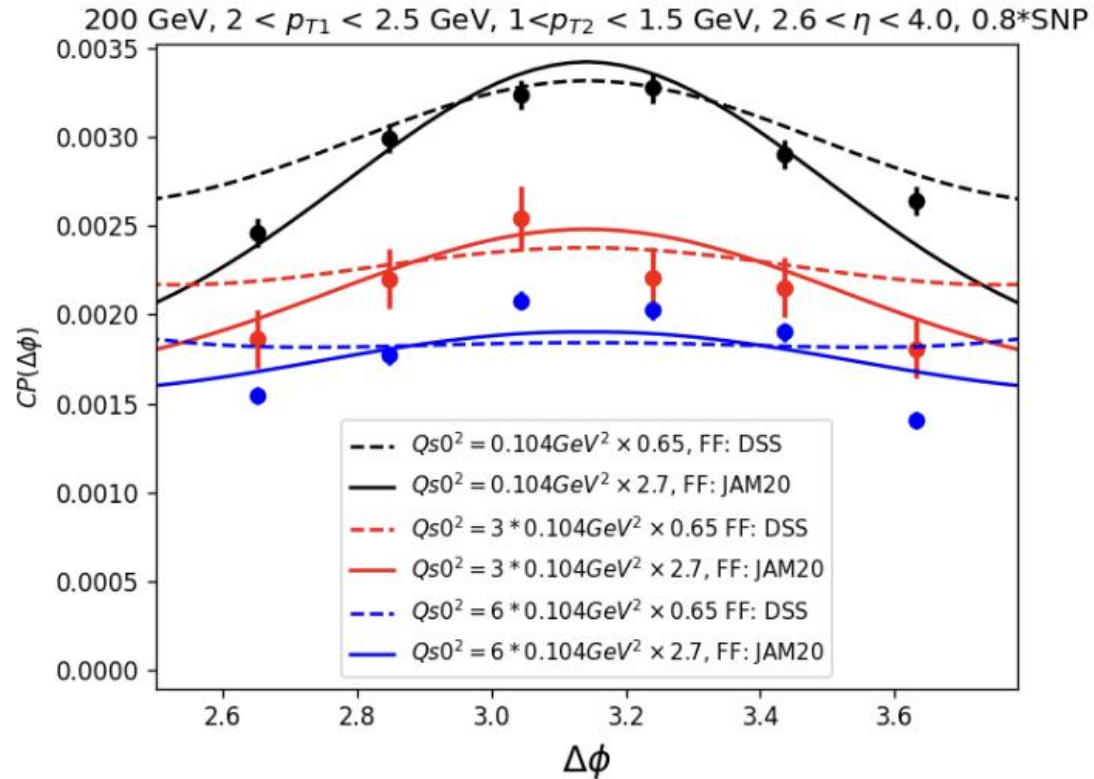


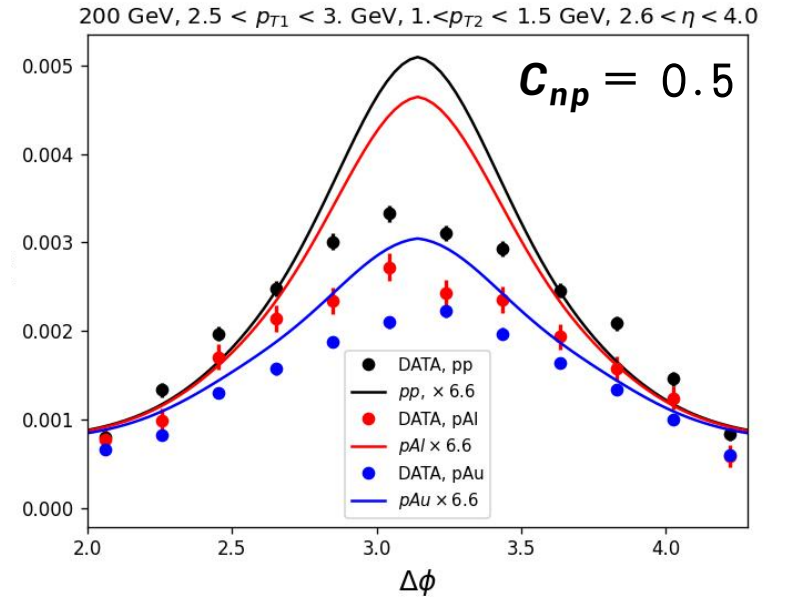
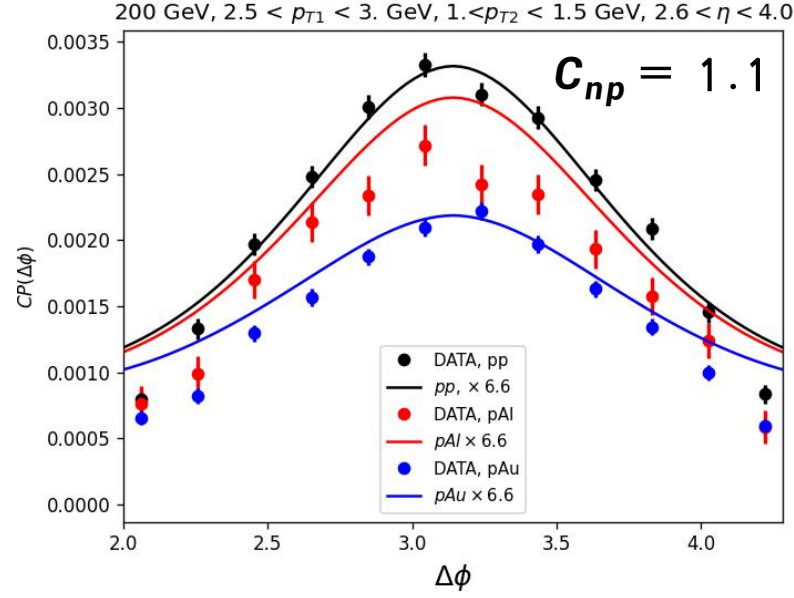
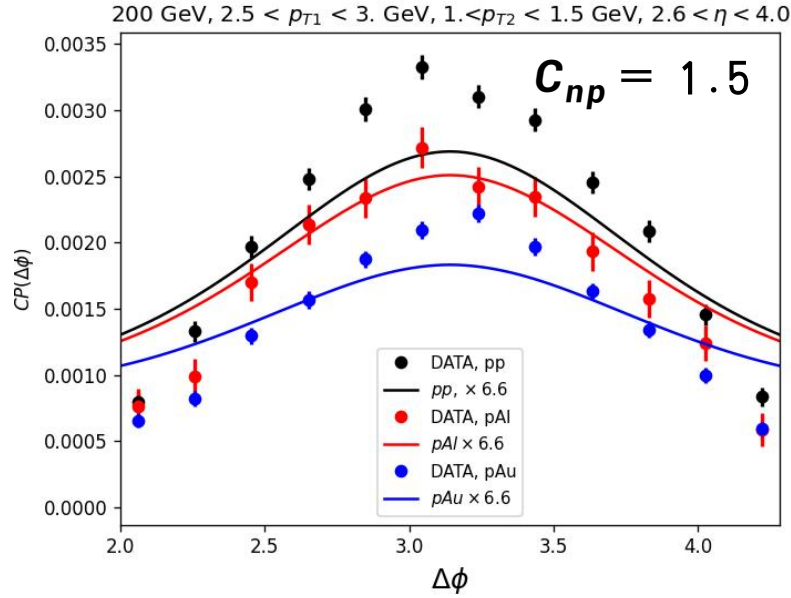
FIG. 3: Saturation scale at $b = 0$ (open symbols) and $b = b_{\text{med}}$. (filled symbols) as a function of A for different x . The saturation scale for the proton is shown at $A = 1$ and by the arrows on the right. Left: IPsat model. Right: bCGC model.

Fragmentation Function uncertainties



- Note, here the initial parameters for the MV is different with the defaulted one, and $Q_{A,0}^2 = A^{1/3} Q_{p,0}^2$.

$CP(\Delta\Phi)$ for different C_{np} .



$$S_{\text{Sud}}^{a+b \rightarrow c+d}(b_{\perp}) = \sum_{i=a,b,c,d} S_p^i(b_{\perp}) + C_{np} \times \sum_{i=a,c,d} S_{np}^i(b_{\perp}),$$

$$\begin{aligned}
\frac{d\sigma^{pA \rightarrow \pi^0 \pi^0 X}}{dy_1 dy_2 d^2p_{1t} d^2p_{2t}} &= \frac{\alpha_s^2}{2C_F} \int_{p_{t1} \frac{e^{y_1}}{\sqrt{s}} / (1 - p_{t2} \frac{e^{y_2}}{\sqrt{s}})}^1 \frac{dz_1}{z_1^2} \int_{p_{t2} \frac{e^{y_2}}{\sqrt{s}} / (1 - \frac{p_{t1}}{z_1} \frac{e^{y_1}}{\sqrt{s}})}^1 \frac{dz_2}{z_2^2} \frac{z(1-z)}{P_t^4} \\
&\left\{ D_{\pi^0/g}(z_1, \mu^2) [x_1 u(x_1, \mu^2) D_{\pi^0/u}(z_2, \mu^2) + x_1 d(x_1, \mu^2) D_{\pi^0/d}(z_2, \mu^2)] P_{gq}(z) \times \right. \\
&\quad \times \left[(1-z)^2 \mathcal{F}_{qg}^{(1)}(x_2, k_t) + \mathcal{F}_{qg}^{(2)}(x_2, k_t) \right] + \\
&+ D_{\pi^0/g}(z_2, \mu^2) [x_1 u(x_1, \mu^2) D_{\pi^0/u}(z_1, \mu^2) + x_1 d(x_1, \mu^2) D_{\pi^0/d}(z_1, \mu^2)] P_{gq}(1-z) \times \\
&\quad \times \left[z^2 \mathcal{F}_{qg}^{(1)}(x_2, k_t) + \mathcal{F}_{qg}^{(2)}(x_2, k_t) \right] + \\
&+ 2 [D_{\pi^0/u}(z_1, \mu^2) D_{\pi^0/u}(z_2, \mu^2) + D_{\pi^0/d}(z_1, \mu^2) D_{\pi^0/d}(z_2, \mu^2)] x_1 g(x_1, \mu^2) P_{gg}(z) \times \\
&\quad \times \left[\mathcal{F}_{gg}^{(1)}(x_2, k_t) - 2z(1-z) (\mathcal{F}_{gg}^{(1)}(x_2, k_t) - \mathcal{F}_{gg}^{(2)}(x_2, k_t)) \right] + \\
&+ D_{\pi^0/g}(z_1, \mu^2) D_{\pi^0/g}(z_2, \mu^2) x_1 g(x_1, \mu^2) P_{gg}(z) \times \\
&\quad \times \left. \left[\mathcal{F}_{gg}^{(1)}(x_2, k_t) - 2z(1-z) (\mathcal{F}_{gg}^{(1)}(x_2, k_t) - \mathcal{F}_{gg}^{(2)}(x_2, k_t)) + \mathcal{F}_{gg}^{(6)}(x_2, k_t) \right] \right\},
\end{aligned}$$

At LO in the CGC we have

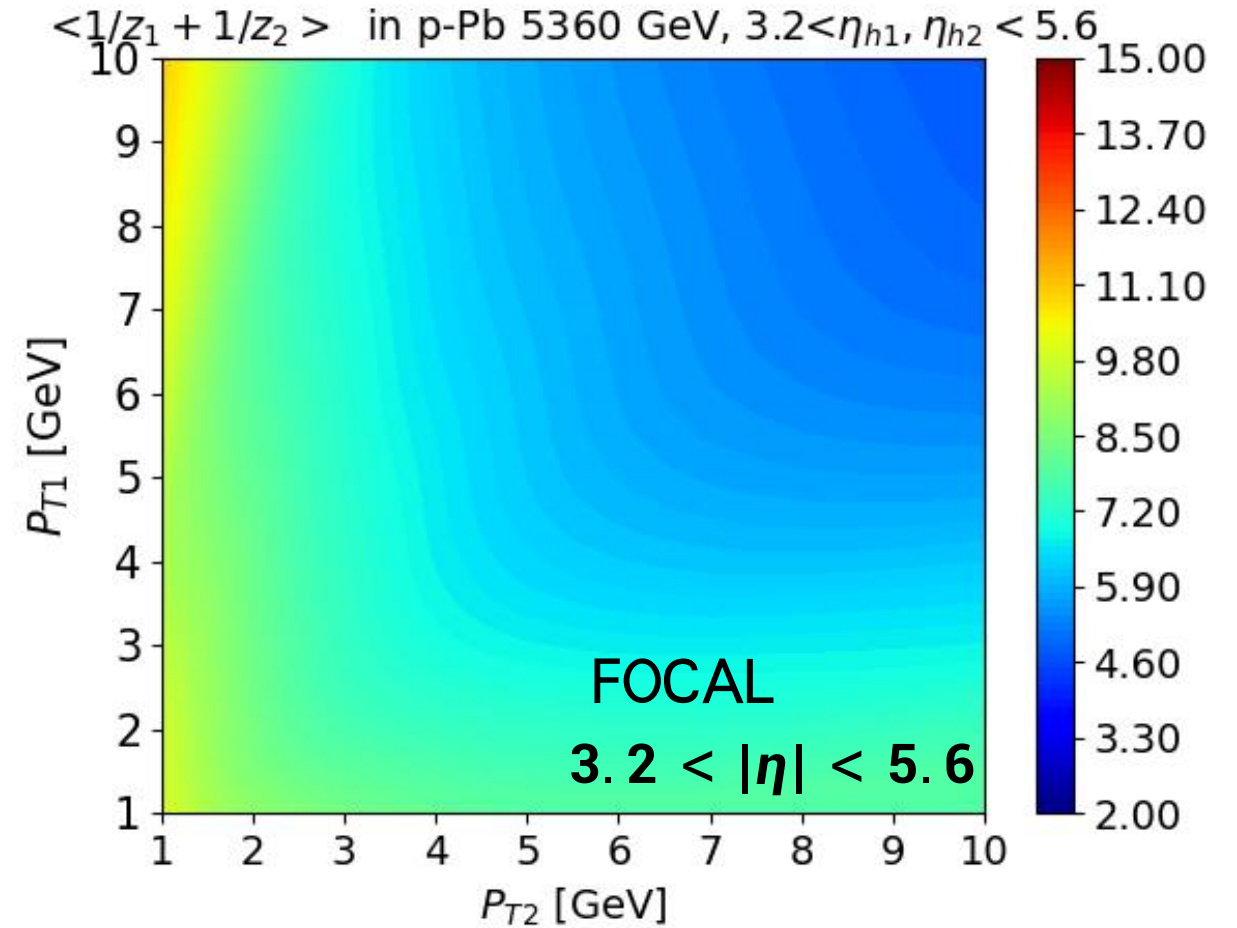
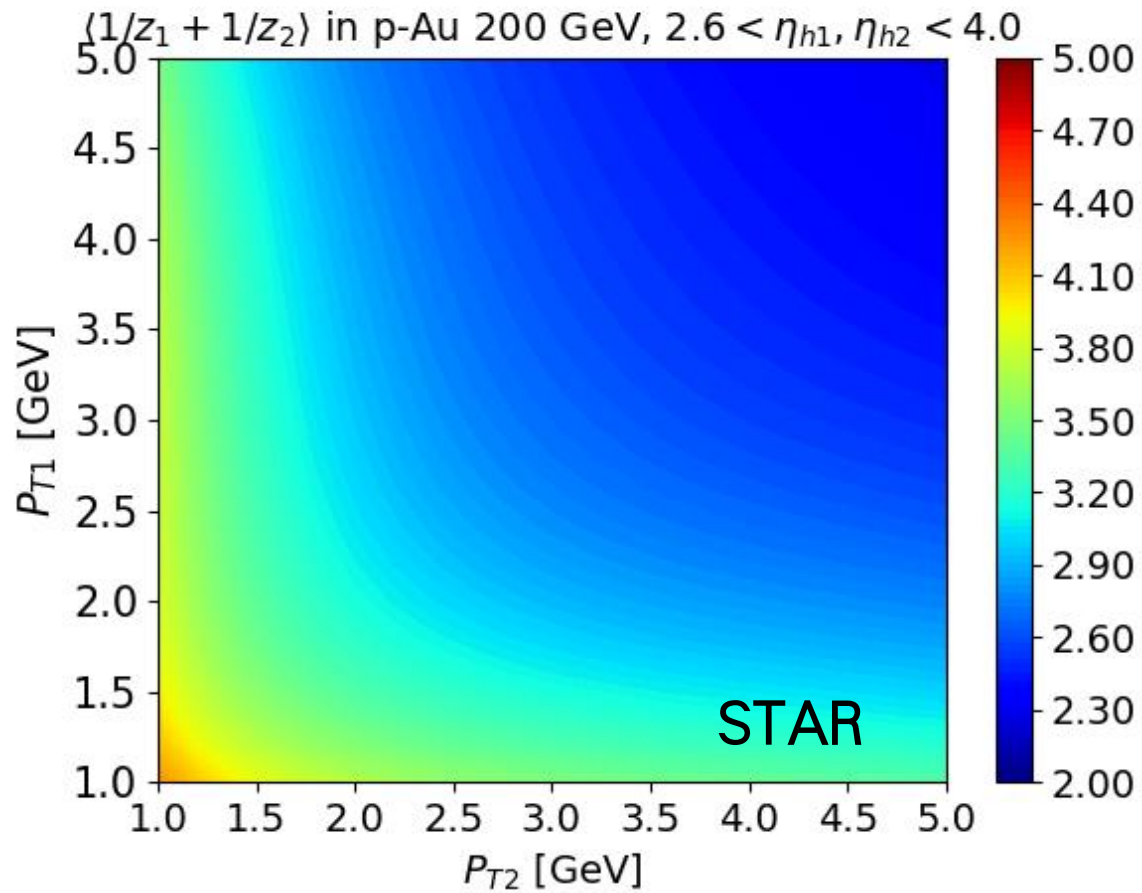
$$\frac{d\sigma^{p(q)A \rightarrow h_1 X}}{d^2\mathbf{p}_{h_1\perp} d\eta_{h_1}} = \int_0^1 \frac{dz_{h_1}}{z_{h_1}^2} \left[\sum_q x_p f_q(x_p, \mu^2) F(\mathbf{k}_\perp, x_A) D_{h_1/q}(z_{h_1}, \mu^2) + x_p g(x_p, \mu^2) F_{\text{Adj}}(\mathbf{k}_\perp, x_A) D_{h_1/g}(z_{h_1}, \mu^2) \right] \quad (207)$$

which includes both the quark and gluon-initiated channels. We introduced the Fourier transform of the dipole in the adjoint representation

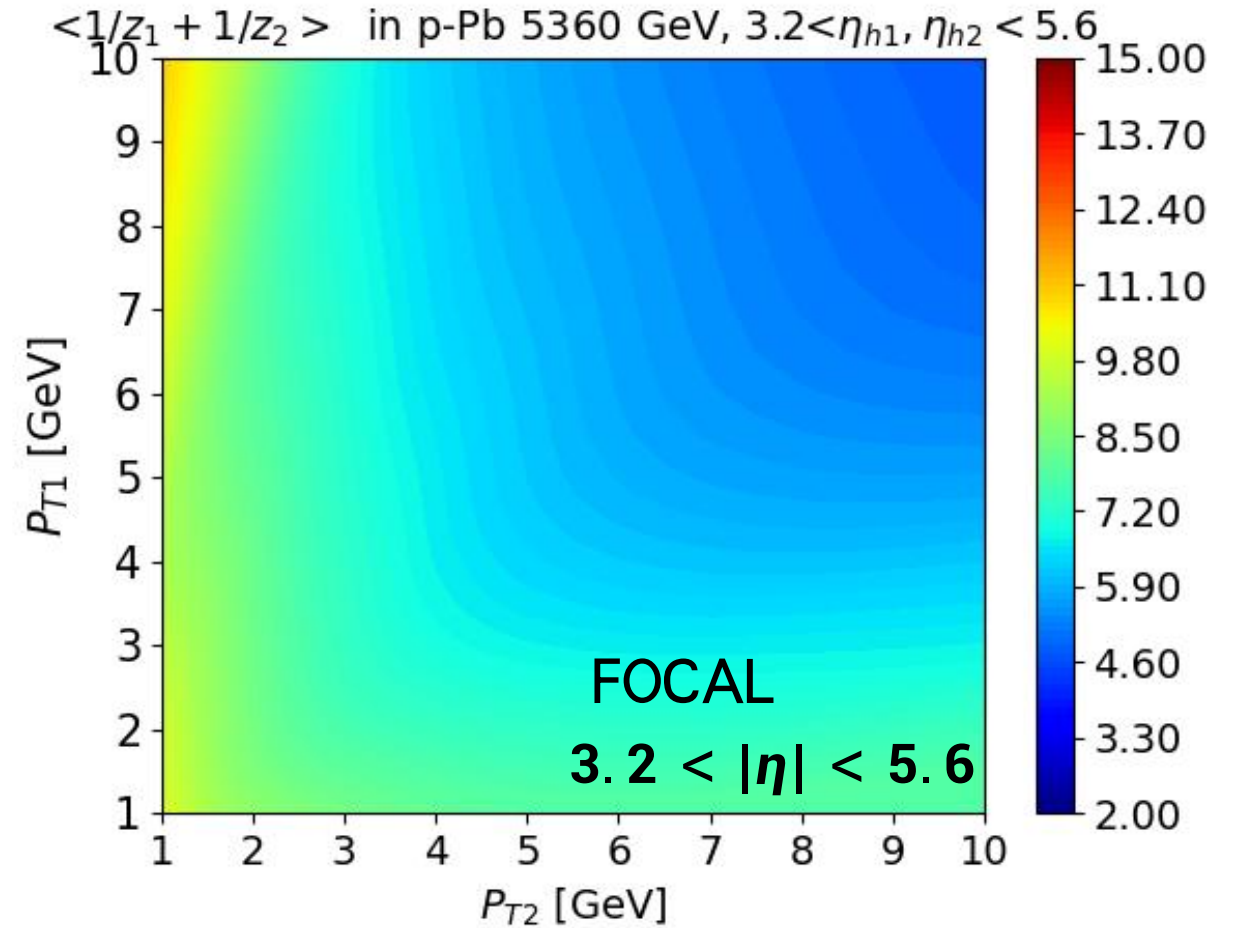
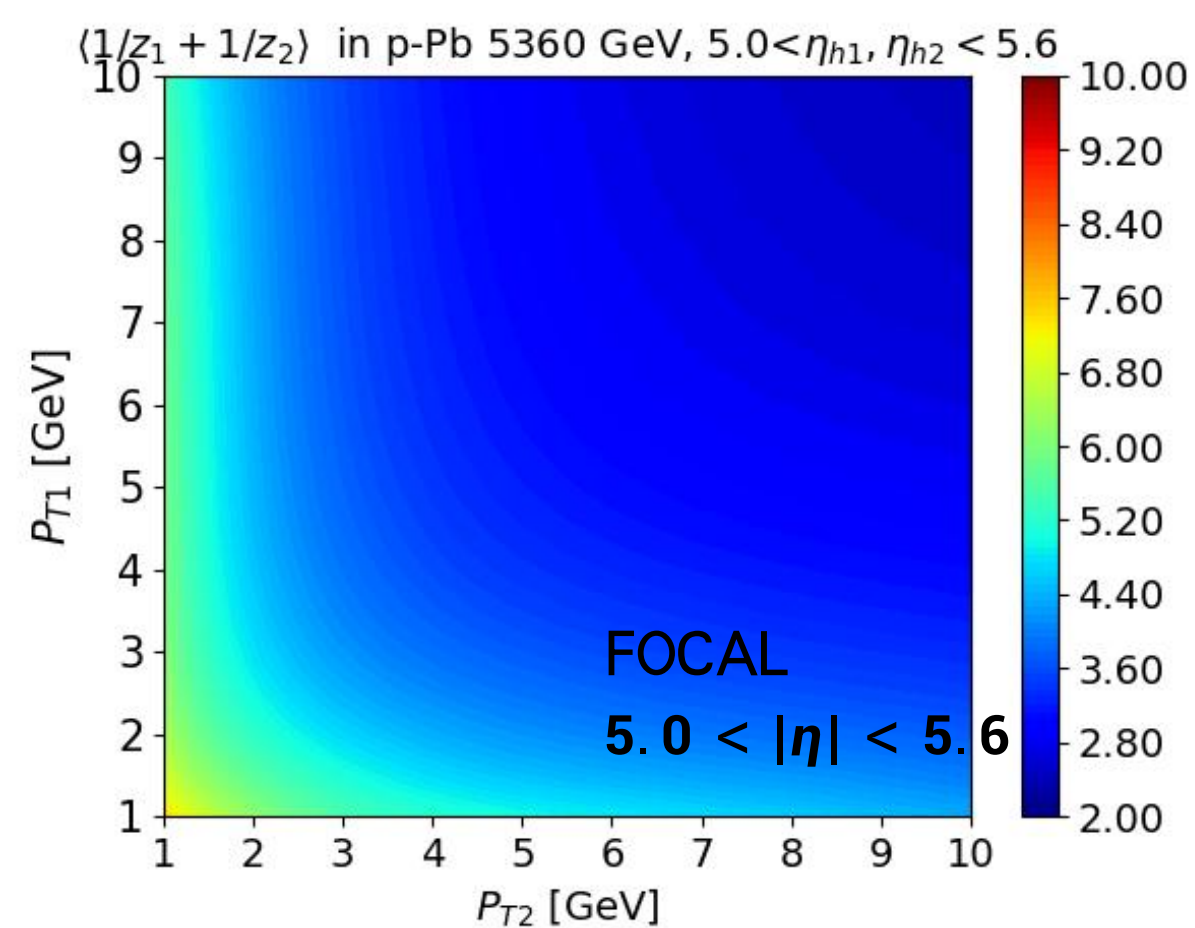
$$F_{\text{Adj}}(\mathbf{k}_\perp, x) = S_\perp \int \frac{r_\perp dr_\perp}{2\pi} J_0(k_\perp r_\perp) S_{\text{Adj}}(r_\perp, x) \quad (208)$$

which can be related to the dipole in the fundamental representation by

$$S_{\text{Adj}}(r_\perp, x) = (S(r_\perp, x))^{N_c/C_F} \quad (209)$$



- STAR has much smaller $\langle 1/z_1 + 1/z_2 \rangle$ than that at FOCAL.



- STAR has much smaller $(1/z_1 + 1/z_2)$ than that at FOCAL.